



Faculty of Graduate Studies

**New Zn(II) Complexes Having Different Coordination Modes
Controlled by the Drug Furosemide in Presence of Bioactive
Nitrogen Based Ligands: Synthesis, Structures and Various
Biological Applications.**

معقدات الزنك ثنائي الشحنة ومختلف طرق الترابط المحكومة بالدواء فوروسميد بوجود
القواعد النيتروجينية النشطة. التحضير، التركيب والتطبيقات البيولوجية المختلفة.

**This thesis is submitted in partial fulfillment of the requirements for the degree
of masters in Applied Chemistry at the Faculty of Graduate Studies, Birzeit
University, Ramallah, Palestine.**

Ghana Raymoni

Under Supervision of

Dr. Hijazi Abu Ali

June, 2018

**New Zn(II) Complexes Having Different Coordination Modes
Controlled by the Drug Furosemide in Presence of Bioactive
Nitrogen Based Ligands: Synthesis, Structures and Various
Biological Applications.**

By

Ghana Raymoni

This thesis was defended successfully on 19/06/2018 and approved by:

Committee Members

Signature

Dr. Hijazi Abu Ali

.....

Supervisor

Department of Chemistry, Birzeit University

Prof. Khalid Swaileh

.....

Member of thesis committee

Department of Biology and Biochemistry, Birzeit University

Dr. Wadie Sultan

.....

Member of thesis committee

Department of Chemistry, Al-Quds University

Acknowledgements:

I am thankful to Allah for giving me the strength and power to complete this work. I am most honored to thank my supervisor Dr. Hijazi Abu Ali for his continuous effort and support to complete this work; his kind understanding it from the beginning to the end is greatly appreciated.

I am very much delighted to thank Prof. Khalid Swaileh and Dr. Wadie Sultan for their valuable time and the great efforts in reading and discussing the present work.

Thanks to everyone in the Chemistry Department who helped me during this work, Mr. Ibrahim Shalash, Mr. Azmi Dodeen and Mr. Assem Mubarak. I do not forget to thank Mr. Ratib Muhammad and Mr. Munther Metani from the Biology Department for helping me to complete the biological activity part of this thesis.

I would like to dedicate this work to my father, mother, and thank them for their continuous encouragement and support during my life. Also I would like to thank my brothers (Nidal, Mohammad and Ahmed) and my sisters (Enas and Samya). Finally, I would like to thank all my friends especially Amani Abu Shamma and all people at Birzeit University who helped me during this work.

Contents:

Acknowledgements:	III
Contents:	IV
List of Figures:	VII
List of Tables:	IX
List of Schemes:	X
Abbreviations:	XI
Abstract:	XII
ملخص بالعربية:	XIV
1. Introduction:	1
1.1 General ideas:	1
1.2 Metals in biological systems:	2
1.2.1 Zinc in biological systems:	4
1.3 Zinc as an element:	6
1.4 Bioactive chelating agents:	7
1.5 Carboxylate and metal carboxylate chemistry:	13
1.6 Zinc carboxylates:	18
1.7 Furosemide:	19
1.7.1 Furosemide metal complexes:	20
1.8 Bis-(4-nitrophenyl) phosphate hydrolysis:	21
1.9 Anti-bacterial activity:	24
1.10 Aim of research:	26
2. Experimental:	26
2.1 Chemicals and reagents:	26
2.2 Instrumentations:	27
2.3 Synthesis and characterization of zinc furosemide complexes:	27

2.3.1 Synthesis of [Zn(furo) ₂ (MeOH) ₂] (1):	27
2.3.2 Synthesis of [Zn(furo) ₂ (2-ampy) ₂] (2):	28
2.3.3 Synthesis of [Zn(furo) ₂ (2-ammepy) ₂] (3):	29
2.3.4 Synthesis of [Zn(furo) ₂ (H ₂ O)(2,2-bipy)](4):	29
2.3.5 Synthesis of [Zn(furo) ₂ (H ₂ O)(4,4-dipy)] (5):	30
2.3.6 Synthesis of [Zn(furo) ₂ (1,10-phen)] (6):	31
2.3.7 Synthesis of [Zn(furo) ₂ (2,9-dmp)] (7):	31
2.3.8 Synthesis of [Zn(furo) ₂ (quin) ₂] (8):	32
2.4 X-ray single crystal diffraction:	33
2.5 Anti-bacterial activity:	35
2.6 BNPP hydrolysis:	36
3. Results and discussion:	37
3.1 Synthesis zinc furosemide complexes:	37
3.2 ¹ H-NMR and ¹³ C NMR:	39
3.3 Infrared spectroscopy:	46
3.4 Electronic absorption spectroscopy:	49
3.5 X-ray spectroscopy:	50
3.5.1 X-ray crystal structure of [Zn(furo) ₂ (H ₂ O)(2,2-bipy)] (4):	50
3.6 Biological activity (<i>In-vitro</i>):	53
3.6.1 Anti-bacterial activity:	53
3.7 BNPP catalytic hydrolysis:	58
3.7.1 Effect of complexes` concentration on BNPP hydrolysis	58
3.7.2 Effect of temperatures on BNPP hydrolysis	59
3.7.3 Effect of pH on BNPP hydrolysis	59
3.8 Mass spectrometry:	62
4. Conclusions:	66

5. References:	67
6. Appendices:	72
Appendix A: Crystal structure data of [Zn(furo)₂(H₂O)(2,2-bipy)] (4)	72
Appendix B: Mass spectra of complexes (1-8)	84

List of Figures:

Figure 1: Elements building up bio-mass, additional essential elements, essential for some groups of organisms, and medically important elements.....	1
Figure 2: Dose-response curve for essential elements.....	2
Figure 3: Diagram of human carbonic anhydrase, with Zn atom shown in the Center.....	5
Figure 4: Few new classes of Schiff base ligands. (I) Bidentate ligand, (II) tridentate Ligand, (III) tetradentate ligand.....	7
Figure 5: Formation of metal complexes through interaction with monodentate and Bidentate ligands.....	8
Figure 6: Example of pyrazolone ligand.....	10
Figure 7: Chemical structure of bioactive ligands (nitrogen heterocyclic) used in the Present work.....	11
Figure 8: Ortep plot of [Cu (benzoic acid) ₂ (phen)(H ₂ O)].....	12
Figure 9: Structure of silver-trifluoroacetate precursor.....	13
Figure 10: Bonding modes of carboxylate ligands (I) ionic modes, (II) monodentate Mode, (III) bidentate chelating, and (IV) bidentate bridging.....	14
Figure 11: Carboxylate bridging modes.....	15
Figure 12: Molecular structure of Zn(methoxy) ₂ -1,10-phenanthroline.....	18
Figure 13: The chemical structure of furosemide.....	19
Figure 14: Molecular structure of Cu(furosemide) ₂ .2MeOH.....	20
Figure 15: Structure of ATP.....	21
Figure 16: Structure of BNPP	22
Figure 17: Oxidative cleavage agent [Cu(phen) ₂] ⁺	22
Figure 18: Proposed mechanism of the BNPP catalytic cleavage.....	24
Figure 19: Molecular structure of compound 4	50

Figure 20: Agar diffusion	56
Figure 21: BNPP hydrolysis at different concentration of complex 7 in DMSO/ HEPES buffer solution under certain conditions ($[BNPP]= 1 \times 10^{-4}$ M, pH = 7.00 and temp = 25 °C)	58
Figure 22: BNPP hydrolysis at different temperature values in DMSO/HEPES buffer Solution under certain conditions ($[BNPP] = 1 \times 10^{-4}$ M, $[complex\ 4] =$ 2×10^{-4} M, and pH = 7.00)	59
Figure 23: BNPP hydrolysis at different pH values in DMSO/HEPES buffer solution under certain conditions ($[BNPP] = 1 \times 10^{-4}$ M, $[complex\ 4] = 2 \times 10^{-4}$ M, and temp = 37 °C)	60
Figure 24: Second order rate for complex 4 with different BNPP concentrations under certain conditions (pH = 7.00, temp = 37 °C and $[complex\ 4] = 2 \times 10^{-4}$ M)	60
Figure 25: Mass spectra of complex 1	62
Figure 26: Mass spectra of complex 2	62
Figure 27: Mass spectra of complex 3	63
Figure 28: Mass spectra of complex 4	63
Figure 29: Mass spectra of complex 5	64
Figure 30: Mass spectra of complex 6	64
Figure 31: Mass spectra of complex 7	65
Figure 32: Mass spectra of complex 8	65

List of Tables:

Table 1: Percentage composition of selected elements in the human body.....	3
Table 2: Zinc content in typical food.....	4
Table 3: Non-steroid anti-inflammatory drugs of the acid type.....	17
Table 4: Crystal data and refinements for complex 4	34
Table 5: Physical properties of complexes (1-8) and their % yields	39
Table 6: ¹ H-NMR spectral data of complex 1 , complex 2 , and furosemide	40
Table 7: ¹³ C-NMR spectral data of complex 1 , complex 2 , and furosemide	41
Table 8: ¹ H-NMR spectral data of Complex 3 , Complex 4 , and complex 5	42
Table 9: ¹³ C-NMR spectral data of complex 3 , complex 4 , and complex 5	43
Table 10: ¹ H-NMR spectral data of complex 6 , complex 7 , and complex 8	44
Table 11: ¹³ C-NMR spectral data of complex 6 , complex 7 , and complex 8	45
Table 12: Assignment IR bands and wave numbers of Na _{furo} and complex 1	46
Table 13: Assignments IR bands and wave numbers of complex 2 , complex 3 , and complex 4	47
Table 14: Assignments IR bands and wave numbers of complex 5 , complex 6 , complex 7 , and complex 8	48
Table 15: UV-visible spectral data for the prepared complexes and pure ligand	49
Table 16: Selected bond distances (Å) and bond angles (°) for complex 4	51
Table 17: Hydrogen bond distances (Å) and bond angles (°)	52
Table 18: <i>In-vitro</i> anti-bacterial activity data for complexes (1-8) against gram negative bacteria	53
Table 19: <i>In-vitro</i> anti-bacterial activity data for complexes (1-8) against gram positive bacteria	54

Table 20: Kinetic parameters of BNPP hydrolysis for complexes (1-8) with different concentration of BNPP61

List of Schemes:

Scheme 1: Proposed synthesis of $[Zn(furo)_2(MeOH)_2]$ (1)37

Scheme 2: Synthesis of complexes 2, 3, 4 and 538

Scheme 3: Synthesis of complexes 6, 7 and 838

Abbreviations:

2-ampy	2-aminopyrdine
2-ammepy	2-aminomethylpyrdine
ATP	Adenosine triphosphate
2,2-bipy	2,2-bipyrdine
BNPP	Bis(4-nitrophenyl) phosphate
¹³ C-NMR	Carbon-13 Nuclear Magnetic Resonance
4,4-dipy	4,4-dipyrdine
2,9-dmp	2,9-Dimethyl-1,10-phenanthroline
DNA	Deoxyribonucleic acid
DMF	Dimethylformamide
DMSO	Dimethyl sulfoxide
E	Erythromycin
Furo	Furosemide
G	Gentamycin
G+	Gram-positive
G-	Gram-negative
h	Hour
HEPES	(4-(2-hydroxyethyl)-1-piperazineethanesulfonic acid)
¹ H-NMR	Proton Nuclear Magnetic Resonance
IR	Infrared
IZD	Inhibition zone diameter
LMCT	Ligand-metal charge transfer
MeOH	Methanol
MLCT	Metal-ligand charge transfer
m.p	Melting point
NMR multiplicities	s = Singlet d = Doublet t = Triplet m = Multiplet
NSAIDs	Non-steroidal anti-inflammatory drugs
1,10-phen quin	1,10-phenanthroline quinoline
RNA	Ribonucleic acid
rt	Room temperature
temp	Temperature
UV-Vis	Ultraviolet-visible
Vo	Initial rate

Abstract

Novel Zn(II) complexes with the general formula: $[\text{Zn}_n(\text{Furo})_m(\text{L})_z]$, ($n = 1, 2\dots$; $m = 1, 2\dots$; $z = 1, 2\dots$) were prepared. The complexes $[\text{Zn}(\text{furo})_2(\text{MeOH})_2]$ (**1**), $[\text{Zn}(\text{furo})_2(2\text{-ampy})_2]$ (**2**), $[\text{Zn}(\text{furo})_2(2\text{-ammepy})_2]$ (**3**), $[\text{Zn}(\text{furo})_2(\text{H}_2\text{O})(2,2\text{-bipy})]$ (**4**), $[\text{Zn}(\text{furo})_2(\text{H}_2\text{O})(4,4\text{-dipy})]$ (**5**), $[\text{Zn}(\text{furo})_2(1,10\text{-phen})]$ (**6**), $[\text{Zn}(\text{furo})_2(2,9\text{-dmp})]$ (**7**), and $[\text{Zn}(\text{furo})_2(\text{quin})_2]$ (**8**) were synthesized and characterized using different techniques such as IR, UV-Vis, $^1\text{H-NMR}$, $^{13}\text{C-NMR}$, LC/MS, single crystal X-ray diffraction and other physical properties. The crystal structure of complex (**4**) was determined using single crystal X-ray diffraction.

The anti-bacterial activity of complexes (**1-8**) was tested using agar diffusion method against three gram-positive (*Staphylococcus aureus*, *Bacillus subtilis* and *Staphylococcus epidermidis*) and three gram-negative bacteria (*Escherichia coli*, *Proteus mirabilis*, *Pseudomonas aeruginosa*). Most of the prepared complexes did not show considerable anti-bacterial activity against gram-negative bacteria except complex **4** and complex **6**. The two complexes **4** and **6** showed anti-bacterial activity against *P.mirbilis* with Inhibition Zone Diameter equals 10.0 mm and complex **6** showed anti-bacterial activity against *E.coli* with IZD equals 11.7 mm. In the case of gram-positive bacteria, only complex **3** showed low anti-bacterial activity against *S. epidermidis* with IZD equals 6.0 mm. Complexes **4** and **5** only showed anti-bacterial activity against *S. aureus* with IZD equals 8.7 mm and 8.0 mm, respectively.

The complexes **2** and **8** didn't show any anti-bacterial activity against gram-positive bacteria. Complex **7** showed anti-bacterial activity for all types of gram-positive

bacteria (*S. aureus*, *B. subtilis*, *S. epidermidis*) with IZD equals 8.0 mm, 8.7 mm and 11.3 mm, respectively. Complex **1** didn't show any anti-bacterial activity against all types of gram positive and gram negative bacteria. In addition, the rate of bis-(4-nitrophenyl) phosphate hydrolysis was measured at different temperatures, pH values and concentrations and the rates for the eight complexes were in the following order: complex **4 > 2 > 5 > 8 > 7 > 6 > 3 > 1**.

ملخص بالعربية

تم تحضير ثمانية مركبات جديدة من الزنك وصيغتها الشكلية كما يلي $[Zn_n(Furo)_m(L)_z]$, ($n = 1, 2, \dots$; $m = 1, 2, \dots$; $z = 1, 2, \dots$)

والمركبات الثمانية هي: $[Zn(furo)_2(2-ampy)_2]$ (2), $[Zn(furo)_2(2-ammpy)_2]$ (3), $[Zn(furo)_2(H_2O)(2,2-bipy)]$ (4), $[Zn(furo)_2(H_2O)(4,4-dipy)]$ (5), $[Zn(furo)_2(1,10-phen)]$ (6), $[Zn(furo)_2(2,9-dmp)]$ (7), and $[Zn(furo)_2(quin)_2]$ (8)

حيث تم تشخيص المركبات الثمانية بأجهزة مختلفة مثل طيف الأشعة تحت الحمراء وجهاز طيف الأشعة فوق البنفسجية والمرئية وجهاز الرنين المغناطيسي وجهاز حيود الأشعة السينية البلورية وجهاز الكروماتوغرافية السائلة والمطياف الكتلي وخصائص فيزيائية أخرى. البنية البلورية للمركب 4 تم تحديدها باستخدام جهاز حيود الأشعة السينية البلورية.

تم اختبار نشاط المركبات (1-8) باستخدام طريقة الانتشار في الآجار ضد ثلاثة أنواع من البكتيريا موجبة غرام (*E. coli*, *P. mirabilis*, *P. aeruginosa*) وثلاثة أنواع من البكتيريا سالبة غرام (*S. aureus*, *B. subtilis* and *S. epidermidis*). معظم المركبات التي تم تحضيرها لم تظهر أي نشاط ضد جميع أنواع بكتيريا سالبة غرام باستثناء مركب 4 ومركب 6. المركبان 4 و 6 اظهرا نشاطا ضد *P. mirabilis* بقطر نطاق تثبيط لهذه البكتيريا يساوي 10.0 ملم. والمركب 6 اظهر نشاطا ضد *E. coli* بقطر نطاق تثبيط يساوي 11.7 ملم. في حالة بكتيريا موجبة غرام، المركب 3 اظهر نشاطا قليلا ضد *S. epidermidis* بقطر نطاق تثبيط يساوي 6.0 ملم. المركبان 4 و 5 اظهرا نشاطا ضد نوع واحد هو *S. aureus* بقطر نطاق تثبيط يساوي 8.0 ملم و 8.7 ملم، بالترتيب.

المركبان 2 و 8 لم يظهر أي نشاطا ضد أي نوع من بكتيريا موجبة غرام. المركب 7 اظهر نشاطا بكتيريا ضد جميع انواع بكتيريا موجبة غرام (*S. epidermidis*, *B. subtilis* and *S. aureus*) بقطر نطاق تثبيط يساوي 8.0 ملم و 8.7 ملم و 11.3 ملم، بالترتيب.

مركب 1 لم يظهر أي نشاطا ضد جميع انواع البكتيريا موجبة و سالبة غرام. بالإضافة، تم قياس سرعة تحلل bis-(4-nitrophenyl) phosphate عند درجات حرارة و قيم pH و تراكيز مختلفة حيث كان ترتيب

المركبات كما يلي: المركب 4 < 2 < 5 < 8 < 7 < 6 < 3 < 1.

(Figure 2).^{2,4} The humans' body needs macro-minerals in amounts greater than 100 mg/day, but micro-minerals are needed in amounts less than 100 mg/day.¹

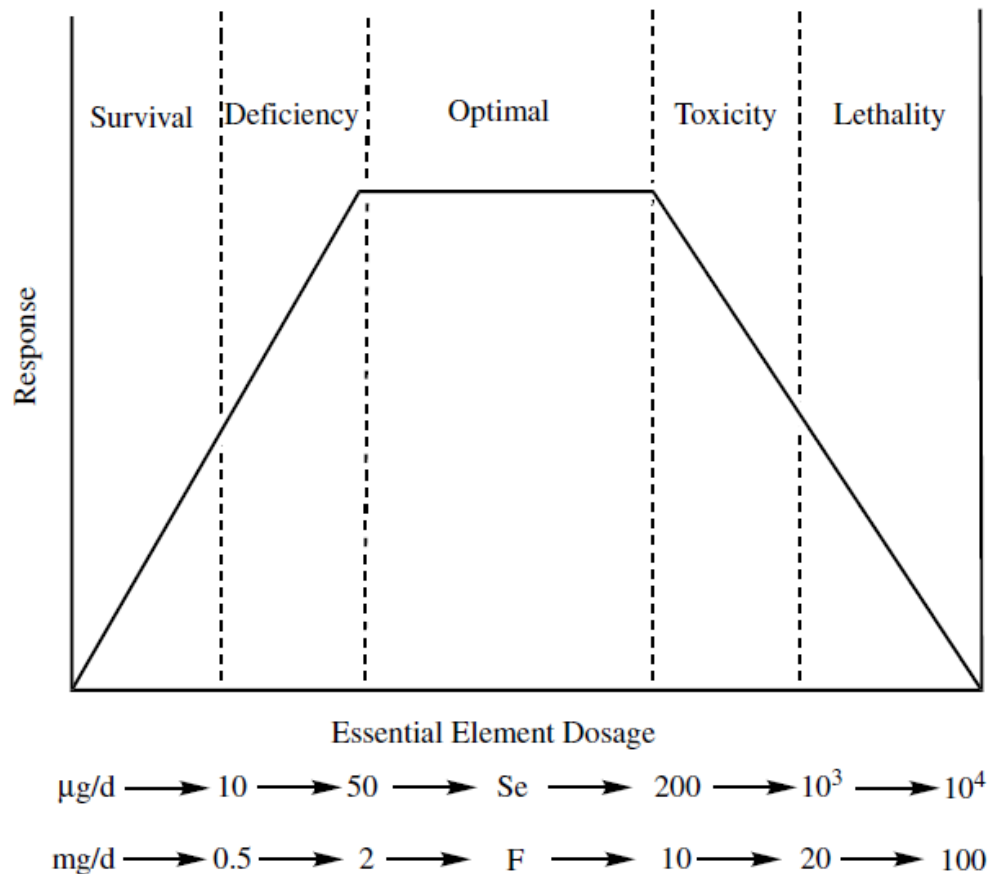


Figure 2: Dose-response curve for essential elements.²

1. 2 Metals in biological systems:

Metal ions play important roles in about one third of enzymes, and can perform many functions including (1) modification of electrons flow in enzymes, by ease of controlling an enzyme-catalyzed reaction (2) binding with active sites in enzymes with appropriate functional group (3) and if the metal has many valence state, they can provide a site for redox reactivity.⁵ A catalyzed biochemical reaction by a certain metalloenzyme might be proceeded slowly or can't be proceeded at all if appropriate metal ion does not exist. These ions being bounded with different groups may bind

with main-chain amino and carbonyl groups, particularly with carboxylate groups of aspartic and glutamic acid.⁵

Metal ions with positive charge greater than one, act as electrophiles. The positive charge makes metal ions capable of forming bond or charge-charge interaction with another atom. Because metal ions have a large ionic volume and high positive charge, they can associate with many ligands around them at the same time.⁵

Metals are essential for plants, animals, and microorganisms, however some of these metals are toxic while others do not have any known biological effects like scandium +2 and +3 ions and in its various isotopic forms.^{6,7} Metals play important roles in life processes as they participate in cellular and sub-cellular functions, such as iron, zinc, cobalt, copper, molybdenum, chromium, vanadium and nickel. Zinc is one of the most abundant metals in human body because it is a component of more than 300 enzymes specially enzymes which are responsible for ribonucleic acid and deoxyribonucleic acid synthesis. The approximate percentages by weight of selected essential elements in the human body are shown in Table 1.^{7,8}

Table 1: Percentage composition of selected elements in the human body.²

Element	Percentage (by weight)	Element	Percentage (by weight)
Oxygen	53.6	Silicon, magnesium	0.04
Carbon	16.0	Iron, fluorine	0.005
Hydrogen	13.4	Zinc	0.003
Nitrogen	2.4	Copper, bromine	2.0×10^{-4}
Sodium, potassium, sulfur	0.10	Selenium, manganese, arsenic nickel	2.0×10^{-5}
Chlorine	0.09	Lead, cobalt	9.0×10^{-6}

1. 2.1 Zinc in biological systems:

Zinc is the second essential trace element after iron in the human body. Its total quantity ranges from two to three grams, being most abundant in muscles, liver, kidneys, bones, prostate and eyes.^{8,9,10} The recommended daily intake of zinc for women is 12 mg/day, 15 mg/day for men, and in the range of 7 – 11 mg/day for children.⁹ Also it is present in plant, animal tissues and all living cells.¹

Zinc is obtained from food such as red meat, eggs, and fish, and low zinc amounts can be obtained from drinking water, fruits and white sugar. However, meat and offal are considered as the richest sources of zinc as shown in Table 2.^{8,11}

Table 2: Zinc content in typical food.⁸

Food groups	Average zinc content (mg/kg)	Food groups	Average zinc content (mg/kg)
Bread	9.8	Green vegetables	3.9
Cereals	9.9	Potatoes	3.3
Meat	52	Other vegetables	2.4
Offal	52	Canned vegetables	4.2
Meat products	25	Fresh fruit	0.85
Poultry	15	Fruit products	0.63
Fish	8.0	Beverages	0.14
Oil & fats	0.5	Milk	3.9
Eggs	13	Milk products	12
Sugars & preserves	5.5	Nuts	30

When zinc enters human body from food and other sources, it is absorbed by small intestine, then it is transported to tissues, or to blood plasma, the place where the zinc

is bound by albumins and globulins.¹⁰ Zinc in biological systems exists in two forms: bound zinc and chemically reactive Zn^{2+} , which is a part of zinc-binding proteins structural and molecules of cellular signaling pathway.¹¹

Zinc has many physiological roles divided into catalytic, structural, regulatory and perform once of many functions, such as:

(1) it is used as a cofactor and it is a part of hormonal complexes and many enzymes like lactate dehydrogenase, alcohol phosphatase, DNA and RNA polymerase, carbonic anhydrase and carboxy peptidase. These enzymes are important to carbon dioxide (CO_2) regulation and proteins digestion, such as carbonic anhydrase which is used to convert CO_2 to bicarbonate and vice versa, without this enzyme the conversion is difficult and slow. Carboxy peptidase enzyme helps in breaking down the peptide bonds during protein digestion.^{1,9-11} Figure 3 shows the structure of human carbonic anhydrase enzyme.

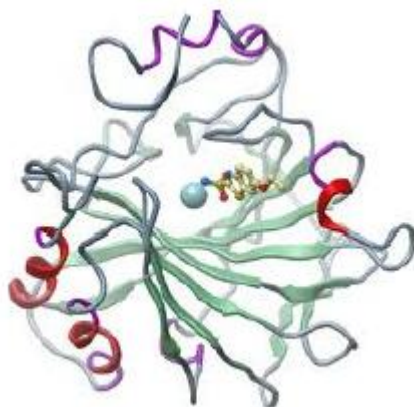


Figure 3: Diagram of human carbonic anhydrase, with Zn atom shown in the center.¹⁰

(2) It has a role in cell replication, cell division, gene expression and it is also used in nucleic acids, amino acids and cellular metabolism.

(3) It is used for protein synthesis, tissue repair, and wound healing because zinc speeds up the healing process after injury

(4) It plays an important role in immune function and zinc ions are effective antimicrobial agents even at low concentration.

(5) Finally, it plays a role in structural composition of zinc fingers, because zinc fingers form transcription factors, which are proteins that recognize DNA base sequences during the replication and transcription of DNA.^{1,10,11}

The deficiency of zinc causes many problems, such as impaired immune function, loss of appetite, hair loss, diarrhea, delayed sexual maturation, impotence, hypogonadism in males, growth retardation, weight loss, delayed healing of wounds, taste abnormalities and skin lesions.¹⁰

Zinc deficiency occurs due to inadequate zinc intake or absorption. Severe Zn deficiency depresses immune function and even mild to moderate degrees of zinc deficiency can impair macrophage, natural killer cell activity and complement activity. The body requires zinc to develop and activate T-lymphocytes.¹⁰

1.3 Zinc as an element:

Zinc has many characteristics that make it different from other elements, such as: it has a lustrous bluish-white color, it is the heaviest metal in first row of the transition elements, and it is among the most 23rd abundant elements in the Earths' crust.^{12,13}

Zinc belongs to group IIB with electronic shell is [Ar] 4s²3d¹⁰, atomic number 30, and its atomic mass is 65 amu. Zinc tends to lose two electrons and form Zn²⁺ ion, and it has five naturally occurring isotopes (⁶⁴Zn, ⁶⁶Zn, ⁶⁷Zn, ⁶⁸Zn, and ⁷⁰Zn). The major

isotopes are ^{64}Zn , ^{66}Zn and ^{68}Zn with percentages 48.6%, 27.9% and 18.8% respectively.^{8,13}

Zn^{2+} ion has a filled d orbital (d^{10}) and it functions as a Lewis acid by accepting two electrons, it does not participate in redox reactions which makes it stable ion in a biological medium since its potential is in constant flux. This ion is a cofactor metal for reaction which needs a redox-stable to play role as a Lewis acid-type catalyst. Since Zn^{2+} ion has filled d orbital (d^{10}), its ligand-field stabilization energy is zero in all geometries.¹⁴

1. 4 Bioactive chelating agents:

There are three types of oxygen, nitrogen and sulfur donors chelating agents: the condensation products of carbonyl compounds associated with primary amines which are **Schiff bases**. These bases are characterized as bidentate, tridentate, tetradentate and polydentate ligands. If these ligands contain functional groups such as -OH, -NH₂, -SH, they can form stable complexes with transition metal ions.¹⁵ Figure 4 shows examples of Schiff base ligands.

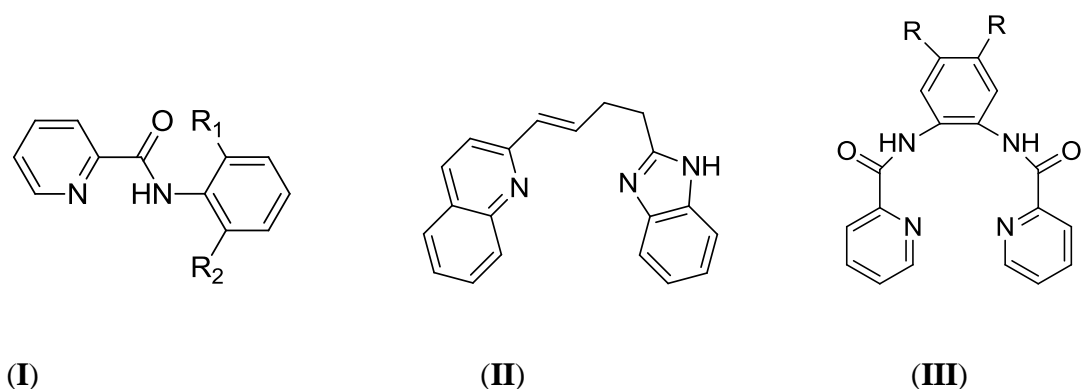


Figure 4: Few new classes of Schiff base ligands. (I) Bidentate ligand, (II) tridentate ligand (III) tetradentate ligand.

When the N-ligands are attached with metal ions, they form strong σ -donors but their π -character depends on the frameworks. In addition to N-, O-, S- and P-ligands also exist, where O-ligands classified as hard but S- and P- ligands are considered soft based on hard-soft acid base pearson's scale.^{15,16}

Schiff bases fall under the name of mixed donor ligands with at least two different functional groups which form bi- or polydentate ligands.^{15,16} The interaction of metal with monodentate and bidentate ligands to form complexes is shown in Figure 5.

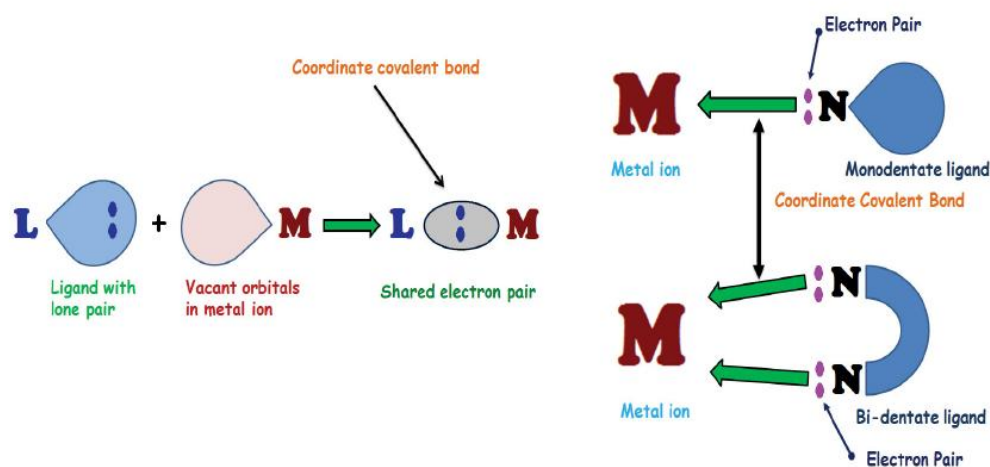


Figure 5: Formation of metal complexes through interaction with monodentate and bidentate ligands.¹⁵

Schiff ligands have wide range of applications due to their characteristics of anti-microbial, anti-tumor, anti-inflammatory, anti-tuberculosis, anti-cardiovascular, and anthelmintic activities.¹⁵

Amino acids, the second chelating agent, consist of a basic amino group (NH_2), acidic carboxyl group ($-\text{COOH}$) and unique R-group. Reduced forms of Schiff bases that contain different amino acid derivatives, are excellent ligands for the formation of multidimensional network structures. The amine ($-\text{NH}_2$) and carboxyl ($-\text{COOH}$) groups of the amino acids are responsible for their ability to act as coordinating

agents. The coordination activity of –SH groups toward heavy metal ions is more versatile when amino acids are present.¹⁵

Amino acids can be linked with (S, N), (N, O), or (S, O) donor atoms, so they act as ambidentate ligands. Amino acids containing negatively charged carboxylate group (COO^-) and positively charged group (-NH_3^+), are considered as ampholytes and can behave as acids or bases.¹⁵

In an organism, amino acids exist as free or bound; the bound amino acids are incorporated into proteins or other biochemical functional structures, whereas the free amino acid are formed as a result of modification of the known amino acids and these are called biogenic amines such as histamine, dopamine, ornithine, taurine, spermine and spermidine.¹⁵

Pyrazolones is another example of bioactive chelating agents. Pyrazolones consists of five membered lactam ring with two adjacent nitrogen atoms and a keto group (C=O) in the same molecule. These compounds have many applications in pharmaceutical fields because they are used as pharmaceutical ingredients particularly in non-steroidal anti-inflammatory drugs. Also they act as anticancer agents, anti-inflammatory, and for treatment of arthritis, and musculoskeletal disorder.¹⁵ In addition, pyrazolones can be used in the solvent extraction of metal ions, and as ligands in complexes with catalytic activity. Recently, many transition metal pyrazolone compounds have been synthesized and characterized.¹⁵ Figure 6 shows an example of pyrazolone ligand (1-phenyl-3-methyl-4-benzoylpyrazolone).

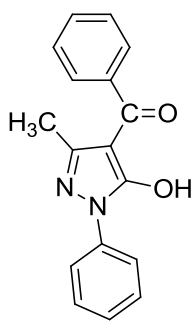


Figure 6: Example of pyrazolone ligand.

Nitrogen heterocycles are the most important ligands in coordination chemistry, they are used in organic and inorganic synthesis. Based on the nature of these ligands and the type of metal ion, anti-bacterial, anti-fungi, anti-microbial and anti-tumor agents were synthesized.^{15,17,18}

When these ligands contain more than two donor atoms or two or more aromatic nitrogen heterocycles into one molecule, they can form numerous chelating and bridging ligands. In addition, these ligands may contain more than one coordination site to link with metal centers. The bridging ligands stabilize the ability of chelation with multiple metal atoms through bidentate donor groups to form a five or six membered chelate ring leading to higher stability and potentially enhance the metal-metal interactions.¹⁵ The chemical structure of bioactive nitrogen heterocyclic compounds such as 1,10-phenanthroline, 2,9-dimethyl-1,10-phenanthroline, 2-aminopyridine, quinoline, 2-aminomethylpyridine, 2,2-bipyridine, 2-methylaminopyridine and 4,4-dipyridine are shown in Figure 7

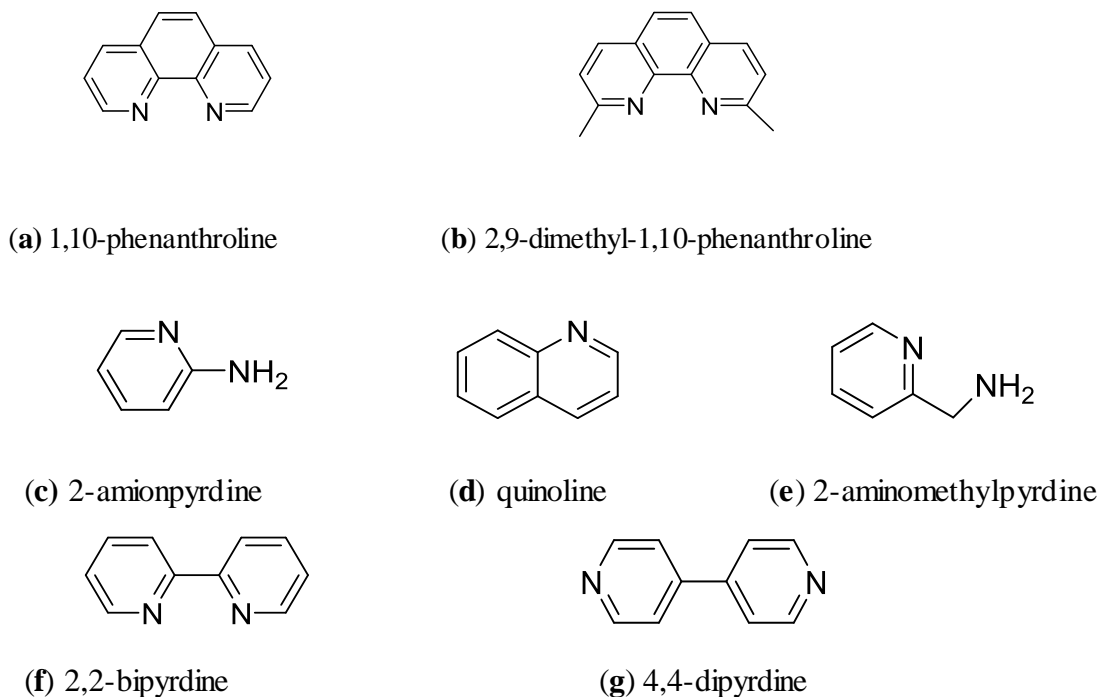


Figure 7: Chemical structures of bioactive ligands (nitrogen heterocyclic) used in the present work.

1,10-phenanthroline is an example of nitrogen heterocyclic and chelating bidentate ligand for metal ions. It has structural features which determine its coordination ability towards metal ions it is a rigid planer, hydrophobic, and its nitrogen is placed in a suitable environment to act cooperatively in cation binding.¹⁵

1,10-phenanthroline plays an important role in the coordination chemistry; it can be used as starting material for the preparation of organic and inorganic compounds. Because 1,10-phenanthroline is a heteroaromatic planer and hydrophobic, it is an appropriate ligand for DNA binding. In addition, it can form non-metal-based compounds which react with DNA to perform certain functions from simple DNA damage to stabilization of particular DNA structures. In addition, 1,10-phenanthroline prevent growth of a sarcoma-37 tumor and inhibits the cell proliferation of Ehrlich ascites.¹⁵

When a hydrophilic group of this chelating agent is masked by metal ions to form neutral compounds, the anti-tumor activity may be enhanced due to its easily entrance through cell membrane and behavior as carriers of antitumor agents.¹⁵

With first row transition metal cations, 1,10-phenanthroline can form octahedral complexes in aqueous solution of the type $[M(\text{Phen})(\text{H}_2\text{O})_4]^{2+}$, $[M(\text{Phen})_2(\text{H}_2\text{O})_2]^{2+}$, and $[M(\text{Phen})_3]^{2+}$. Figure 8 shows an X-ray for structure determination of Cu(II) complex containing 1,10-phenanthroline ligand.^{15,19}

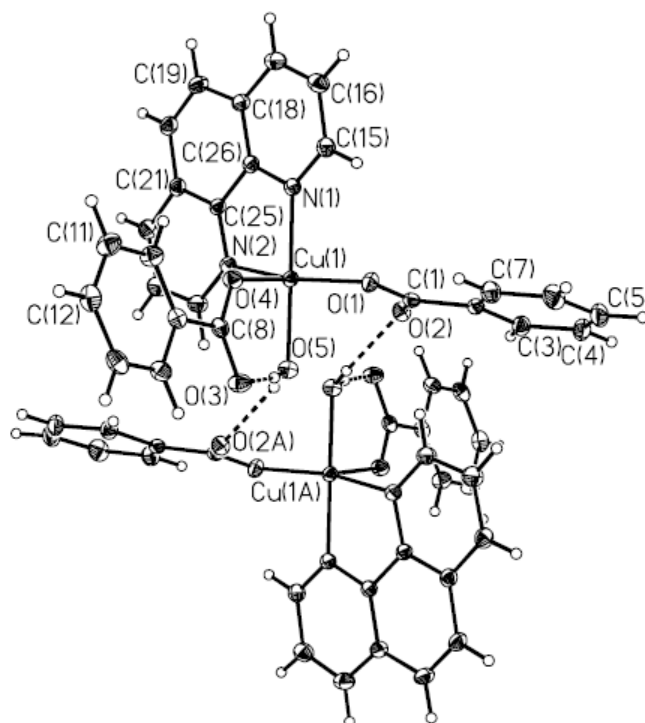


Figure 8: Ortep plot of $[\text{Cu}(\text{benzoic acid})_2(\text{phen})(\text{H}_2\text{O})]$.

Another example of nitrogen heterocyclic ligand is 2,2'-bipyridine, it which has been used since several decades as a chelating bridging ligands. This ligand has many applications in different fields especially in coordination chemistry. Because of its characteristics such as its robust redox stability and relative functionalization, its interconnection with metal centers was well defined spatial arrangements.¹⁵

1.5 Carboxylate and metal carboxylate chemistry:

In coordination chemistry, carboxylic acid complexes continue to receive great attention since the 19th century due to their ability to act as ligands and as anti-microbial agents in foods, drugs, anti-bacterial and anti-inflammatory drugs.^{20,21} Carboxylic acids can interact with metal ions and form a variety of metal-carboxylate complexes.²⁰ Recently, many transition metal carboxylate complexes have been prepared and have shown different applications which are commercially available, and cheap precursors in catalysts` synthesis.^{20,22,23} Figure 9 shows example of precursors (silver-trifluoroacetate)

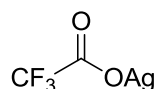


Figure 9: Structure of silver-trifluoroacetate precursor

There are different approaches for the preparation of metal carboxylates:

- (1) fusion method which depends on refluxing a metal or metal oxide, hydroxide, or carbonate with appropriate molar ratio of carboxylic acid.²³
- (2) Precipitation method, in which water soluble metal salts are treated with stoichiometric amounts of the desired carboxylic acid alkali salts in aqueous solution.²³
- (3) and reactions in non-aqueous media, this reaction is useful for the preparation of carboxylates of less electropositive metals.²³ The sol-gel method is used for electrochemical synthesis of transition metal carboxylates.²³

The binding of the carboxylate group with metal ions may increase the biological activities when compared to the free ligands.²³⁻²⁵ The carboxylate group binds with metal ions in different modes of interaction, such as:

- (1) ionic or uncoordinated: this mode is found in the carboxylate of highly electropositive elements such as sodium and potassium.
- (2) unidentate or monodentate coordination: this mode exist in lithium and cobalt acetate.
- (3) bidentate chelating coordinations, which is the least favored coordination mode; there are two types of this mode: (A) symmetrical and (B) asymmetrical bidentate.
- (4) the last coordination mode is the bidentate bridging mode which is the most favored interaction.

The structure of the carboxylate group, the nature of the solvent, the nature of ligand and metal ion are the key factors in determining the mode of interaction.²³⁻²⁵ Figure 10 shows the various binding modes of the carboxylate ligands.

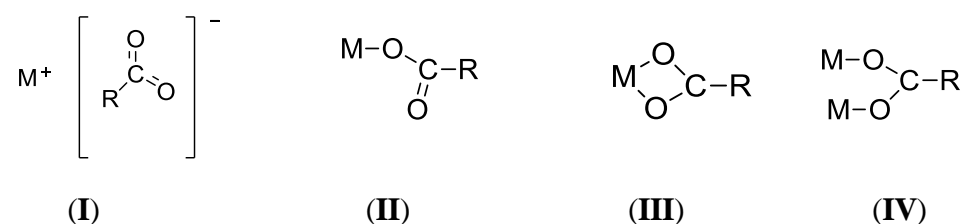


Figure 10: Binding modes of carboxylate ligands. (I) ionic mode, (II) monodentate mode, (III) bidentate chelating, and (IV) bidentate bridging.

There are four types of carboxylate bridging modes: anti-anti, syn-syn, anti-syn and monatomic bridge. Anti-anti, and anti-syn bridging form array of metallo-organo polymers. These polymers consist of the association of dimeric units with other dimeric units by bridging carboxylates. Syn-syn form clustered structures with metal-

metal bonds by bringing metal atoms close enough from each other. Poly-nuclear chromium(III) carboxylates are examples of this type. Figure 11 shows the four types of carboxylate bridges.²³

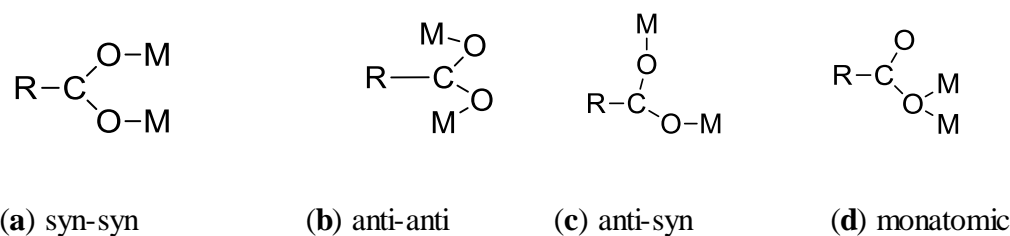


Figure 11: Carboxylate bridging modes.

The simple carboxylic acids contains keto functional group (C=O) which absorbs strongly in the 1760-1770 cm^{-1} region. In metal carboxylate compound, the C=O band appears as COO^- symmetrical or asymmetrical stretches. These peaks are formed because bond order of the two C-O groups in carboxylate are equal because of electron delocalization, the degree of interaction between cationic metal and carboxylate group effects on delocalization and the stretching frequencies of carboxylate ion.²³ The asymmetrical COO^- stretching mode appears as strong absorption in the range 1550-1620 cm^{-1} , while the symmetrical COO^- group appears as weaker absorption around 1400 cm^{-1} .

Infrared spectroscopy is one of the mostly used techniques to determine the type of coordination between metals and ligands based on differences between frequency of symmetrical and asymmetrical stretches of the COO^- groups ($\Delta\nu = \nu_{\text{asym}} - \nu_{\text{sym}}$) of the carboxylate group.^{23,25} Also the difference between the symmetric and asymmetric stretches for the carboxylate ion ($\Delta\nu_{\text{COO}^-}$) to determine binding mode in a carboxylate compound was proposed by Nakamoto and co-workers as a follow:

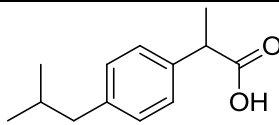
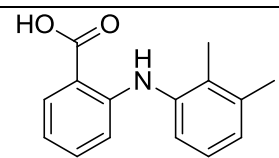
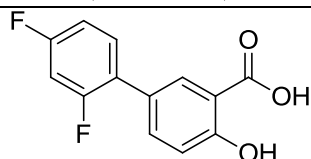
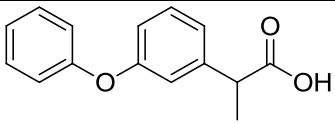
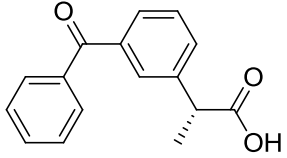
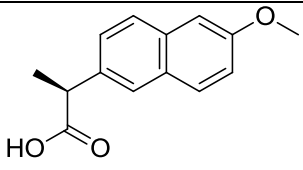
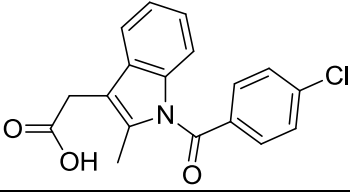
(1) If $\Delta v(\text{COO}^-)_{\text{complex}} \ll \Delta v(\text{COO}^-)_{\text{Na}}$, then the binding mode in a carboxylate compound is bidentate chelating.

(2) If $\Delta v(\text{COO}^-)_{\text{complex}} \approx \Delta v(\text{COO}^-)_{\text{Na}}$, then the binding mode is a carboxylate compound is bidentate bridging.

(3) If $\Delta v(\text{COO}^-)_{\text{complex}} \gg \Delta v(\text{COO}^-)_{\text{Na}}$, then the binding mode in a carboxylate compound is unidentate.

A group of chemically varied substances which have analgesic, anti-pyretic, and anti-inflammatory effects are called anti-inflammatory drugs. Examples of chemicals used in NSAIDs of the acid type with carboxyl functional group are salicylic acid, phenylalkanoic acids, oxicams and anthralinic acids. The most widely used NSAIDs involve ibuprofen, aspirin and paracetamol.²⁵ The anti-inflammatory activity of NSAIDs is derived from the inhibition of the conversion of arachidonic acid to prostaglandin which are the mediators of inflammatory processes. NSAIDs have many functions such as: they are potential inhibitors of cyclooxygenase in vivo and in vitro, they decrease the synthesis of prostaglandin, prostacyclin, and thromboxane. Table 3 shows some examples of non-steroid anti-inflammatory drugs of the acid type.²⁴

Table 3: Non-steroid anti-inflammatory drugs of the acid type.

Generic name	IUPAC name	Formula	Application
Ibuprofen	(RS)-2-(4-(2-methylpropyl)propanoic acid		Acute and chronic pain, osteoarthritis, rheumatoid arthritis
Mefenamic acid	2-(2,3-dimethylphenyl)aminobenzoic acid		Pain, including menstrual pain, migraine headaches
Diflunisal	2,4-difluoro-4-hydroxybi-phenyl-3-carboxylic acid		Prostaglandin production inhibition, an anti-pyretic
Fenoprofen	2-(3-phenoxyphenyl)propanoic acid		Rheumatoid arthritis, osteoarthritis, and mild to moderate pain
Ketoprofen	(RS)-2-(3-benzoyl phenyl) propanoic acid		Analgesic and anti-pyretic effects
Naproxen	(+)-(S)-2-(6-methoxynaphthalen-2-yl) propanoic acid		For relief of a wide variety of pain, fever, inflammations, stiffness
Indomethacin	2-{1-[(4-chlorophenyl)carbonyl] 5-methoxy-2-methyl-1H-indol-3-yl}		To reduce fever, pain, stiffness, and swelling

1.6 Zinc carboxylates:

Zinc carboxylates have been studied because of their wide applications in biochemical systems, catalysis, separation, sorption, non-linear optical properties and material chemistry. This may be due to the diversity of the COO^- moiety and the wide range of coordination modes that the carboxylate group can bind with metal ions. Recently, many zinc carboxylate compounds with various biological activities have been synthesized and fully characterized. For example zinc acetylsalicylate was used as anti-inflammatory agent and 3-aminobenzoic acid zinc complex which was used to inhibit the carcinogenic effect of N-2-fluorenyl acetamide which is responsible for liver tumor in animals. Ibuprofen and 2,2-bipyridine zinc compounds showed anti-bacterial activity and zinc methoxyacetic acid with 1,10-phenanthroline complex also showed anti-bacterial activity.²⁶⁻³⁰ Figure 12 shows an X-ray structure of Zn(II) complex containing methoxyacetic acid and 1,10-phenanthroline ligand.

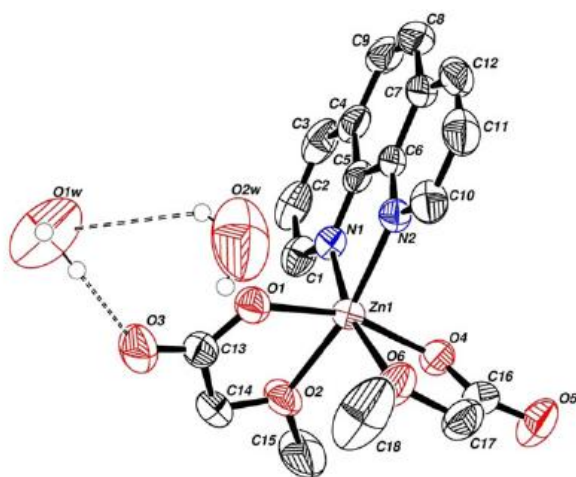


Figure 12: Molecular structure of $\text{Zn}(\text{methoxy})_2$ 1,10-phenanthroline.³⁰

1.7 Furosemide:

Furosemide 4-chloro-N-furfuryl-5-sulphamoylanthranilic acid or 5-(aminosulfonyl)-4-chloro-2-[2-furanylmethylamino] benzoic acid, also commercially known as lasix is a white microcrystalline powder.³² Furosemide is slightly soluble in water, chloroform, ethanol, and diethyl ether, but it is soluble in acetone, methanol, and dimethyl formamide. Furosemide is soluble in aqueous solutions with a pH above 8.³¹⁻

³³ Figure 13 shows the structure of furosemide

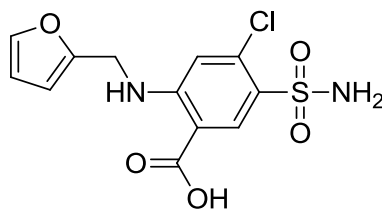


Figure 13: The chemical structure of Furosemide.

Furosemide is extensively used in human and veterinary medicine as a potent diuretic. Furosemide inhibits the electrolyte absorption in the loop of Henle, therefore it is effective for persons who do not respond to thiazide diuretics. In addition, it can be used in the treatment of edema associated with congestive heart failure and hypertension, oliguria, and asthma. In addition, furosemide and other diuretic agents showed *in vitro* anti-oxidant activities.³¹⁻³⁶

The normal oral dose is from 20-80 mg/day, but certain cases may require higher doses up to 600 mg/day. Furosemide is also administered intravenously at 40-80 mg/day.³³ Higher dosage of furosemide can affect the fluid and electrolyte balance causing side effects such as hyponatremia, hypokalemia and hypochloremic alkalosis.³⁵

1.7.1 Furosemide metal complexes:

When metals interact with ligands containing $-\text{SO}_2$ and NH_2 groups such as furosemide, the obtained complexes indicate interesting chemical, structural, pharmaceutical, and biological properties.³⁷ Silver, copper, zinc and iron are metals which form complexes with furosemide for different purposes, silver-furosemide complexes showed anti-bacterial activity against Gram-positive such as *Staphylococcus aureus* and Gram negative such as *Escherichia coli* and *Pseudomonas aeruginosa*.³⁸

To detect the presence of furosemide in tablets, pharmaceutical preparation, plasma, and urine, spectrophotometric methods were used through the complexation of this drug with copper (II), the reaction of furosemide with Fe(III) chloride was also used for the determination of furosemide content.³⁹⁻⁴¹ Figure 14 shows X-ray of copper-furosemide complex.

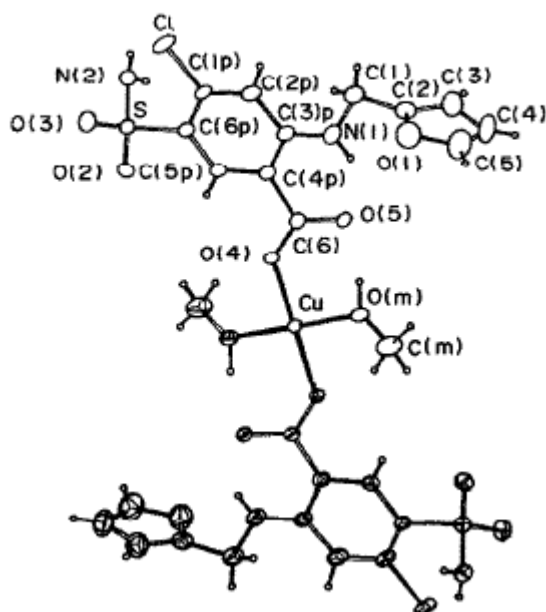


Figure 14: Molecular structure of $\text{Cu}(\text{furosemide})_2 \cdot 2\text{MeOH}$.⁴⁰

Zn(II) with 1,4-bis(imidazol-1-ylmethyl)benzene and furosemide complex demonstrated fluorescence properties` changes in which the fluorescence intensity increases with increasing furosemide. Based on this, a spectro-fluorometric method was developed to determine the furosemide contents in tablets, this method showed many advantages such as simplicity, rapidity, and sensitivity.⁴²

In the present work zinc(II)-furosemide complex was prepared and reacted with different nitrogen based ligands, the new complexes were characterized using various techniques, and their biological activities were tested and studied.

1.8 Bis-(4-nitrophenyl) phosphate hydrolysis:

Phosphate esters play different important roles in biological processes, such as information storage and utilization of (DNA/RNA), cellular signaling communication and energy transduction (ATP). Figure 15 shows structure of ATP. In addition, phosphate esters have been used as pesticides for many decades.^{43,44} Despite of their positive impacts, phosphate esters can be harmful effects to humans.⁴³

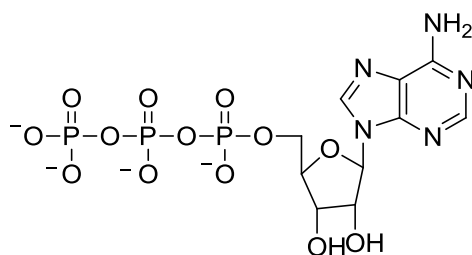


Figure 15: Structure of ATP.

Hydrolysis of phosphate esters have essential roles in nature, biological processes and in chemistry and in biochemistry fields.^{45,46} Bis-p-nitrophenyl phosphate (BNPP) is a type of phosphodiester compound that can be used as an example to study the cleavage or the formation of P-O bonds, but the hydrolysis of this compound and

other types of phosphate esters is difficult and complicated because these compounds are highly stable and have high resistance to undergo hydrolytic cleavage. The BNPP molecule has half life time ($t_{1/2}$) of 2000 years in water at 20 °C and 53 years in water at 50 °C.^{43,47,48} Figure 16 shows the structure of BNPP.

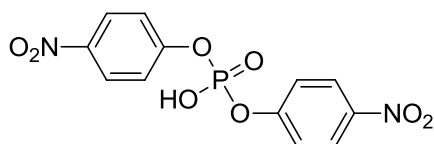


Figure 16: Structure of BNPP.

Because of the high stability of these compounds, scientists developed highly reactive artificial enzymes that speed up the hydrolysis of phosphate esters under physiological conditions.^{44,47,49} Many studies in recent decades have shown that Mn(III), Cu(II), Zn(II), Ni(II), Fe(III), Co(III) and Ln(III) metal complexes with Schiff base ligands can act as potent catalysts to hydrolyse the phosphate esters rapidly. These metal ions may perform many functions such as activation of the phosphate group and a nucleophilic molecule and stabilizing the penta-coordinate phosphorus transition state by cooperative action in metalloenzymes.^{47,48,50,51} [Fe(II) EDTA] and [Cu(I) (1,10-phenanthroline)₂] are examples of redox active coordination complexes that are able to cleave the phosphate diester bonds at neutral pH and ambient temperature.⁴⁴ Figure 17 shows the structure of [Cu(I) (phen)₂].

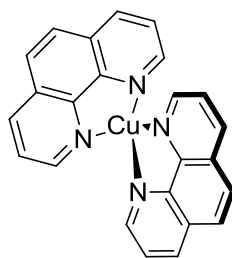


Figure 17: Oxidative cleavage agent [Cu(phen)₂]⁺.

Metallo-enzymatic model systems consisting of phosphate monoesterases, diesterases, and triesterases have shown high catalytic activity and selectivity due to their high Lewis acidity and as a result, these enzymes can be activated by two or more metal ions.^{46,49} The lanthanide ion and its compounds play important roles when compared to other metal complexes due to their Lewis acidity, higher oxidation state, and high ligand exchange rates.⁴⁸ These properties make lanthanide ions act as catalytic centers in the development of artificial enzymes.⁴⁸

The suggested mechanism of action of the metal complexes that act as enzymes to speed up the rate of hydrolysis of the phosphate diester depend on the intramolecular attack of a nucleophilic group on the positive phosphorus atom.⁴⁶

The proposed mechanism of BNPP catalytic cleavage is shown in Figure 18. The first step is the deprotonation of metal-water complex to form aqua-hydroxide active complex **A**. Next, BNPP coordinates with complex **A** to form the catalyst-substrate complex (C-S) which is active enough to convert an intermolecular reaction to intramolecular one as indicated in step I of Figure 18. In the Third step, the metal (Mn(III))-hydroxide anion (base) attacks the positive phosphorus atom (Lewis acid) in BNPP to release one of the p-nitrophenolate anion (first order rate constant (k)). This step (II) is the rate determining step. Finally, the product from BNPP hydrolysis in step (II) of Figure 18 (p-nitrophenyl phosphate (NPP)) is used to release another p-nitrophenolate anion rapidly to form active complex **A** (step (III)), and the catalysis will start again and continue.⁴⁶

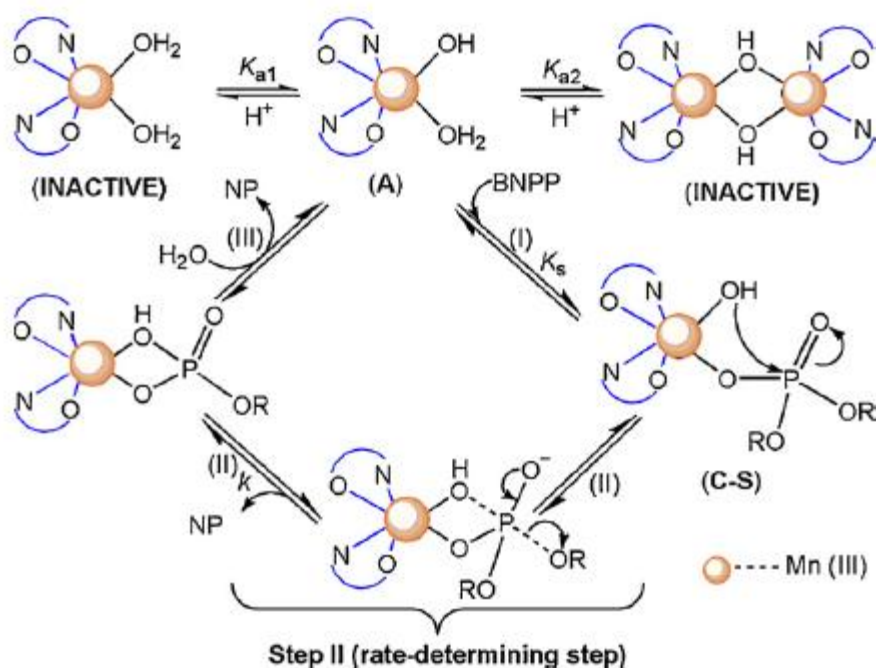


Figure 18: Proposed mechanism of the BNPP catalytic cleavage.⁴⁶

1.9 Anti-bacterial activity:

Many infectious diseases that are caused by microorganisms resistant to current antibiotics, have killed a considerable number of humans. Throughout the years, researchers discovered new compounds which have antimicrobial activities and still they are trying their best to prepare new specific and selective anti-bacterial agents.^{52,53}

The treatment from infectious diseases caused by different pathogens is an important and challenging problem, so medical microbiology is used to study the prevention and treatment of diseases which are caused by micro-organisms. This area of medical science has sub-disciplines such as virology, bacteriology, mycology, phycology, and protozoology. Anti-microbial agents work as preventers or inhibitors of many diseases caused by different microorganisms.^{54,55}

Anti-microbial agents are classified into three main groups based on their applications and spectrum activities:

(1) Antibiotics and chemically synthesized chemotherapeutic agents, these antibiotics formed by micro-organisms or chemically synthesized and they may be of microbial origin, semi-synthetic, or synthetic such as sulfonamides, nitrofurans, 4-quinoline anti-bacterials, and imidazole derivatives.⁵⁴

(2) Non-antibiotics chemotherapeutic agents (disinfectants, antiseptics, and preservatives), such as acids, alcohols and related compounds, iodine, and heavy metals (silver, copper, mercury and zinc).⁵⁴

(3) and immunological products such as vaccines, and monoclonal antibodies.⁵⁴

Researchers have found that complexes which formed from interaction between metal ions and ligands enhanced anti-microbial activity compared to their free ligands. Moreover, metal ions play an important role during the biological process of drug utilization in the body.^{52,56} The complex containing Cu(II) metal ion and the pyridazine ligand, and complexes of (Cu(II), Ni(II), Co(II), and Ag(I)) metal ions with sulfamethoxypyridazine ligand showed enhanced anti-inflammatory and anti-microbial activity against Gram-positive bacteria.⁵⁷

The first effective chemotherapeutic agents are called sulfonamides and are used for the prevention and cure of bacterial infections in humans. They are used as anti-bacterial agents. N-substituted sulfonamides are among the most anti-bacterial agents used worldwide because of their properties such as low cost, low toxicity, and excellent activity against bacterial diseases.⁵³ Copper with five membered

heterocyclic sulfonamides such as $[\text{Cu}(\text{L})_2]\cdot\text{H}_2\text{O}$, and $[\text{Cu}(\text{L})_2(\text{H}_2\text{O})_4]\cdot n\text{H}_2\text{O}$ have antibacterial activity compared to the free sulfonamides.⁵³

1.10 Aim of the research:

The main goal of the current research is to synthesize and characterize new zinc furosemide complexes with different nitrogen based ligands using 1,10-phenanthroline, 2-aminopyridine, 2-aminomethylpyridine, 2,2-bipyridine, 4,4-dipyridyl, 2,9-dimethyl-1,10-phenanthroline, and quinoline. The general formula of the prepared complexes is: $[\text{Zn}_n(\text{Furosemide})_m(\text{L})_z]$, ($n = 1, 2, \dots$; $m = 1, 2, \dots$; $Z = 1, 2, \dots$).

The formula and the structure of each of the prepared complexes will be determined using different techniques including IR, UV-Vis, $^1\text{H-NMR}$, $^{13}\text{C-NMR}$, LC/MS, and single crystal X-ray diffraction. The prepared complexes will be tested for their biological activity and their BNPP hydrolysis application.

2. Experimental:

2.1 Chemicals and reagents:

Chemicals, reagents and solvents used in this work were purchased from commercial sources without any further purification (analytical reagent grade). All types of bacteria (*Escherichia coli*, *Staphylococcus aureus*, *Bacillus subtilis*, *Proteus mirabilis*, *Pseudomonas aeruginosa* and *Staphylococcus epidermidis*) were obtained from Biology and Biochemistry Department at Birzeit University.

2.2 Instrumentations:

IR spectra for the compounds were measured using a Bruker TENSOR II in the 200-4000 cm^{-1} region. Agilent 8453 photodiode array spectrophotometer was used to obtain UV-Vis spectra of the complexes and their parent ligands in the 200-800 nm region using MeOH as a solvent. Melting points were measured using Electrothermal melting point apparatus. NMR spectra were recorded on Varian Unity Spectrometer operating at 300 MHz for ^1H and 75 MHz for ^{13}C nucleus.

2.3 Synthesis and characterization of zinc furosemide complexes:

All zinc furosemide complexes were prepared at room temperature.

2.3.1 Synthesis of $[\text{Zn}(\text{furo})_2(\text{MeOH})_2]$ (1):

Sodium hydroxide (37.4 mmol, 1.5 g) was added with stirring to furosemide (37.4 mmol, 12.4 g) in 180 ml MeOH. Then zinc chloride was added (18.7 mmol, 2.5 g) to the previous solution and the whole mixture was stirred for 3.5 h. Then the solvent was evaporated in air and the product was extracted by dichloromethane and ethyl ether. The dichloromethane and ether were evaporated, then the product was washed with petroleum ether to give yellow solid.

$[\text{Zn}(\text{C}_{12}\text{H}_{10}\text{ClN}_2\text{O}_5\text{S})_2(\text{CH}_3\text{OH})_2]$ (1). 77 % yield; m.p. = 182 °C (d); ^1H NMR (CDCl_3): δ (ppm) 4.43 (d, 2H, CH_2 , $^3J_{\text{H-H}} = 5.7$ Hz), 6.30 (d, 1H, CH), 6.36 (t, 1H, CH), 6.82 (s, 1H, CH), 7.14 (NH_2), 7.56 (d, 1H, CH), 8.45 (s, 1H, CH), 9.60 (NH); $^{13}\text{C}\{^1\text{H}\}$ -NMR (CDCl_3): δ (ppm) 39.08 (CH_2), 107.68 (CH), 110.88 (CH), 112.53 (CH), 113.72 (CH), 126.17 (CH), 133.88 (C), 134.03 (C), 142.88 (C), 152.38 (CH), 152.57 (C), 170.78(C=O); IR(cm^{-1}): 3303, 1605, 1556, 1498, 1423, 1382, 1299, 1159,

1071, 1011, 945, 803, 738, 583, 514, 388, 270; UV-Vis (MeOH, λ (nm)): 229, 275;
ESI m/z: 787 [M+H]⁺.

2.3.2 Synthesis of [Zn(furo)₂(2-ampy)₂] (2):

Zn-furo (2.7 mmol, 2.0 g) was dissolved in 35 ml MeOH (soluble) and 2-ampy (5.5 mmol, 0.5 g) dissolved in minimum amount of MeOH was added to the zn-furo solution with stirring, then the clear reaction mixture was stirred for additional 3.5 h, the solution was evaporated then ethyl ether and petroleum ether were added and evaporated to form solid product.

[Zn(C₁₂H₁₀ClN₂O₅S)₂(H₂NC₅H₄N)₂] (2). 45 % yield; m.p. = 185-190 °C (d); ¹H NMR (CDCl₃): δ (ppm) 4.42 (d, 2H, CH₂), 6.02 (NH₂), 6.29 (d, 1H, CH), 6.36 (t, 1H, CH), 6.44 (t, 1H, CH, ³J_{H-H} = 6.6 Hz), 6.47 (d, 1H, CH, ³J_{H-H} = 6), 6.80 (s, 1H, CH), 7.36 (t, 1H, CH, ³J_{H-H} = 7.6 Hz), 7.56 (d, 1H, CH), 7.89 (d, 1H, CH, ³J_{H-H} = 4.5 Hz), 8.44 (s, 1H, CH), 9.80 (NH); ¹³C{¹H}-NMR(CDCl₃): δ (ppm) 39.08 (CH₂), 107.63 (CH), 108.91 (CH), 110.88 (CH), 112.18 (CH), 112.32 (CH), 126.03 (CH), 134.06 (C), 137.83 (C), 142.85 (C), 147.86 (CH), 152.48 (CH), 152.62 (C), 160.10 (C), 170.63 (C=O); IR (cm⁻¹): 3568, 3322, 3223, 1607, 1560, 1496, 1447, 1374, 1298, 1262, 1150, 976, 942, 803, 770, 737, 686, 582, 520, 474, 334; UV-Vis (MeOH, λ (nm)): 230, 276; ESI m/z: 911 [M+H]⁺.

2.3.3 Synthesis of [Zn(furo)₂(2-ammepy)₂] (3):

Zn-furo (2.7 mmol, 2.0 g) was dissolved in 35 ml MeOH, then 2-ammepy (10.9 mmol, 1.3 g) dissolved in minimum amount of MeOH was added with stirring to the previous solution. The clear reaction mixture was formed and was stirred for additional 3.5 h, the solution was then evaporated, ethyl ether and petroleum ether were added and evaporated to give the desired solid product.

[Zn(C₁₂H₁₀ClN₂O₅S)₂(C₆H₈N₂)₂] (3). 28 % yield; m.p. = 140-145°C; ¹H-NMR (DMSO, δ): 4.03 (s, 2H, CH₂), 4.40 (d, 2H, CH₂, ³J_{H-H} = 5.1 Hz), 6.30 (d, 1H, CH), 6.38 (t, 1H, CH), 6.75 (s, 1H, CH), 7.38 (t, 1H, CH, ³J_{H-H} = 11.7 Hz), 7.49 (d, 1H, CH, ³J_{H-H} = 7.8 Hz), 7.58 (d, 1H, CH), 7.86 (t, 1H, CH, ³J_{H-H} = 7.8 Hz), 8.41 (s, 1H, CH), 8.51 (d, 1H, CH, ³J_{H-H} = 3.9 Hz), 10.19 (NH₂); ¹³C{¹H}-NMR (DMSO, δ): 39.08 (CH₂), 44.43 (CH₂), 107.57 (CH), 110.90 (CH), 111.95 (CH), 117.96 (CH), 122.81 (CH), 123.47 (CH), 125.82 (CH), 132.95 (C), 133.80 (C), 138.47 (CH), 142.87 (C), 148.38 (CH), 152.65 (CH), 152.74 (C), 156.02 (C), 170.58 (C=O); IR (cm⁻¹): 3259, 2933, 2075, 1604, 1549, 1497, 1440, 1364, 1295, 1262, 1138, 943, 817, 744, 712, 683, 629, 577, 495, 408, 333, 281, 225; UV-Vis (MeOH, λ (nm)): 229, 274; ESI m/z: 940 [M+H]⁺.

2.3.4 Synthesis of [Zn(furo)₂(H₂O)(2,2-bipy)] (4):

Compound (1) (2.7 mmol, 2.0 g) was dissolved in 35 ml MeOH and 2,2-bipy (2.7 mmol, 0.4 g) dissolved in minimum amount of MeOH were mixed with stirring, then the clear reaction mixture was formed and was stirred for additional 3.5 h, the solvent was evaporated to give a solid product. Recrystallization of the complex from MeOH by slow evaporation gave single crystals suitable for X-ray determination.

[Zn(C₁₂H₁₀ClN₂O₅S)₂(H₂O)(C₁₀H₈N₂)] (4). 51 % yield; m.p. = 226-229 °C; ¹H NMR (CDCl₃): δ (ppm) 4.42 (d, 2H, CH₂, ³J_{H-H} = 5.4), 6.27 (d, 1H, CH, ³J_{H-H} = 3.0 Hz), 6.35 (t, 1H, CH, ³J_{H-H} = 4.2 Hz), 6.84 (s, 1H, CH), 7.16 (NH₂), 7.57 (t, 1H, 2CH), 8.09 (t, 1H, 2CH), 8.46 (s, 1H, CH), 8.50 (d, 1H, 2CH, ³J_{H-H} = 7.2 Hz), 8.74 (d, 1H, 2CH, ³J_{H-H} = 3.6 Hz), 9.49 (NH); ¹³C{¹H}-NMR (CDCl₃): δ (ppm) 39.08 (CH₂), 107.69 (CH), 110.90 (CH), 112.67 (CH), 115.26 (CH), 121.72 (2CH), 126.26 (CH), 134.08 (C), 134.21 (C), 142.88 (C), 149.49 (2CH), 152.33 (CH), 152.54 (C), 171.09 (C=O); IR(cm⁻¹): 3467, 3265, 3117, 1607, 1553, 1496, 1437, 1382, 1306, 1265, 1151, 1066, 1017, 970, 947, 902, 834, 807, 755, 687, 625, 585, 510, 478, 386; UV-Vis (MeOH, λ (nm)): 230, 276; ESI m/z: 901 [M+H]⁺.

2.3.5 Synthesis of [Zn(furo)₂(H₂O)(4,4-dipy)] (5):

Compound (1) (2.7 mmol, 2.0 g) was dissolved in 35 ml MeOH and 4,4-dipy (2.7 mmol, 0.4 g) dissolved in minimum amount of MeOH were mixed with stirring, then the clear reaction mixture was formed and was stirred for additional 3.5 h, the solvent was evaporated to give a solid product.

[Zn(C₁₂H₁₀ClN₂O₅S)₂(H₂O)(C₁₀H₈N₂)] (5). 58 % yield; m.p. = 201-202 °C; ¹H NMR (CDCl₃): δ (ppm) 4.46 (d, 2H, CH₂, ³J_{H-H} = 4.8), 6.31 (d, 1H, CH), 6.36 (t, 1H, CH), 6.88 (s, 1H, CH), 7.20 (NH₂), 7.56 (d, 1H, CH), 7.87 (d, 1H, 4CH, ³J_{H-H} = 4.2), 8.48 (s, 1H, CH), 8.74 (d, 1H, 4CH, ³J_{H-H} = 3.6), 9.35 (NH); ¹³C{¹H}-NMR (CDCl₃): δ (ppm) 39.08 (CH₂), 107.74 (CH), 110.91 (CH), 112.85 (CH), 122.02 (4CH), 126.42 (CH), 134.35 (C), 141.23 (C), 142.94 (C), 145.10 (2C), 150.88 (4CH), 152.22 (CH), 152.53 (C); IR (cm⁻¹): 3260, 1608, 1559, 1497, 1415, 1372, 1307, 1265, 1159, 1070,

945, 806, 739, 686, 628, 580, 511; UV-Vis (MeOH, λ (nm)): 228, 275; ESI m/z: 901 [M+H]⁺.

2.3.6 Synthesis of [Zn(furo)₂(1,10-phen)] (6):

Compound (1) (2.7 mmol, 2.0 g) was dissolved in 35 ml MeOH and 1,10-phen (2.7 mmol, 0.5 g) dissolved in minimum amount of MeOH were mixed with stirring and the reaction mixture was stirred for additional 3.5 h, the solvent was evaporated to give solid product.

[Zn(C₁₂H₁₀ClN₂O₅S)₂(C₁₂H₈N₂)] (6). 49 % yield; m.p. 191-192 °C; ¹H NMR (CDCl₃): δ (ppm) 4.38 (s, 2H, CH₂, ³J_{H-H} = 5.7 Hz), 6.28 (d, 1H, CH, ³J_{H-H} = 3 Hz), 6.37 (t, 1H, CH), 6.74 (s, 1H, CH), 7.09 (NH₂), 7.57 (d, 1H, CH), 7.90 (t, 1H, 2CH, ³J_{H-H} = 6.1 Hz), 8.14 (d, 1H, 2CH), 8.42 (s, 1H, CH), 8.70 (d, 1H, 2CH, ³J_{H-H} = 7.5 Hz), 8.99 (d, 1H, 2CH), 10.22 (NH); ¹³C{¹H}-NMR (CDCl₃): δ (ppm) 39.08 (CH₂), 107.57 (CH), 110.88 (CH), 111.92 (CH), 118.11 (CH), 125.06 (2CH), 125.79 (CH), 127.38 (2CH), 129.04 (2C), 132.90 (C), 133.79 (C), 141.23 (2C), 142.85 (C), 149.90 (2CH), 152.63 (CH), 152.73 (C), 170.51 (C=O); IR (cm⁻¹): 3569, 3317, 3224, 3077, 1604, 1555, 1501, 1421, 1371, 1309, 1262, 1152, 1011, 941, 805, 724, 577, 532, 473, 333; UV-Vis (MeOH, λ (nm)): 229, 272; ESI m/z: 903 [M+H]⁺.

2.3.7 Synthesis of [Zn(furo)₂(2,9-dmp)] (7):

Compound (1) (2.7 mmol, 2.0 g) was dissolved in 35 ml MeOH and 2,9-dmp (2.7 mmol, 0.57 g) dissolved in minimum amount of MeOH were mixed with stirring, then the reaction mixture was formed and was stirred for additional 3.5 h, the solvent was evaporated to give solid product.

[Zn(C₁₂H₁₀ClN₂O₅S)₂(C₁₄H₁₂N₂)] (7). 32 % yield; m.p. = 261-265 °C (d); ¹H NMR (CDCl₃): δ (ppm) 2.49 (s, 3H, 2CH₃), 4.44 (d, 2H, CH₂, ³J_{H-H} = 5.4 Hz), 6.28 (d, 1H, CH), 6.36 (t, 1H, CH), 6.90 (s, 1H, CH), 7.23 (NH₂), 7.55 (d, 1H, CH), 8.05 (d, 1H, 2CH, ³J_{H-H} = 8.4 Hz), 8.14 (d, 1H, 2CH), 8.49 (s, 1H, CH), 8.80 (d, 1H, 2CH, ³J_{H-H} = 8.4 Hz), 8.89 (NH); ¹³C{¹H}-NMR (CDCl₃): δ (ppm) 24.67 (2CH₃), 39.08 (CH₂), 107.89 (CH), 110.93 (CH), 113.25 (CH), 126.66 (2CH), 126.83 (CH), 127.41 (2CH), 134.55 (C), 135.27 (C), 139.48 (2CH), 141.23 (C), 143.05 (2C), 152.92 (CH), 152.42 (C), 158.16 (2C), 170.26 (C=O); IR (cm⁻¹): 3398, 3313, 3222, 3072, 1628, 1585, 1499, 1420, 1350, 1257, 1165, 1071, 1008, 962, 925, 863, 758, 688, 617, 583, 550, 520, 410, 326, 266; UV-Vis (MeOH, λ (nm)): 229, 275; ESI m/z: 931 [M+H]⁺.

2.3.8 Synthesis of [Zn(furo)₂(quin)₂] (8):

Compound (1) (2.7 mmol, 2.0g) was dissolved in 35 ml MeOH and quino (11.1 mmol, 1.4 g) dissolved in minimum amount of MeOH were mixed with stirring, then the reaction mixture was stirred for additional 3.5 h, the solvent was evaporated then ethyl ether and petroleum ether were added and evaporated to form solid product.

[Zn(C₁₂H₁₀ClN₂O₅S)₂(C₉H₇N)₂] (8). 92 % yield; m.p. = 198-199 °C; ¹H NMR (DMSO): δ (ppm) 4.45 (d, 2H, CH₂, ³J_{H-H} = 4.5 Hz), 6.33 (d, 1H, CH), 6.36 (t, 1H, CH), 6.87 (s, 1H, CH), 7.21 (NH₂), 7.58 (m, 1H, 2CH), 7.77 (m, 1H, 2CH), 8.01 (m, 1H, 2CH), 8.37 (d, 1H, CH, ³J_{H-H} = 8.1 Hz), 8.50 (NH); ¹³C{¹H}-NMR (CDCl₃): δ (ppm) 39.08 (CH₂), 107.74 (CH), 110.91 (CH), 112.79 (CH), 121.94 (CH), 126.37 (CH), 127.04 (CH), 128.38 (C), 129.33 (C), 130.00 (2CH), 134.34 (CH), 136.55 (CH), 141.23 (C), 142.91(C), 148.12 (C), 151.03 (CH), 152.28 (CH), 152.56 (C), 171.16 (C=O); IR (cm⁻¹): 3282, 3055, 2917, 1611, 1557, 1501, 1379, 1301, 1261,

1153, 1079, 945, 806, 732, 688, 584, 549, 516, 478, 386, 280; UV-Vis (MeOH, λ (nm)): 204, 225; ESI m/z: 981 [M+H]⁺.

2.4 X-ray single crystal diffraction:

Single crystal X-ray diffraction of compound (4) was attached to a glass fiber, with epoxy glue. The measurements of this single crystal were performed on a Bruker SMART APEX CCD X-ray diffractometer system. The crystal which was attached to a glass fiber to -150 °C and mounted on the three-circle goniometer with χ fixed at +54.76°, was done by a Bruker KRYOFLEX nitrogen cryostat. The system is equipped with a graphite monochromator and it was controlled by a Pentium-based (PC) used for running the SMART software package. This graphite monochromator appeared on a phosphor screen at -44°C which was held at 6.0 cm from the crystal. After data collection at room temperature (rt) using Mo- k_{α} radiation at $\lambda = 0.71073 \text{ \AA}$ and detector array of 512 * 512 Pixels (Pixel size is 120 μm), the raw data frames were transferred rapidly to a second PC computer for integration and reduction by the SAINT program package (SAINT-NT V5.0, BRUKER AXS GMBH, D-76181 Karlsruhe). To update the background frame information, following equation was used: $B' = (7B+C)/8$

Where B' is the updated pixel value, B is the background pixel value before updating and C is the pixel value through the current frame.⁵⁸ Finally, the SHELXTL software package was used to solve and refine the structure.⁵⁸⁻⁶² Crystal data and structure refinements are shown in Table 4.

Table 4: Crystal data and structure refinements for complex **4**.

Property	Complex 4
Empirical formula	C ₃₅ H ₃₄ Cl ₂ N ₆ O ₁₂ S ₂ Zn
Formula weight	931.07
Temperature	293(1) K
Wavelength	0.71073 Å
Crystal system	Triclinic
Space group	P-1
Unit cell dimensions	a = 11.632(2) Å α = 94.742(3)° b = 12.104(2) Å β = 104.071(3)° c = 15.572(3) Å γ = 108.523(3)°
Volume	1985.7(6) Å ³
Z	2
Density (calculated)	1.557 Mg/m ³
Absorption coefficient	0.928 mm ⁻¹
F(000)	956
Crystal size	0.49 x 0.29 x 0.27 mm ³
Theta range for data collection	2.13 to 27.00°
Index ranges	-14<=h<=14, -15<=k<=15, -19<=l<=19
Reflections collected	21179
Independent reflections	8415 [R(int) = 0.0223]
Completeness to theta = 27.00°	97.0%
Absorption correction	Semi-empirical from equivalents
Max. and Min. transmission	0.7878 and 0.6592
Refinement method	Full-matrix least-squares on F ²
Data/restraints/parameters	8415/0/532
Goodness-of-fit on F ²	1.004
Final R indices [I>2sigma(I)]	R ₁ = 0.0475, wR ₂ = 0.1197
R indices (all data)	R1 = 0.0537, wR2 = 0.1246
Largest diff. peak and hole	0.902 and -0.417e.Å ³

2.5 Anti-bacterial activity:

Three gram negative bacteria (*Escherichia coli*, *Proteus mirabilis*, and *Pseudomonas aeruginosa*) and three gram positive bacteria (*Staphylococcus aureus*, *Bacillus subtilis*, and *Staphylococcus epidermidis*) were used to test anti-bacterial activities of the new zinc complexes.

Agar diffusion method was used to test anti-bacterial activities of complexes (1-8) *in vitro*. The sterile saline solution was formed by dissolving 0.5 g of NaCl in 500 ml of water (0.9% of NaCl), then the solution was autoclaved. The saline solution was used to dissolve single bacterial colonies until the turbidity of the suspended cells reached to the McFarland 0.5 standard, then the bacterial inoculate were spread on the surface of Muller Hinton nutrient agar by using a sterile cotton swab. The wells (diameter = 6 mm) in the agar plate were formed by using sterile glassy borer. After that, zinc complexes which were dissolved in DMSO (concentration = 6 mg/ml) were added into respective wells in plates by using 25 μ L pipette. Finally, the plates were incubated at 37 °C for 12-24 h.^{28,63}

Gentamicin and Erthromycin were used as positive control, but DMSO was used as negative standard. By measuring IZD (inhibition zone diameter) in millimeter (mm), the activities of complexes were determined also, the results were determined by calculating the average of three trials, and these results are stated as average \pm standard error.^{28,63}

2.6 BNPP hydrolysis:

To determine the optimum conditions of the BNPP hydrolysis, the kinetic experiments were performed in three trials, then the graphs of absorbance vs. released p-nitrophenol concentration were plotted. The perfect graphs were chosen to determine the optimum conditions.

HEPES buffer (4-(2-hydroxyethyl)-1-piperazineethanesulfonic acid) was used to keep the pH constant. The buffer solutions were prepared by dissolving 50 μM of HEPES in minimum amount of deionized water, then the pH was adjusted by NaOH or HCl to obtain the required pH. After that, the BNPP was dissolved in HEPES buffer to obtain a final volume of 100 ml using 100 ml volumetric flask.⁶³⁻⁶⁵

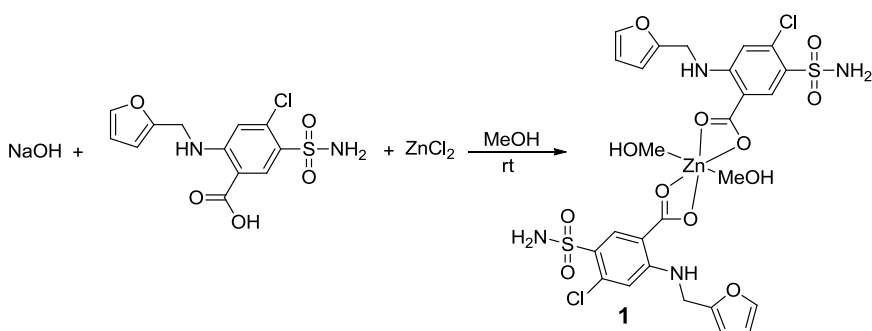
Zinc(II) complexes were used as catalysts in the BNPP hydrolysis process, these complexes were prepared in DMSO solution with different concentration. UV-Vis spectrophotometer ($\lambda = 400 \text{ nm}$, $\epsilon = 13400 \text{ L/mol.cm}$) was used to calculate the rate of p-nitrophenol formation. After the two solutions were placed in the water bath for 10 minutes at constant temperature, 1.5 ml of zinc complexes and 1.5 ml of BNPP solutions were added and mixed in a quartz cell at fixed temperature and the kinetic measurement was performed.⁶³⁻⁶⁵

3. Results and discussion:

3.1 Synthesis zinc furosemide complexes:

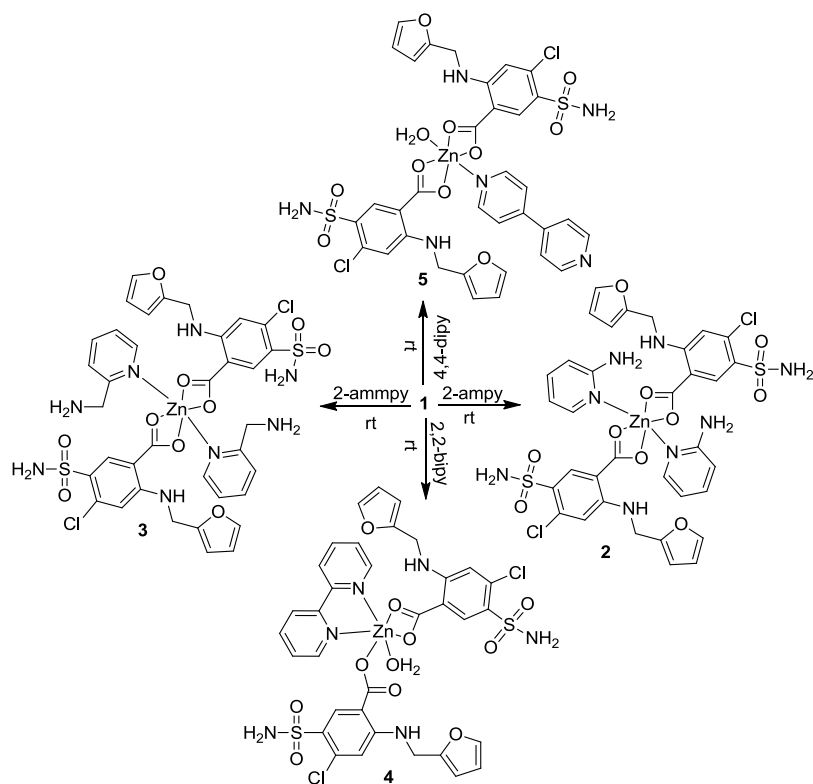
1 equivalent of ZnCl_2 was reacted with 2 equivalents of NaOH and 2 equivalents of furosemide at rt to form $[\text{Zn}(\text{furo})_2(\text{MeOH})_2]$ (**1**) as shown in Scheme 1. The obtained complex has a light yellow color with 77% yield.

Scheme 1: Proposed synthesis of $[\text{Zn}(\text{furo})_2(\text{MeOH})_2]$ (**1**)



Zinc furosemide was reacted with different molar ratios of nitrogen based ligands to form zinc furosemide complexes (**2-5**) as shown in Scheme 2 and Scheme 3. Table 5 shows the physical properties and the percent yields of the complexes (**1-8**).

Scheme 2: Synthesis of complexes **2**, **3**, **4** and **5**.



Scheme 3: Synthesis of complexes **6**, **7** and **8**.

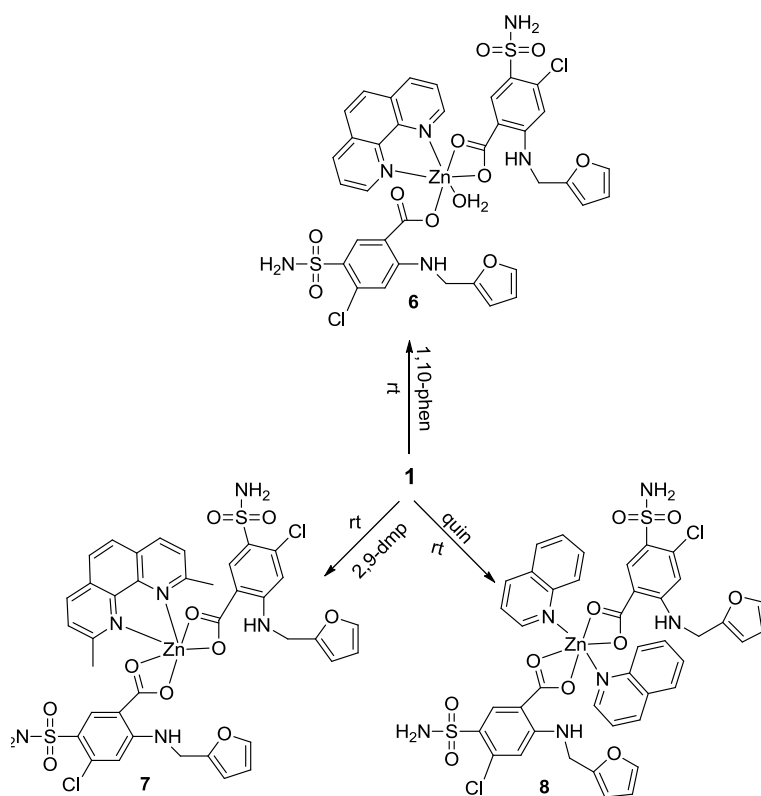


Table 5: Physical properties of complexes (**1-8**) and their % yields.

Complex	m.p (°C)	% Yield	Solubility
[Zn(furo) ₂ (MeOH) ₂] (1)	182 ^d	77	Methanol, ethanol, acetone, DMSO, DMF, slightly soluble in CHCl ₃
[Zn(furo) ₂ (2-ampy) ₂] (2)	185-190 ^d	45	Acetone, DMSO, slightly soluble in methanol, ethanol, DMF, and acetonitrile
[Zn(furo) ₂ (2-ammpy) ₂] (3)	140-145	28	DMSO, DMF, slightly soluble in methanol, and acetone
[Zn(furo) ₂ (H ₂ O)(2,2-bipy)] (4)	226-229	51	DMSO, DMF, slightly soluble in methanol, and acetone
[Zn(furo) ₂ (H ₂ O) ₂ (4,4-dipy)] (5)	201-202	58	DMSO, DMF, slightly soluble in methanol, and acetonitrile
[Zn(furo) ₂ (1,10-phen)] (6)	191-192	49	DMSO, DMF, slightly soluble in methanol and acetone
[Zn(furo) ₂ (2,9-dmp)] (7)	261-265 ^d	32	DMSO, DMF, slightly soluble in methanol and acetone
[Zn(furo) ₂ (quin) ₂] (8)	198-199	92	DMSO, DMF, slightly soluble in methanol

d: decomposed

3.2 ¹H-NMR and ¹³C NMR:

Table 6 and Table 7 show the ¹H-NMR and ¹³C-NMR spectral data of complex **1**, H-furo, and complex **2**. The intensities of ¹H-NMR signals indicated good correlation with the proposed structures. In addition, the resonance chemical shifts of the parent ligands slightly down field shifted compared to the same resonance in complexes **1** and **2** which may be due to the complexation with the Zn metal cation. The O-H

resonance in complex **1** and complex **2** was absent, and supporting the coordination mode with the metal center. In addition, C=O in complex **1** and complex **2** shifted downfield compared to H-furo in the ^{13}C -NMR, due to electron density donation (deshielding effect) from the carboxylate group in furosemide to center of Zn(II).

Table 6: ^1H -NMR spectral data of complex **1**, complex **2** and furosemide, δ (ppm).

Complex 1	H-furo	Complex 2
—	13.25 (OH)	—
4.43 (d, 2H, CH ₂)	4.55 (d, 2H, CH ₂ , $^3J_{\text{H-H}} = 5.7$ Hz)	4.42 (d, 2H, CH ₂)
6.30 (d, 1H, CH)	6.34 (d, 1H, CH)	6.29 (d, 1H, CH)
6.36 (t, 1H, CH)	6.39 (t, 1H, CH)	6.36 (t, 1H, CH)
6.82 (s, 1H, CH)	7.03 (s, 1H, CH)	6.80 (s, 1H, CH)
7.56 (d, 1H, CH)	7.59 (d, 1H, CH)	7.56 (d, 1H, CH)
8.45 (s, 1H, CH)	8.37 (s, 1H, CH)	8.44 (s, 1H, CH)
9.60 (NH)	8.59 (t, 1H, NH, $^3J_{\text{H-H}} = 5.7$)	9.80 (NH)
7.14 (NH ₂)	7.31 (NH ₂)	6.02 (NH ₂)
—	—	6.44 (t, 1H, CH)
—	—	6.47 (d, 1H, CH)
—	—	7.36 (t, 1H, CH)
—	—	7.89 (d, 1H, CH)

Table 7: ^{13}C -NMR spectral data of complex **1**, complex **2** and furosemide, δ (ppm).

Complex 1	H-furo	Complex 2
170.78 C=O	169.06 C=O	170.63 C=O
39.08 CH ₂	39.51 CH ₂	39.08 CH ₂
107.68 CH	108.07 CH	107.63 CH
110.88 CH	108.48 CH	110.88 CH
112.53 CH	110.96 CH	112.18 CH
113.72 CH	114.01 CH	112.32 CH
126.17 CH	127.21 CH	126.03 CH
133.88 C	133.73 C	134.06 C
134.03 C	136.63 C	137.83 C
142.88 C	143.16 C	142.85 C
152.38 CH	151.75 CH	152.48 CH
152.57 C	152.79 C	152.62 C
—	—	108.91 CH
—	—	147.86 CH

Table 8 and Table 10 show the resonance chemical shifts of the complexes **3**, **4**, **5**, **6**, **7** and **8**, some of the resonance chemical shifts of these complexes are slightly upfield shifted and others are downfield shifted compared to the same resonance in H-furo which may be due to the complexation with the Zn metal cation. OH group was absent in complexes may be also due to complexation with the Zn(II) center. In addition, C=O of the complexes **3**, **4**, **5**, **6**, **7** and **8** in ^{13}C -NMR was shifted downfield

compared to H-furo as shown in Table 9 and Table 11. This downfield shift is due to the deshielding effect of carboxylate group. The intensities of $^1\text{H-NMR}$ of the all complexes signals showed good correlation with the proposed structures.

Table 8: $^1\text{H-NMR}$ spectral data of Complex 3, Complex 4 and complex 5, δ (ppm).

Complex 3	Complex 4	Complex 5
4.40 (d, 2H, CH ₂ , $^3J_{\text{H-H}} = 5.1$ Hz)	4.42 (d, 2H, CH ₂)	4.46 (d, 1H, CH ₂)
6.30 (d, 1H, CH)	6.27 (d, 1H, CH)	6.31 (d, 1H, CH)
6.38 (t, 1H, CH)	6.35 (t, 1H, CH)	6.36 (t, 1H, CH)
6.75 (s, 1H, CH)	6.84 (s, 1H, CH)	6.88 (s, 1H, CH)
7.49 (d, 1H, CH, $^3J_{\text{H-H}} = 7.8$ Hz)	7.57 (t, 1H, 2CH)	7.56 (d, 1H, CH)
8.41 (s, 1H, CH)	8.46 (s, 1H, CH)	8.48 (s, 1H, CH)
10.19 (NH)	9.49 (NH)	9.35 (NH)
4.03 (s, 2H, CH ₂)	7.16 (NH ₂)	7.20 (NH ₂)
7.38 (t, 1H, CH, $^5J_{\text{H-H}} = 11.7$ Hz)	8.09 (t, 1H, 2CH)	7.87 (d, 1H, 4CH)
7.58 (d, 1H, CH)	8.50 (d, 1H, 2CH)	8.74 (d, 1H, 4CH)
7.86 (t, 1H, CH ₃ , $^3J_{\text{H-H}} = 7.8$ Hz)	8.74 (d, 1H, 2CH)	—
8.51 (d, 1H, CH)	—	—

Table 9: ^{13}C -NMR spectral data of complex **3**, complex **4** and complex **5**, δ (ppm).

Complex 3	Complex 4	Complex 5
170.58 C=O	171.09 C=O	171.15 C=O
39.08 CH ₂	39.08 CH ₂	39.08 CH ₂
107.57 CH	107.69 CH	107.74 CH
110.90 CH	110.92 CH	110.91 CH
111.95 CH	112.67 CH	112.85 CH
117.96 CH	115.26 CH	122.02 4CH
125.82 CH	126.26 CH	126.42 CH
132.95 C	134.08 C	134.35 C
133.80 C	134.21 C	141.23 C
142.87 C	142.88 C	142.49 C
152.65 CH	152.33 CH	152.22 CH
152.74 C	152.54 C	152.53 C
44.43 CH ₂	121.72 2CH	145.10 2C
122.81 CH	149.49 2CH	150.88 4CH
123.47 CH	—	—
138.47 CH	—	—
148.38 CH	—	—
156.02 C	—	—

Table 10: $^1\text{H-NMR}$ spectral data of complex **6**, complex **7** and complex **8**, δ (ppm).

Complex 6	Complex 7	Complex 8
4.38 (s, 2H, CH ₂ , $^3J_{\text{H-H}} = 5.7$ Hz)	4.44 (d, 2H, CH ₂ , $^3J_{\text{H-H}} = 5.4$ Hz)	4.45 (d, 2H, CH ₂)
6.28 (d, 1H, CH)	6.28 (d, 1H, CH)	6.33 (d, 1H, CH)
6.37 (t, 1H, CH)	6.36 (t, 1H, CH)	6.36 (t, 1H, CH)
6.74 (s, 1H, CH)	6.90 (s, 1H, CH)	6.87 (s, 1H, CH)
7.57 (d, 1H, CH)	7.55 (d, 1H, CH)	7.58 (m, 1H, 2CH)
8.42 (s, 1H, CH)	8.49 (s, 1H, CH)	7.77 (m, 1H, 2CH)
10.22 (NH)	8.89 (NH)	8.50 (NH)
7.09 (NH ₂)	7.23 (NH ₂)	7.21 (NH ₂)
7.90 (t, 1H, 2CH, $^3J_{\text{H-H}} = 6.1$ Hz)	8.05 (d, 1H, 2CH, $^3J_{\text{H-H}} = 8.4$ Hz)	8.01 (m, 1H, 2CH)
8.14 (d, 1H, 2CH)	8.14 (d, 1H, 2CH)	8.37 (d, 1H, CH, $^3J_{\text{H-H}} = 8.1$ Hz)
8.70 (d, 1H, 2CH, $^5J_{\text{H-H}} = 7.5$ Hz)	8.80 (d, 1H, 2CH, $^5J_{\text{H-H}} = 8.4$ Hz)	—
8.99 (d, 1H, 2CH)	2.49 (s, 3H, 2CH ₃)	—

Table 11: ^{13}C -NMR spectral data of complex **6**, complex **7** and complex **8**, δ (ppm)..

Complex 6	Complex 7	Complex 8
170.51 C=O	170.26 C=O	171.16 C=O
39.08 CH ₂	39.08 CH ₂	39.08 CH ₂
107.57 CH	107.89 CH	107.74 CH
110.88 CH	110.93 CH	110.91 CH
111.92 CH	113.25 CH	112.79 CH
118.11 CH	126.66 2CH	121.94 CH
125.79 CH	126.83 CH	126.37 CH
132.90 C	134.55 C	134.34 CH
133.79 C	135.27 C	141.23 C
142.85 C	141.23 C	142.91 C
152.63 CH	152.92 CH	152.28 CH
152.73 C	152.42 C	152.56 C
125.06 2CH	24.67 (2CH ₃)	127.04 CH
127.38 2CH	127.41 2CH	128.38 CH
129.04 2C	139.48 2CH	129.33 C
141.23 2C	143.05 2CH	130.00 2CH
149.90 2CH	158.16 2C	136.55 CH
—	—	148.12 C
—	—	151.03 CH

3.3 Infrared spectroscopy:

The IR spectra in the range of (200-4000) cm^{-1} was used to characterize the prepared zinc complexes. Table 12 shows the bands assignment and their corresponding wave numbers for Na_{furo} and complex **1**. The IR spectra for complex **1** shows two (COO^-) stretching bands symmetric and asymmetric, $\nu_{\text{s}}(\text{COO}^-)$ at 1383 cm^{-1} and $\nu_{\text{as}}(\text{COO}^-)$ at 1605 cm^{-1} . The difference between two bands ($\Delta\nu(\text{COO}^-) = 222 \text{ cm}^{-1}$) which is less than ($\Delta\nu(\text{COO}^-) = 229 \text{ cm}^{-1}$) of Na_{furo} indicating chelating bidentate coordination modes zinc and furosemide. The $\nu(\text{M-O})$ and $\nu(\text{M-N})$ bands for metal complexes occur in the range of (430-520) cm^{-1} and (542-576) cm^{-1} as weak bands, respectively.

Table 12: Assignment IR bands and wave numbers of Na_{furo} and complex **1**.

Assignments	Na_{furo} (cm^{-1})	Complex 1 (cm^{-1})
$\nu(\text{C-H})_{\text{alph}}$	2988	—
$\nu(\text{C-H})_{\text{ar}}$	3020	—
$\nu_{\text{s}}(\text{NH}_2)$	3285	3303
$\nu_{\text{as}}(\text{NH}_2)$	3326	—
$\nu(\text{N-H})$	3222	—
$\nu_{\text{as}}(\text{COO}^-)$	1602	1605
(N-H) bending	1558	1556
$\nu_{\text{s}}(\text{COO}^-)$	1373	1383
$\nu_{\text{as}}(\text{SO}_2)$	1315	1299
$\nu(\text{C-O})$	1149	1159
$\nu_{\text{s}}(\text{SO}_2)$	1060	1071
(O-H) out of plane	941	945
$\delta(\text{COO}^-)$	736	738
$\nu(\text{C-Cl})$	576	583
$\nu(\text{Zn-O})$	—	514
$\nu(\text{Na-O})$	471	—
$\Delta(\text{COO}^-)$	229	222

In complex **2**; $\Delta\nu(\text{COO}^-) = 233 \text{ cm}^{-1}$ is greater than $\Delta\nu(\text{COO}^-)$ of Na_{furo} , indicating monodentate coordination mode. Also in complex **3**; $\Delta\nu(\text{COO}^-) = 240 \text{ cm}^{-1}$ is greater than $\Delta\nu(\text{COO}^-)$ of Na_{furo} , indicating monodentate coordination mode. In complex **4**; $\Delta\nu(\text{COO}^-) = 225 \text{ cm}^{-1}$ is less than $\Delta\nu(\text{COO}^-)$ of Na_{furo} , indicating chelating bidentate coordination mode, but X-ray structure analysis indicates bidentate coordination mode for the first carboxylate group and monodentate for the second, respectively. In complex **5**; $\Delta\nu(\text{COO}^-) = 191 \text{ cm}^{-1}$ is less than $\Delta\nu(\text{COO}^-)$ of Na_{furo} , chelating bidentate is expected. In complex **6**; $\Delta\nu(\text{COO}^-) = 183 \text{ cm}^{-1}$ is less than $\Delta\nu(\text{COO}^-)$ of Na_{furo} , this also indicates chelating bidentate. In complex **7**; $\Delta\nu(\text{COO}^-) = 208 \text{ cm}^{-1}$, less than $\Delta\nu(\text{COO}^-)$ of Na_{furo} , therefore indicating chelating bidentate coordination mode. In complex **8**; $\Delta\nu(\text{COO}^-) = 232 \text{ cm}^{-1}$, greater than $\Delta\nu(\text{COO}^-)$ of Na_{furo} , indicating monodentate coordination mode.

Table 13: Assignments IR bands and wave numbers of complex **2**, complex **3** and complex **4**.

Assignments	Complex 2	Complex 3	Complex 4
$\nu(\text{C-H})_{\text{alph}}$	—	2933	—
$\nu(\text{C-H})_{\text{ar}}$	—	—	3117
$\nu_{\text{s}}(\text{NH}_2)$	3322	—	—
$\nu_{\text{as}}(\text{NH}_2)$	3568	—	3467
$\nu(\text{N-H})$	3223	3259	3265
$\nu_{\text{as}}(\text{COO}^-)$	1607	1604	1607
(N-H) bending	1560	1549	1553
$\nu_{\text{s}}(\text{COO}^-)$	1374	1364	1382
$\nu_{\text{as}}(\text{SO}_2)$	1298	1295	1306
$\nu(\text{C-O})$	1150	1138	1151
$\nu_{\text{s}}(\text{SO}_2)$	—	—	1066
(O-H) out of plane	942	943	947
$\delta(\text{COO}^-)$	737	744	755
$\nu(\text{C-Cl})$	582	577	585
$\nu(\text{Zn-O})$	520	495	510
$\Delta(\text{COO}^-)$	233	240	225

Table 14: Assignments IR bands and wave numbers of complex **5**, complex **6**, complex **7** and complex **8**.

Assignments	Complex 5	Complex 6	Complex 7	Complex 8
$\nu(\text{C-H})_{\text{alph}}$	—	—	—	2917
$\nu(\text{C-H})_{\text{ar}}$	—	3077	3072	3055
$\nu_{\text{s}}(\text{NH}_2)$	3260	3317	3313	3282
$\nu_{\text{as}}(\text{NH}_2)$	—	3569	3397	—
$\nu(\text{N-H})$	—	3224	3222	—
$\nu_{\text{as}}(\text{COO}^-)$	1606	1604	1628	1611
(N-H) bending	1559	1555	1585	1557
$\nu_{\text{s}}(\text{COO}^-)$	1415	1421	1420	1379
$\nu_{\text{as}}(\text{SO}_2)$	1307	1309	1350	1301
$\nu(\text{C-O})$	1159	1152	1165	1153
$\nu_{\text{s}}(\text{SO}_2)$	1070	—	1071	1079
(O-H) out of plane	945	941	962	945
$\delta(\text{COO}^-)$	739	723	758	732
$\nu(\text{C-Cl})$	580	577	583	584
$\nu(\text{Zn-O})$	511	473	520	516
$\Delta(\text{COO}^-)$	191	183	208	232

3.4 Electronic absorption spectroscopy:

In coordination chemistry there are three types of electronic transition: First, the forbidden d-d transition in the metal ion, such transition is called ligand-field transition. Ligand-field transition occurs in the visible and near infrared regions. The intensity of these bands is weak due to Laporte rule. Second, intra ligand transitions which normally occurs in the ultraviolet region and is similar to that of general organic compounds. Third, charge-transfer transitions which occur due to electron transition from metal orbitals to ligands orbitals or from ligand orbitals to metal orbitals. Charge-transfer are very intense because they are allowed according to Laport rule and occur mainly in the ultraviolet region and as some complexes in the visible region.⁶⁷

MLCT transition primary occur in the (201-296) nm region.⁶³⁻⁶⁷ Table 15 shows no (LMCT), because Zn(II) is a d^{10} cation with completely filled d-orbitals. In addition, d-d electronic transition will not happen for the same reason. The origin of the observed bands in complexes are due to (MLCT) and intra-ligand transitions. The spectra of the Zn(II) complexes are similar to the spectra of the parent ligands with very small blue or red shifts.

Table 15: UV-visible spectral data for the prepared complexes and pure ligand.

Complexes	λ_{\max} (nm)	Parent ligands	λ_{\max} (nm)
[Zn(furo) ₂] (1)	229, 275	Furo	233, 274
[Zn(furo) ₂ (2-ampy) ₂] (2)	234, 296	2-ampy	230, 276
[Zn(furo) ₂ (2-ammepy) ₂] (3)	229, 274	2-ammepy	206, 261
[Zn(furo) ₂ (H ₂ O)(2,2-bipy)] (4)	230, 276	2,2-bipy	236, 282
[Zn(furo) ₂ (4,4-dipy)] (5)	228, 275	4,4-dipy	204, 241
[Zn(furo) ₂ (1,10-phen)] (6)	229, 272	1,10-phen	230, 264
[Zn(furoe) ₂ (2,9-dmp)] (7)	229, 275	2,9-dmp	229, 270
[Zn(furo) ₂ (quin) ₂] (8)	204, 225	quin	224, 275

3.5 X-ray spectroscopy:

Crystal structure of complex **4** was determined and suitable crystal was obtained by recrystallization from MeOH. Crystallographic information files (CIF) are given in Appendix A.

3.5.1 X-ray crystal structure of $[\text{Zn}(\text{furo})_2(\text{H}_2\text{O})(2,2\text{-bipy})]$ (**4**):

The orotp structure of complex **4** is shown in Figure 19 with one monodentate, one bidentate furosemide, one bidentate 2,2-bipy and one water molecule formed distorted octahedral arrangement around the metal center. 2,2-bipy ligand formed stable five member ring with Zn metal center. Selected bond distances and bond angles for complex **4** are shown in Table 16.

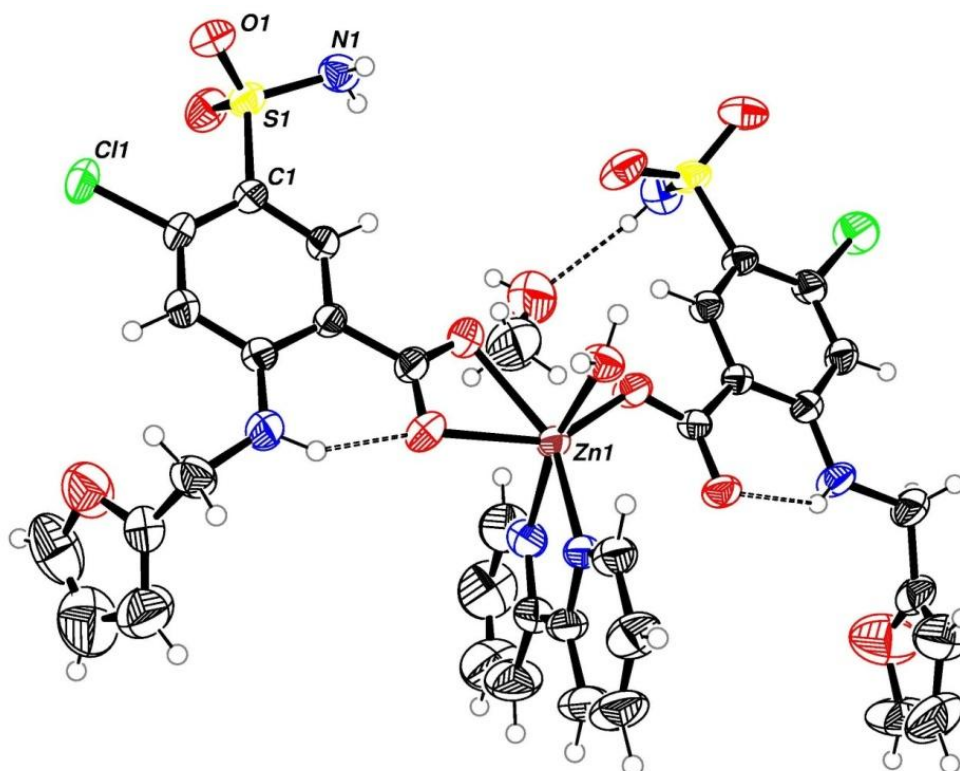


Figure 19: Molecular structure of complex **4**.

Table 16: Selected bond distances (Å) and bond angles (°) for complex **4**.

Bond	Distance (Å)	Bonds	Angle (°)
O(3)-Zn(1)	2.336(2)	N(6)-Zn(1)-O(3)	152.66(8)
O(4)-Zn(1)	2.159(2)	O(4)-Zn(1)-O(3)	57.90(8)
O(8)-Zn(1)	1.9912(19)	O(1W)-Zn(1)-O(3)	91.14(8)
O(1W)-Zn(1)	2.100(2)	O(8)-Zn(1)-O(3)	84.04(8)
C(7)-O(3)	1.252(4)	N(5)-Zn(1)-O(4)	94.22(10)
C(7)-O(4)	1.268(4)	N(6)-Zn(1)-O(4)	94.76(9)
C(19)-O(8)	1.261(3)	O(1W)-Zn(1)-O(4)	93.21(9)
C(19)-O(9)	1.246(3)	O(8)-Zn(1)-O(4)	141.91(8)
N(5)-Zn(1)	2.134(3)	O(8)-Zn(1)-O(1W)	88.40(9)
N(6)-Zn(1)	2.125(2)	O(8)-Zn(1)-N(6)	123.29(8)
C(29)-N(5)	1.339(5)	O(1W)-Zn(1)-N(6)	90.55(9)
C(25)-N(5)	1.334(4)	O(8)-Zn(1)-N(5)	92.88(9)
C(30)-N(6)	1.350(4)	O(1W)-Zn(1)-N(5)	166.22(9)
C(34)-N(6)	1.343(4)	N(6)-Zn(1)-N(5)	77.28(10)
		N(5)-Zn(1)-O(3)	102.64(9)
		C(19)-O(8)-Zn(1)	124.52(17)

Hydrogen bonds formation depend on molecular recognition of complementary parts of the molecules containing donor and acceptor groups and molecular stereochemistry. This type of interaction is strongly directional and is used in supra-molecular chemistry and crystal engineering to produce novel (bio) nano-material. Hydrogen bonds play an important role in the stability of crystal structures and therefore can be used in identification of the protein structures, and is a key building block in the DNA formation. The bond formed between –OH of one molecule and the –N of another molecule leads to tight crystal packing.⁶⁸⁻⁷⁰

The bond distances of O-Zn (2.336(2) Å, 2.159(2) Å, 1.9912(19) Å and 2.100(2) Å) are similar to previously reported values (1.84-2.33).⁷¹ N-Zn bond distances 2.134(3) Å, and 2.125(2) Å are smaller than previously reported values (2.169-2.197).⁷² Complex **4** formed a distorted octahedral geometry around Zn(II) center due to unsymmetrical bond angles. O(4)-Zn(1)-O(3) = 57.90(8)°, O(8)-Zn(1)-O(3) = 84.04(8)°, O(8)-Zn(1)-O(1W) = 88.40(9)°, O(1W)-Zn(1)-O(4) = 93.21(9)°, O(1W)-Zn(1)-O(3) = 91.14(8)°, N(5)-Zn(1)-O(3) = 102.64(9)°, N(6)-Zn(1)-N(5) = 77.28(10)°, O(1W)-Zn(1)-N(5) = 166.22(9)°, O(8)-Zn(1)-N(5) = 92.88(9)°, O(1W)-Zn(1)-N(6) = 90.55(9)°, O(8)-Zn(1)-N(6) = 123.29(8)°, N(6)-Zn(1)-O(4) = 94.76(9)°, N(5)-Zn(1)-O(4) = 94.22(10)°, and N(6)-Zn(1)-O(3) = 152.66(8)°.

Intra-hydrogen bonds were formed between a lone pair of electrons on one of O(9), O(2), O(4), O(6), O(3), O(7) and a hydrogen atom bonded to one of the N(1), N(2), N(3), N(4) and O(1W), whereas inter-hydrogen bonds were formed between hydrogen of N(3) and lone pair of electrons of O(1ME) and hydrogen of O(1ME) and lone pair of electrons of O(1). Table 17 shows the hydrogen bond distances in (Å) and their angles in (°).

Table 17: Hydrogen bond distances (Å) and bond angles (°).

D-H...A	d(D-H)	d(H...A)	d(D...A)	<(DHA)
N(1)-H(1AN)...O(9)#1	0.92	1.93	2.841(3)	170.7
N(1)-H(1BN)...O(2)#2	0.87	2.03	2.897(3)	172.6
N(2)-H(2N)...O(4)	0.87	1.93	2.656(4)	140.4
N(3)-H(3AN)...O(6)#3	0.91	2.16	3.023(4)	159.4
N(3)-H(3BN)...O(1ME)	0.81	2.20	2.984(5)	163.5
N(4)-H(4N)...O(9)	0.89	1.99	2.703(3)	136.7
O(1W)-H(1W)...O(3)#1	0.83	1.93	2.754(3)	172.2
O(1W)-H(2W)...O(7)#1	0.85	2.03	2.840(3)	160.2
O(1ME)-H(1ME)...O(1)#2	0.82	2.25	3.000(4)	151.5

Symmetry transformations used to generate equivalent atoms:

#1 -x+1,-y,-z+1 #2 -x,-y,-z+1 #3 -x+1,-y,-z+2

3.6 Biological activity (*In-vitro*):

3.6.1 Anti-bacterial activity:

The anti-bacterial activity of complexes (1-8) were tested using agar diffusion method against gram-positive and gram-negative bacteria. The results are shown in Table 18 and in Table 19 for gram-negative and gram-positive bacteria, respectively.

Table 18: *In-vitro* anti-bacterial activity data for complexes (1-8) against gram negative bacteria.

Compounds	<i>E. coli</i>	<i>P. mirabilis</i>	<i>P. aeruginosa</i>
Gentamycin	13.7 ± 1.2	14.0 ± 1.0	11.7 ± 0.6
Erythromycin	11.3 ± 0.6	9.3 ± 1.2	10.7 ± 1.2
ZnCl ₂	-	-	-
Furo	-	-	-
DMSO	-	-	-
Complex 1	-	-	-
Complex 2	-	-	-
2-ampy	-	-	-
Complex 3	-	-	-
2-ammepy	-	-	-
Complex 4	-	10.0 ± 1.0	-
2,2-bipy	10.3 ± 0.6	13.0 ± 1.0	-
Complex 5	-	-	-
4,4-dipy	-	-	-
Complex 6	11.7 ± 0.6	10.0 ± 1.0	-
1,10-phen	16.0 ± 1.0	19.3 ± 3.2	-
Complex 7	-	-	-
2,9-dmp	-	-	-
Complex 8	-	-	-
quin	-	-	-

Inhibition zone diameter (millimeter (mm)) ± Standard error

Table 19: *In-vitro* anti-bacterial activity data for complexes (1-8) against gram positive bacteria.

Compounds	<i>S. aureus</i>	<i>B. subtilis</i>	<i>S. epidemidis</i>
Gentamycin	13.3 ± 0.6	13.7 ± 1.5	19.0 ± 3.0
Erythromycin	19.3 ± 0.6	18.3 ± 1.2	20.7 ± 1.2
ZnCl ₂	-	-	6.3 ± 0.6
Furo	-	-	-
Complex 1	-	-	-
Complex 2	-	-	-
2-ampy	-	-	-
Complex 3	-	-	6.0 ± 1.0
2-ammepy	-	-	-
Complex 4	8.7 ± 1.5	-	-
2,2-bipy	8.3 ± 0.6	9.3 ± 0.6	11.7 ± 0.6
Complex 5	8.0 ± 1.4	-	-
4,4-dipy	-	-	-
Complex 6	11.7 ± 0.6	8.0 ± 0.0	13.7 ± 0.6
1,10-phen	18.7 ± 1.2	16.3 ± 0.6	22.0 ± 1.0
Complex 7	8.0 ± 0.0	8.7 ± 0.6	11.3 ± 0.6
2,9-dmp	11.0 ± 0.0	7.0 ± 1.0	16.3 ± 0.6
Complex 8	-	-	-
quin	-	-	-

Inhibition zone diameter (millimeter (mm)) ± Standard error

Most of the prepared complexes did not show considerable anti-bacterial activity against gram-negative bacteria except complex 4 and complex 6. This minor activity is possibly due to the fact that gram-negative bacteria contain cytoplasmic inner membrane and an outer membrane that contains lipopolysaccharide molecules. The space between the two membranes contains peptidoglycan cell wall and many unique proteins where the outer membrane acts as a protective membrane preventing the noxious compounds from reaching the cell.⁶⁶ Complex 4 showed anti-bacterial activity against *P.mirabilis* with IZD equals 10.0 mm and complex 6 showed anti-bacterial activity against *E.coli* and *P.mirabilis* with IZD equals 11.7 mm and 10.0 mm, respectively. The parent ligand 2,2-bipy shows higher anti-bacterial activity against *P.mirabilis* with IZD equals 13.0 mm compared to complex 4. Also 2,2-bipy

shows anti-bacterial activity against *E.coli* with IZD equals 10.3 mm, but complex **4** didn't show any anti-bacterial activity against this type of gram negative bacteria. In addition, 1,10-phen shows higher anti-bacterial activity against *E.coli* and *P.mirabilis* compared to complex **6** with IZD equals 16.0 mm and 19.3 mm, respectively.

Because 1,10-phen exist in small amount in complex **6**, the anti-bacterial activity of complex **6** comes from the complex not from 1,10-phen only.

The anti-bacterial activity for complexes **4** and **6** is lower than G, but higher than E against *p.mirabilis*. Also complex **6** has slightly higher anti-bacterial activity than E, but lower than G against *E.coli*.

In the case of gram positive bacteria, more prepared complexes show anti-bacterial activity when compared with gram negative bacteria as presented in Table 19.

ZnCl₂, furo, and Complexes **1**, **2** and **8** didn't show any anti-bacterial activity against gram-negative and gram-positive bacteria except ZnCl₂ showed very low anti-bacterial activity against *S. epidermidis* with IZD equals 6.3 mm.

Complex **3** showed low anti-bacterial activity against *S. epidermidis* with IZD equals 6.0 mm and this value is very lower than values of G and E. Complex **4** only showed anti-bacterial activity against *S. aureus* with IZD equals 8.7 mm and this value is very lower when compared with G and E while the parent ligand 2,2-bipy showed higher anti-bacterial activity against all tested microorganisms.

Complex **5** showed anti-bacterial activity against *S. aureus* with IZD equals 8.0 mm and this value is lower than values of G and E, the parent ligand didn't show anti-bacterial activity against any types of gram positive bacteria. Complex **6** showed anti-bacterial activity against all tested gram-positive bacteria (*S. aureus*, *B. subtilis*, *S.*

epidermidis) with IZD equals 11.7 mm, 8.0 mm, and 13.7 mm, respectively and these values lower than values of G and E. However the parent ligand 1,10-phen showed higher anti-bacterial activity than complex **6** for all tested bacteria.

Complex **7** showed anti-bacterial activity for all type of gram-positive bacteria (*S. aureus*, *B. subtilis*, *S. epidermidis*) with IZD equal 8.0 mm, 8.7 mm, and 11.3, respectively and these values are lower than values of G and E while the parent ligand 2,9-dmp showed higher anti-bacterial activity compared to complex **7** except *B. subtilis* where it showed slightly higher anti-bacterial activity than its parent ligand.

The quantity of parent ligands 1,10-phen and 2,9-dmp in complexes **6** and **7** are small quantities, this means the overall anti-bacterial activity of these complexes comes from complexes not from parent ligands only.

The complexation of zinc furosemide with nitrogen donor ligands showed low inhibition activity against gram-positive bacteria compared to the positive controls (E and G). Figure 20 shows agar diffusion.



Figure 20: Agar diffusion.

Destructions of bacterial cell walls of *S. aureus* by Zn(II) ion is due to the inhibition of peptidoglycan elongation by the activations of peptidoglycan autolysins of amidases, but the destruction of *E.coli* cell wall is caused by damage of outer membrane structure by degradative enzymes of lipoproteins at N-and C-terminals, the inhibition of peptidoglycan elongation in this type of bacteria is depend on the activation of peptidoglycan hydrolases and autolysins of amidase and carboxypeptidase-transpeptidase. DNA damages may be due to Zn ion complex formation by Zn^{2+} substitution into hydrogen bonds in DNA.⁷³

The anti-microbial activity of metal complexes depend on many factors: (1) the chelate effect of the ligands; (2) the nature of the N-donor ligands; (3) the total charge of the complex; (4) the existence and the nature of the ionic complex; (5) the nuclearity of the metal center in the complex. In the complexes (1-8) the first of these factors are only present, such as the chelate effect of the ligand. This factor may be the main reasons for the diverse anti-bacterial activity which were shown by the complexes.⁷⁴

3.7 BNPP catalytic hydrolysis:

All zinc furosemide complexes were tested for their catalytic activity in BNPP hydrolysis. The rate of BNPP hydrolysis was performed at different temperatures, pH and concentrations. The optimum conditions for BNPP hydrolysis were determined by varying one of the above factors and keeping the other two factors constant.

3.7.1 Effect complexes` concentration on BNPP hydrolysis:

Figure 21 shows the relationship between absorbance and time at different concentration of complex **7** and constant temp, pH and concentration of BNPP. The initial rates were determined to be 3.8×10^{-9} and 5.6×10^{-9} mol/L.S for 1×10^{-4} M, 2×10^{-4} M, respectively. By measuring the absorbance of p-nitrophenol vs. time at 400 nm, the initial rate of BNPP hydrolysis can be determined.

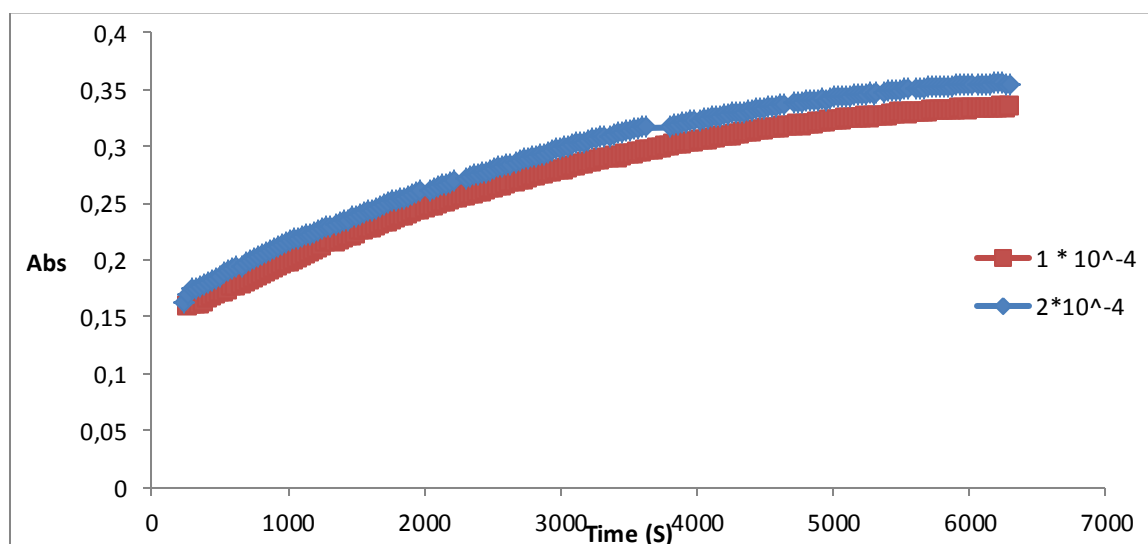


Figure 21: BNPP hydrolysis at different concentrations of complex **7** in DMSO/HEPES buffer solution under certain conditions ($[BNPP] = 1 \times 10^{-4}$ M, $pH = 7.00$ and $temp = 25$ °C).

3.7.2 Effect of temperatures on BNPP hydrolysis:

The absorbance vs. time for complex **4** is plotted in Figure 22 at different temperature values while pH, concentrations of BNPP and complex were maintained constant. The values of initial rates at 25 °C, 37 °C, and 40 °C are 8.6×10^{-9} , 9.9×10^{-9} , and 9.2×10^{-9} (mol/L.S) respectively with maximum initial rate observed at 37 °C for complex **4**.

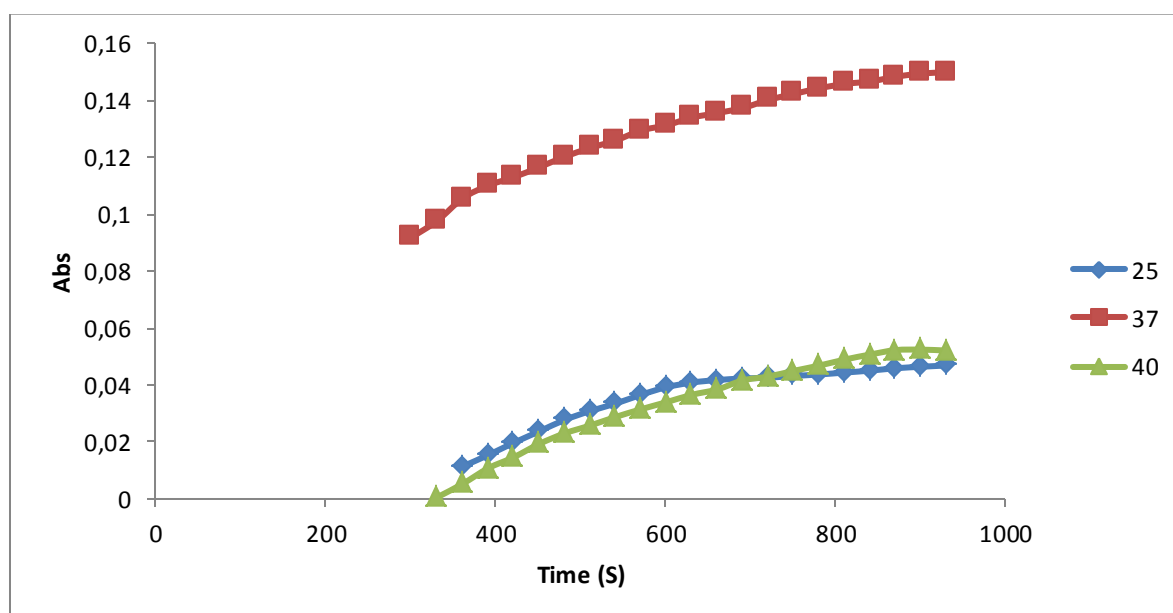


Figure 22: BNPP hydrolysis at different temperature values in DMSO/HEPES buffer solution under certain conditions ($[BNPP] = 1 \times 10^{-4}$ M, $[complex \ 4] = 2 \times 10^{-4}$ M, and pH = 7.00).

3.7.3 Effect of pH on BNPP hydrolysis:

Figure 23 shows the relationship between absorbance and time for complex **4** at different pH values and a temperature of 37 °C and constant concentration of both BNPP and complex. The initial rate values 9.9×10^{-9} , 6.4×10^{-9} , and 7.8×10^{-9} (mol/L.S) were obtained for pH = 7.00, 7.54, and 7.92, respectively. The maximum initial rate value for catalytic activity of complex **4** on the hydrolysis of BNPP was observed at pH = 7.00.

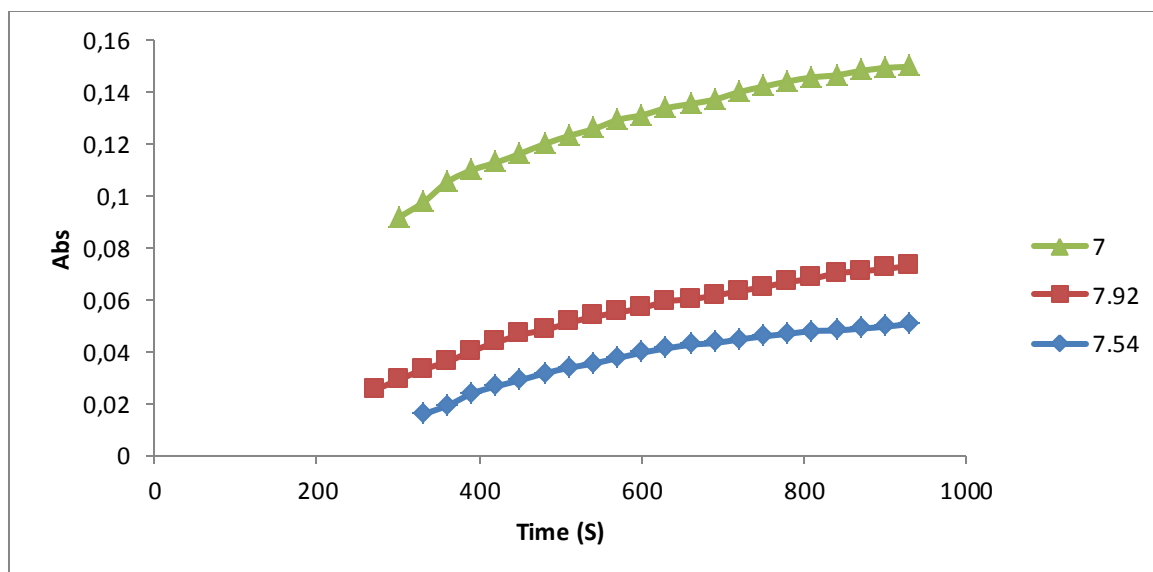


Figure 23: BNPP hydrolysis at different pH values in DMSO/HEPES buffer solution under certain conditions ($[BNPP] = 1 \times 10^{-4} \text{ M}$, $[\text{complex } 4] = 2 \times 10^{-4} \text{ M}$ and $\text{temp} = 37 \text{ }^\circ\text{C}$).

Figure 24 shows the relationship between the reciprocal the concentration of BNPP and rate of hydrolysis for complex 4 according to Michaelis- Menten equation ($1/ V_o = 1/ V_{\text{max}} + K_m/V_{\text{max}}[BNPP]$).⁷⁵ All complexes 1, 2, 3, 4, 5, 6, 7 and 8 have the similar relationship.

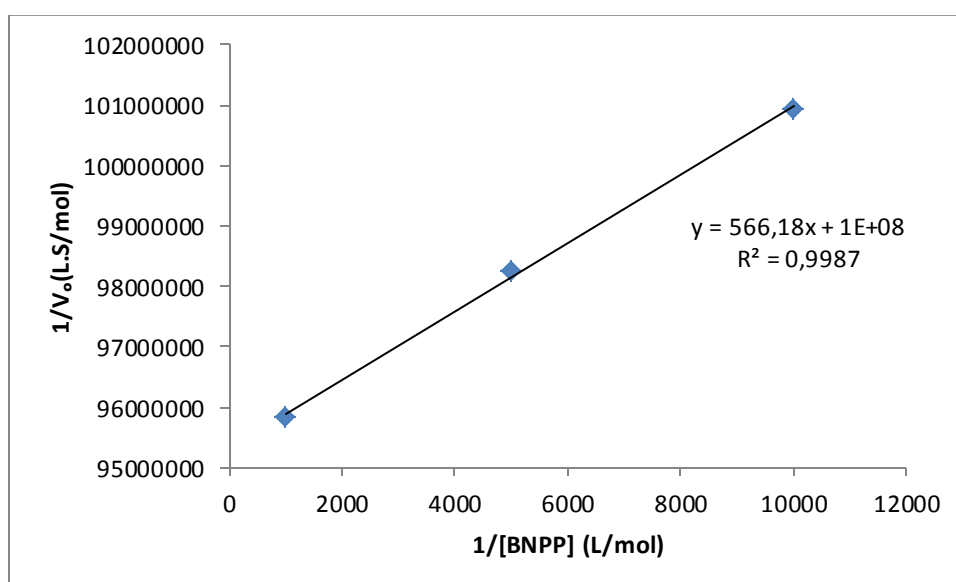


Figure 24: Second order rate for complex 4 with different BNPP concentrations under certain conditions ($\text{pH} = 7.00$, $\text{temp} = 37 \text{ }^\circ\text{C}$ and $[\text{complex } 4] = 2 \times 10^{-4} \text{ M}$).

The rate of BNPP hydrolysis using complexes as catalysts was in the following order: complex **4** > **2** > **5** > **8** > **7** > **6** > **3** > **1**. Table 20 shows the kinetic parameters of BNPP hydrolysis.

Table 20: Kinetic parameters of BNPP hydrolysis for complexes (**1-8**) with different concentration of BNPP.

Concentration of complexes (M)	Concentration of BNPP (M)	V_o (mol/L.S)	V_{max} (mol/L.S)	K_m (mol/L)	K_{cat}^* (S^{-1})	2-order rate $K_{BNPP}^{\#}$ (L/mol. S)
1 (2×10^{-4})	1×10^{-3}	6.84×10^{-9}	1.00×10^{-8}	1.20×10^{-4}	5.00×10^{-5}	0.42
1 (2×10^{-4})	2×10^{-4}	5.01×10^{-9}	1.00×10^{-8}	1.20×10^{-4}	5.00×10^{-5}	0.42
1 (2×10^{-4})	1×10^{-4}	3.92×10^{-9}	1.00×10^{-8}	1.20×10^{-4}	5.00×10^{-5}	0.42
2 (2×10^{-4})	1×10^{-3}	1.01×10^{-8}	1.11×10^{-8}	6.06×10^{-5}	5.55×10^{-5}	0.91
2 (2×10^{-4})	2×10^{-4}	8.24×10^{-9}	1.11×10^{-8}	6.06×10^{-5}	5.55×10^{-5}	0.91
2 (2×10^{-4})	1×10^{-4}	6.76×10^{-9}	1.11×10^{-8}	6.06×10^{-5}	5.55×10^{-5}	0.91
3 (2×10^{-4})	1×10^{-3}	6.98×10^{-9}	1.00×10^{-8}	1.01×10^{-4}	5.00×10^{-5}	0.49
3 (2×10^{-4})	2×10^{-4}	5.53×10^{-9}	1.00×10^{-8}	1.01×10^{-4}	5.00×10^{-5}	0.49
3 (2×10^{-4})	1×10^{-4}	4.13×10^{-9}	1.00×10^{-8}	1.04×10^{-4}	5.00×10^{-5}	0.49
4 (2×10^{-4})	1×10^{-3}	1.04×10^{-8}	1.00×10^{-8}	5.66×10^{-6}	5.00×10^{-5}	8.83
4 (2×10^{-4})	2×10^{-4}	1.01×10^{-8}	1.00×10^{-8}	5.66×10^{-6}	5.00×10^{-5}	8.83
4 (2×10^{-4})	1×10^{-4}	9.90×10^{-9}	1.00×10^{-8}	5.66×10^{-6}	5.00×10^{-5}	8.83
5 (2×10^{-4})	1×10^{-3}	9.33×10^{-9}	1.00×10^{-8}	5.08×10^{-5}	5.00×10^{-5}	0.98
5 (2×10^{-4})	2×10^{-4}	8.05×10^{-9}	1.00×10^{-8}	5.08×10^{-5}	5.00×10^{-5}	0.98
5 (2×10^{-4})	1×10^{-4}	6.55×10^{-9}	1.00×10^{-8}	5.08×10^{-5}	5.00×10^{-5}	0.98
6 (2×10^{-4})	1×10^{-3}	6.78×10^{-9}	1.00×10^{-8}	5.39×10^{-5}	5.00×10^{-5}	0.93
6 (2×10^{-4})	2×10^{-4}	5.82×10^{-9}	1.00×10^{-8}	5.39×10^{-5}	5.00×10^{-5}	0.93
6 (2×10^{-4})	1×10^{-4}	4.97×10^{-9}	1.00×10^{-8}	5.39×10^{-5}	5.00×10^{-5}	0.93
7 (2×10^{-4})	1×10^{-3}	8.28×10^{-9}	1.00×10^{-8}	4.24×10^{-5}	5.00×10^{-5}	1.17
7 (2×10^{-4})	2×10^{-4}	7.24×10^{-9}	1.00×10^{-8}	4.24×10^{-5}	5.00×10^{-5}	1.17
7 (2×10^{-4})	1×10^{-4}	6.29×10^{-9}	1.00×10^{-8}	4.24×10^{-5}	5.00×10^{-5}	1.17
8 (2×10^{-4})	1×10^{-3}	11.72×10^{-9}	1.00×10^{-8}	4.57×10^{-5}	5.00×10^{-5}	1.09
8 (2×10^{-4})	2×10^{-4}	7.23×10^{-9}	1.00×10^{-8}	4.57×10^{-5}	5.00×10^{-5}	1.09
8 (2×10^{-4})	1×10^{-4}	6.41×10^{-9}	1.00×10^{-8}	4.57×10^{-5}	5.00×10^{-5}	1.09

(*) $K_{cat} = V_{max}/[complex]$, (#) $K_{BNPP} = K_{cat}/K_m$

3.8 Mass spectrometry:

Figures 25-32 show mass spectra of all complexes (1-8). The average molecular weight of complex 1 equal 787 amu as shown in Figure 25.

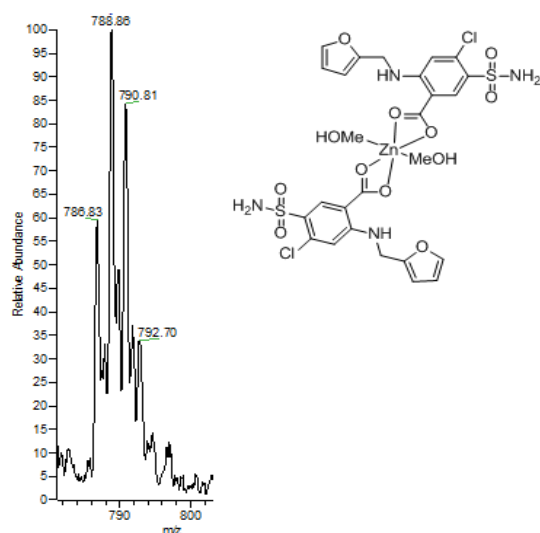


Figure 25: Mass spectra of complex 1

The average molecular weight of complex 2 equal 911 amu as shown in Figure 26.

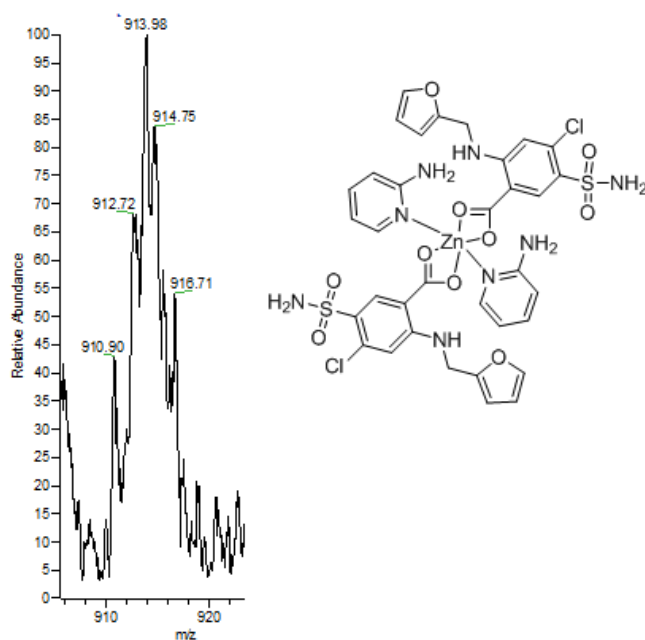


Figure 26: Mass spectra of complex 2.

The average molecular weight of complex **3** equal 939 amu as shown in Figure 27.

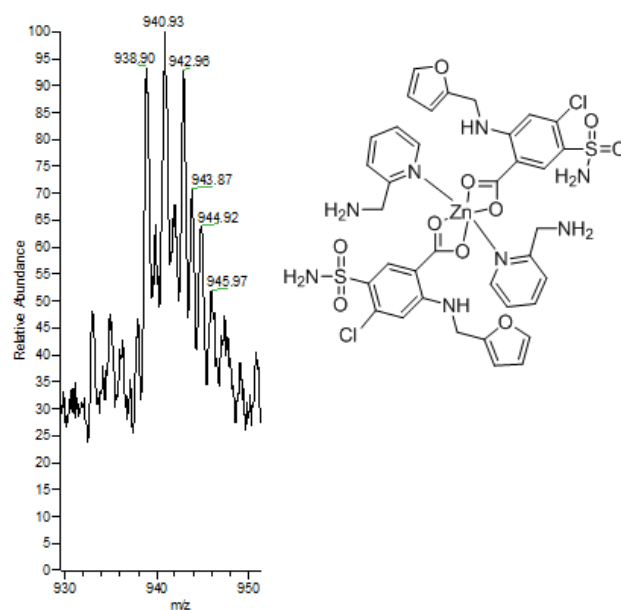


Figure 27: Mass spectra of complex **3**.

The average molecular weight of complex **4** equal 901 amu as shown in Figure 28.

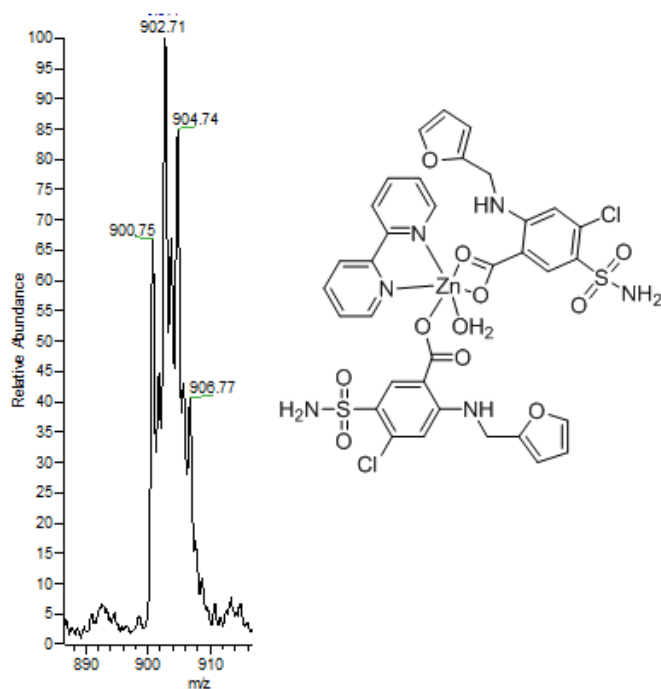


Figure 28: Mass spectra of complex **4**.

The average molecular weight of complex **5** equal 901 amu as shown in Figure 29.

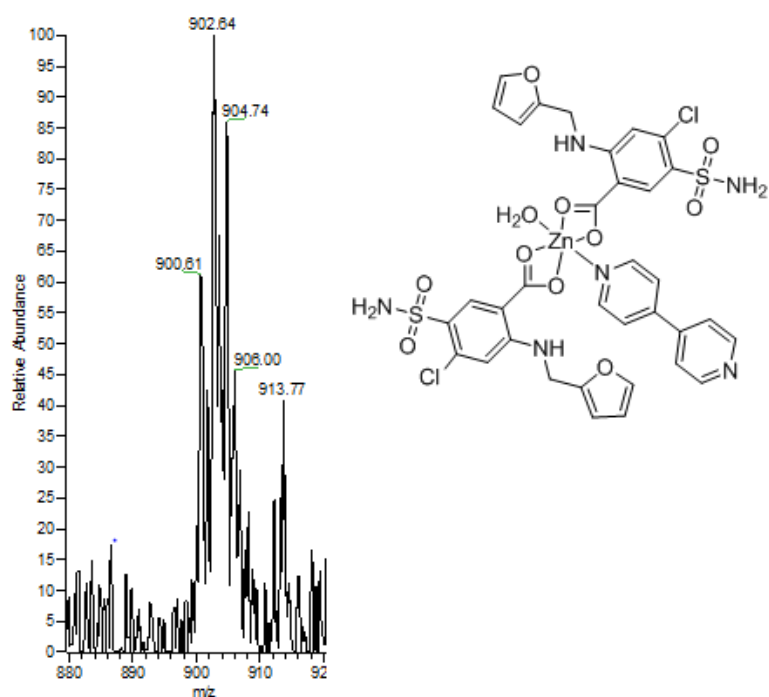


Figure 29: Mass spectra of complex **5**.

The average molecular weight of complex **6** equal 903 amu as shown in Figure 30.

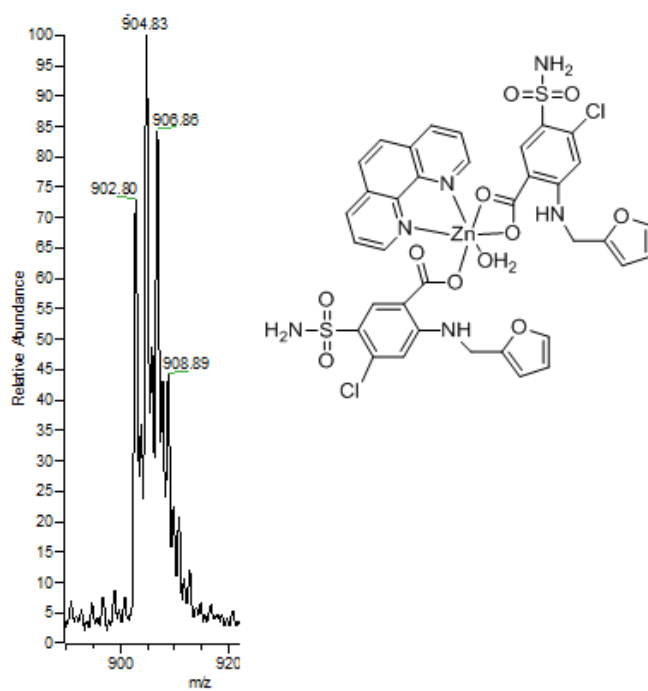


Figure 30: Mass spectra of complex **6**.

The average molecular weight of complex **7** equal 931 amu as shown in Figure 31.

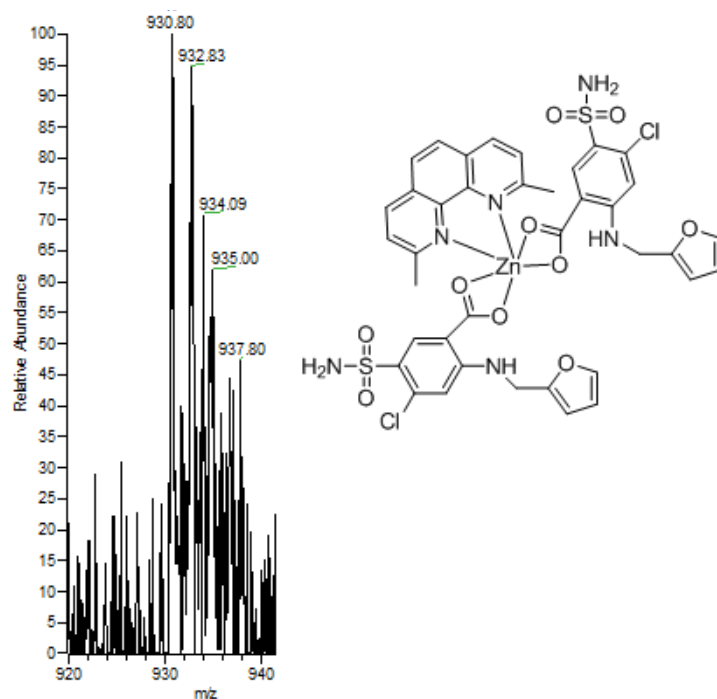


Figure 31: Mass spectra of complex **7**.

The average molecular weight of complex **8** equal 981 amu as shown in Figure 32.

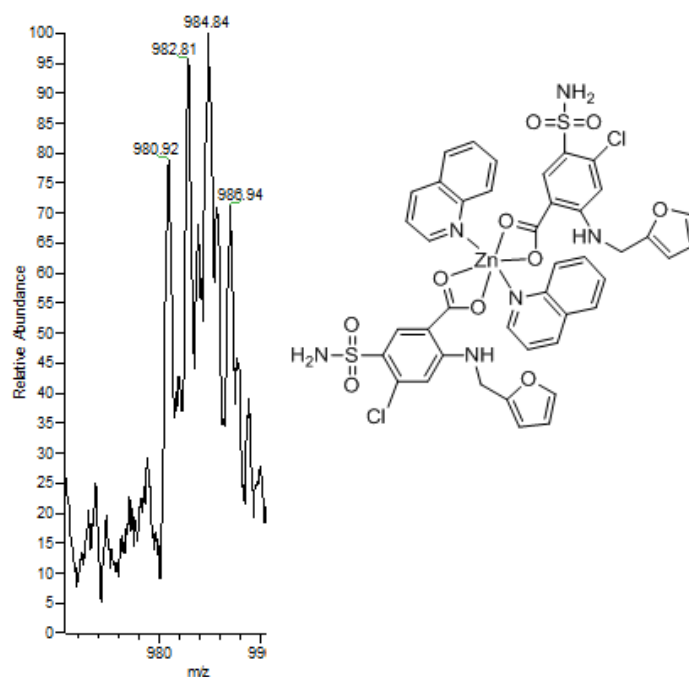


Figure 32: Mass spectra of complex **8**.

4. Conclusion:

The prepared zinc complexes with furosemide in the presence of N-donor ligands were synthesized and characterized by using different techniques such as IR, UV-Vis, $^1\text{H-NMR}$, $^{13}\text{C-NMR}$, LC/MS and single crystal X-ray diffraction and other physical properties. The prepared complexes were $[\text{Zn}(\text{furo})_2(\text{MeOH})_2]$ (**1**), $[\text{Zn}(\text{furo})_2(2\text{-ampy})_2]$ (**2**), $[\text{Zn}(\text{furo})_2(2\text{-ammepy})_2]$ (**3**), $[\text{Zn}(\text{furo})_2(\text{H}_2\text{O})(2,2\text{-bipy})]$ (**4**), $[\text{Zn}(\text{furo})_2(\text{H}_2\text{O})(4,4\text{-dipy})]$ (**5**), $[\text{Zn}(\text{furo})_2(1,10\text{-phen})]$ (**6**), $[\text{Zn}(\text{furo})_2(2,9\text{-dmp})]$ (**7**), and $[\text{Zn}(\text{furo})_2(\text{quino})_2]$ (**8**).

The crystal structure of complex **4** was determined using single crystal X-ray diffraction. Complex **4** revealed distorted octahedral geometry with one bidentate furosemide carboxylate group, one monodentate furosemide carboxylate, one bidentate 4,4-bipy, and one water molecule. for the first carboxylate group and monodentate for the second one.

Most of the prepared complexes did not show considerable anti-bacterial activity against gram-negative bacteria except complex **4** and complex **6**, and some of the prepared complexes showed anti-bacterial activity against gram-positive bacteria. In general, the complexation of zinc furosemide with nitrogen donor ligands showed slightly low inhibition activity against gram-positive bacteria compared to the positive controls (E and G).

The rate of BNPP hydrolysis was tested in order to determine the effect of zinc complexes on the phosphates hydrolysis. The results showed that the hydrolysis rate of BNPP for the following complexes was in the following order: **4** > **2** > **5** > **8** > **7** > **6** > **3** > **1**.

5. References:

1. Soetan, K.; Olaiya, C.; Oyewole, O. *African Journal of Food Science*. **2010**, *4*(5), 200-222.
2. Roat-Malone, R. M. *Bioinorganic chemistry: A Short Course*, 1st ed.; John Wiley and Sons: New Jersey, **2002**.
3. Rehder, D. *Introduction to Bioinorganic Chemistry*, **2008**
4. Bertini, I.; Gray, H.; Lippard, S.; Valentine, J. *Bioinorganic chemistry*. **1994**.
5. Glusker, J.; Katz, A.; Bock, C. *The Rigaku Journal*, **2000**, *16*, 8-17.
6. Hamada, K. *Electronic Journal of Biology*. **2016**.
7. https://authors.library.caltech.edu/25052/2/BioinCh_chapter1.pdf (accessed Feb 6, 2018)
8. Frassinetti, S.; Croce, C. *Journal of Environmental Pathology, Toxicology, and Oncology*, **2006**, *25*(3), 597-610.
9. Livingstone, C. *American Society of Parenteral and Enteral Nutrition*, **2015**, 1-12.
10. Osredkar, J.; Sustar, N. *Journal of Clinical Toxicology*. **2011**, 1-18.
11. Bogutska, K.; Sklyarov, Y.; Prylutsky, Y. *Ukrainica Bioorganica Acta*, **2013**, *1*, 9-16.
12. <https://www.lenntech.com/periodic/elements/zn.htm>. (accessed Feb 7, 2018)
13. weppi.gtk.fi/publ/foregsatlas/text/Zn.pdf. (accessed Feb 7, 2018)
14. A. McCall, K.; Huang, C.; A. Fierke, C. *American Society of Nutritional Sciences*, **2010**, 1437-1446.
15. Selvaganapathy, M.; Raman, N. *Journal of Chemical Biology and Therapeutics*, **2016**, *1*(2), 1-17.
16. Ravasio, A.; Boggioni, L.; Tritto, I. *Olefin Upgrading Catalysis by Nitrogen – based Metal Complexes*, **2011**, 27-118.
17. Bujdosova, Z.; Gyoryova, K.; Kovarova, J.; Hudecova, D.; Halas, L.; J. Therm. Ana. Calorim. **2009**, *98*, 151.

18. Abu Ali, H.; Darawsheh, M.; Abuhijleh, A.; Rappoccio, E.; Akkawi, M.; Jaber, S.; Maloul, S.; Hussein, Y. *European Journal of Medicinal Chemistry*. **2014**, *82*, 152-163.
19. Devereux, M.; Shea, D.; Kellett, A; McCann, M.; Walsh, M.; Egan, D.; Deegan, C.; Kedziora, K.; Rosair, G.; Bunz, H. *Journal of Inorganic Chemistry*, **2007**, 881-892.
20. Kumar, N.; A.V.G.S, P. *International Journal of Basic Applied Chemical Sciences*, **2015**, *5(1)*, 52-57.
21. Abu Hijleh, A. L.; Abu Ali, H.; Emwas, A. *J. Organometal. Chem.* **2009**, 694, 3590.
22. wiredspace.wits.ac.za/bitstream/.../Chapter%201%20Introduction.pdf. (accessed Feb 21, 2018)
23. www.springer.com/cda/content/document/.../9783211993101-c1.pdf. (accessed Feb 21, 2018)
24. Krstic, N.; Nikolic, R.; Stankovic, M.; Nikolic, N.; Dordevic, D. *Tropical Journal of Pharmaceutical Research*, **2015**, *14(2)*, 337-349.
25. Papageorgiou, S.; Kouvelos, E.; Favvas, E.; Sapalidis, A.; Romanos, G.; Katsaros, F. *Carbohydrate Research*, **2010**, *345*, 469-473.
26. Palanisami, N.; Rajakannu, P.; Murugavel, R. *Inorganic Chimica Acta*, **2013**, *405*, 522-531.
27. Baca, S. *International Research Journal of Pure and Applied Chemistry*, **2012**, *2(1)*, 1-24.
28. Abu Ali, H.; Jabali, B. *polyhedron*, **2016**, *16*, 1-35.
29. Abu Ali, H.; Omar, S.; Darawsheh, M.; Fares, H. *Journal of Coordination Chemistry*. **2016**, 1-28
30. Abu Ali, H.; Kamel, S.; Abu Shamma, A. *Applied Organometallic Chemistry*, **2017**, 1-13.
31. Granero, G.; Longhi, M.; Mora, M.; Junginger, H.; Midha, K.; Shah, V.; Stavchansky, S.; Dressman, J.; Barends, D. *Journal of Pharmaceutical Sciences*, **2009**, *99(6)*, 2544-2556.
32. Rowbotham, P. C.; Stanford, J. B.; Sugden, J. K. *Pharm Acta Helv.*, **1976**, *51*, 304.
33. Shin, S C, Kim, J. *Int J Pharm*, **2003**, *251*, 79.
34. Lebedev, A.; Mironova, L.; Pleshakov, I. *Pharmaceutical Chemistry Journal*, **1985**, *19(10)*, 697-700.

35. Al Omar, I.; Al Shban, R.; Shah, A. *Research Journal of Pharmacology*, **2009**, 3(4), 63-77.
36. Lahet, J.; Lenfant, F.; Courderot-Masuyer, C.; Ecartot-Laubriet, E.; Vergely, C.; Durnet-Archeray, M.; Freysz, M.; Rochette, L. *Life Sciences*. **2003**, 73, 1075-1082.
37. Hondrellis, V.; Kabanos, T.; Perlepes, S.; Tsangaris, J. *Monatshette für Chemie*, **1988**, 119, 1091-1101.
38. Lustri, W.; Lazarini, S.; Lustri, B.; Corbi, P.; Silva, M.; Nogueira, F.; Filho, O.; Massabni, A.; Barud, H. *Journal of Molecular Structure*, **2016**, 1-39.
39. Gölcü, A. *Journal of Analytical Chemistry*, **2006**, 61, 784-754.
40. Pontchev, P.; Kadum, H.; Gochev, G.; Evtimova, B. *polyhedron*, **1992**, 11, 1973-1980.
41. Zivanović, L.; Agatonović, S.; Radulović, D. *Mikrochim Acta*, **1990**, I, 49-54.
42. Liu, Y.; Wang, H.; Wang, J.; Li, Y. *The Journal of Biology and Chemical Luminescence*, **2012**, 28, 882-887.
43. Valle-Orta, M.; Dłaz, D.; Dubé, Inti.; Quiñonez, J.; Guerrero, R. *Journal of Physics*, **2017**, 838, 1-9.
44. Young, M. Faculty of Graduate Studies and Research Phosphate Diester Cleavage Mediated by Transition Metal Complexes, Mc Gill University, 1996.
45. Floriá, J.; Warshel, A. *J. Phys. Chem. B*, **1998**, 102, 719-734.
46. Jiang, W.; Xu, B.; Lin, Q.; Li, J.; Liu, F.; Zeng, X.; Chem, H. *Collids Surfaces A: Physicochem. Eng. Aspects*, **2008**, 315, 103-109.
47. Jiang, W.; Xu, B.; Zhong, J.; Li, J.; Liu, F. *J. Chem. Sci*, **2008**, 120(4), 411-417.
48. Xie, J.; Li, C.; Wang, M.; Jiang, B. *Chemical Papers*, **2013**, 67(4), 365-371.
49. Xie, J.; Jiang, B.; Kou, X.; Hu, C.; Zeng, X. *Transition Metal Chemistry*, **2003**, 28, 782-787.
50. Li, J.; Li, H.; Zhou, B.; Zeng, W.; Qin, S. *Transition Metal Chemistry*, **2005**, 30, 278-284.
51. Jancsó, A.; Török, I.; Hegetschweiler, K.; Gajda, T. *Issue in Honor of Prof Harri Lonnberg*, **2009**, (iii), 217-224.

52. Santos, A. F.; Brotto, D. F.; Favarin, L.R. V.; Cabeza, N. A.; Andrade, G. R.; Batistote, M.; Cavalherio, A. A.; Neves, A.; Rodrigues, D. C. M.; Anjos, A. D. *Brazilian Journal of Pharmacognosy*, **2014**, *24*, 309-315.
53. <https://www.intechopen.com/...antibacterial-agents/metal-complexes-...pdf> (accessed Mar 03, 2018)
54. shodhganga.inflibnet.ac.in/bitstream/10603/.../11_chapter%204.pdf (accessed Mar 03, 2018)
55. Rizzotto, M. *A Search Antibact. Agents*. **2012**.
56. Efthimiadou, E. K.; Sanakis, Y.; Katsaros, N.; Karaliota, A.; Psomas, G. *Polyhedron*, **2007**, *26*, 1148-1158.
57. Sönmez, M.; Berber, I.; Akbas, E. *European Journal of Medicinal Chemistry*, **2006**, *41*, 101-105.
58. SMART-NT V5.6 , B. A. G., D-76181 Karlsruhe, Germany, 2002.
59. SAINTL-NT V5.0, B. A. G., D-76181 Karlsruhe, Germany, 2002.
60. SHELXTL-NT V6.1, B. A. G., D-76181 Karlsruhe, Germany, 2002.
61. Rahman, A.; Choudhary, M. I.; Thomsen, W. J. Bioassay techniques for drug development; Harwood academic: Amsterdam, **2001**.
62. <science.sciencemag.org/highwire/filestream/.../0/bino-SOM.pdf> (accessed Mar 12, 2018)
63. Abu Shamma, A.; Abu Ali, H.; Kamel, S. *Applied Organometallic Chemistry*, **2017**, *32(1)*, 1-12.
64. Torres, J.; Brusoni, M.; Peluffo, F.; Kremer, C.; Domínguez, S.; Mederos, A.; Kremer, E. *Inorganic Chimica Acta*, **2005**, *358*, 3320-3328.
65. Abuhijleh, A. *Polyhedron*, **1997**, *16(4)*, 733-740.
66. Nikaido, H.; Nakae, T. *Advances in Microbial Physiology*, **1980**, *20*, 163-250.
67. Xin-Min, S.; Hai-Yan, W.; Yan-Bing, LI.; Jing-Xin, Y.; Lei, C.; Ge, H.; Wei-Ging, X.; Bing, Z. *Chem. Res. Chinese Universities*, **2010**, *26(6)*, 1011-1015.
68. Cruz Cabeza, A.; Day, G.; Samuel Motherwell, W.; Jones, W. *Crystal Growth and Design*, **2007**, *7(1)*, 100-107.
69. Kojić-Prodić, B.; Molčanov, K. *Acta Chim. Slov*, **2008**, *55*, 692-708.
70. Saluja, H.; Mehanna, A.; Panicucci, R.; Atef, E. *Molecules*, **2016**, *21*, 1-16.

71. Shalash, A.; AbuAli, H. Faculty of Graduate Studies Non-steroidal Zn (II) and Co (II) Sulindac Drugs and Bioactive bacterial Effect , Anti-malarial Effect and The Use as Phosphate Hydrolyzing Enzymes, Birzeit University, 2015.
72. Yadav, Y.; Mastropietro, T.; Szerb, E.; Talarico, A.; Pirillo, S.; Pucci, D.; Crispini, A.; Ghedini, M. *New J. Chem*, **2013**, *37*, 1486-1493.
73. T, Ishida. *J Genes Proteins*, **2017**, *1(1)*, 1-7.
74. Efthimiadou, E.; Sanakis, Y.; Katsaros, N.; Karaliota, A.; Psomas, G. *Polyhedron*, **2007**, *26*, 1148-1158.
75. Abu Shamma, A.; Abu Ali, H. Faculty of Graduate Studies New mixed ligand Cobalt (II/III) complexes based on the drug sodium valproate and bioactive Nitrogen-donor ligands. Synthesis, structure and biological properties. Birzeit University, **2016**.

6. Appendices:

Appendix A: Crystal structure data of [Zn(furo)₂(H₂O)(2,2-bipy)] (4)

Table 2: Atomic coordinates ($\times 10^4$) and equivalent isotropic displacement parameters ($\text{\AA}^2 \times 10^3$) for complex 4. U(eq) is defined as one third of the trace of the orthogonalized U_{ij} tensor.

	x	y	z	U(eq)
C(1)	431(2)	-284(2)	3248(2)	34(1)
C(2)	29(3)	13(3)	2404(2)	43(1)
C(3)	852(3)	708(3)	2011(2)	45(1)
C(4)	2167(3)	1148(2)	2442(2)	37(1)
C(5)	2585(2)	915(2)	3319(2)	33(1)
C(6)	1711(2)	208(2)	3693(2)	33(1)
C(7)	3940(3)	1393(2)	3869(2)	41(1)
C(8)	2683(3)	2137(3)	1166(2)	51(1)
C(9)	2409(3)	3252(3)	1215(2)	53(1)
C(10)	3094(5)	4358(4)	1206(4)	98(2)
C(11)	2339(7)	5055(5)	1298(5)	114(2)
C(12)	1261(7)	4346(6)	1344(4)	96(2)
C(13)	6643(2)	1089(2)	8421(2)	33(1)
C(14)	7762(3)	1501(3)	9133(2)	37(1)
C(15)	8876(3)	2217(3)	9028(2)	40(1)
C(16)	8947(2)	2576(2)	8197(2)	33(1)
C(17)	7836(2)	2118(2)	7460(2)	30(1)
C(18)	6726(2)	1400(2)	7596(2)	32(1)
C(19)	7790(2)	2339(2)	6517(2)	30(1)
C(20)	11235(3)	3760(3)	8806(2)	55(1)
C(21)	12139(3)	4825(3)	8610(2)	53(1)
C(22)	12854(5)	4820(4)	8084(3)	77(1)
C(23)	13521(5)	6021(7)	8078(5)	116(2)
C(24)	13125(7)	6650(5)	8555(4)	114(2)
C(25)	7594(3)	4654(3)	4688(2)	48(1)
C(26)	7883(4)	5869(3)	4843(4)	79(1)
C(27)	7372(5)	6358(4)	5408(4)	97(2)
C(28)	6569(5)	5646(4)	5797(4)	91(2)

C(29)	6282(4)	4445(4)	5603(3)	69(1)
C(30)	8184(3)	4059(3)	4150(2)	43(1)
C(31)	9135(4)	4676(3)	3794(3)	60(1)
C(32)	9650(4)	4073(4)	3314(3)	69(1)
C(33)	9214(4)	2862(4)	3179(3)	62(1)
C(34)	8276(3)	2286(3)	3552(2)	46(1)
Cl(1)	-1576(1)	-453(1)	1837(1)	76(1)
Cl(2)	7785(1)	1102(1)	10181(1)	65(1)
N(1)	187(2)	-1579(2)	4581(2)	43(1)
N(2)	2997(2)	1772(3)	2032(2)	50(1)
N(3)	4736(3)	1108(3)	9135(2)	54(1)
N(4)	10029(2)	3353(2)	8112(2)	43(1)
N(5)	6771(3)	3952(2)	5050(2)	45(1)
N(6)	7768(2)	2866(2)	4037(2)	36(1)
O(1)	-1367(2)	-2285(2)	3098(2)	47(1)
O(2)	-1308(2)	-556(2)	4076(2)	50(1)
O(3)	4243(2)	1293(2)	4680(2)	54(1)
O(4)	4788(2)	1908(2)	3510(2)	56(1)
O(5)	1263(3)	3213(3)	1273(2)	80(1)
O(6)	5219(2)	-695(2)	8971(2)	55(1)
O(7)	4290(2)	13(2)	7628(1)	57(1)
O(8)	6732(2)	1846(2)	5937(1)	42(1)
O(9)	8767(2)	2951(2)	6347(1)	40(1)
O(10)	12162(4)	5914(3)	8868(3)	109(1)
O(1W)	6384(2)	411(2)	4280(1)	42(1)
S(1)	-631(1)	-1218(1)	3739(1)	37(1)
S(2)	5143(1)	267(1)	8515(1)	39(1)
Zn(1)	6348(1)	2101(1)	4667(1)	32(1)
C(1ME)	4414(5)	2916(6)	7083(5)	116(2)
O(1ME)	4062(4)	2717(4)	7909(3)	116(1)

Table 2: Bond lengths [\AA] and angles [$^\circ$] for complex **4**.

C(1)-C(6)	1.385(4)
C(1)-C(2)	1.401(4)
C(1)-S(1)	1.762(3)
C(2)-C(3)	1.362(4)
C(2)-Cl(1)	1.740(3)
C(3)-C(4)	1.413(4)
C(3)-H(3)	0.9300
C(4)-N(2)	1.350(4)
C(4)-C(5)	1.418(4)
C(5)-C(6)	1.387(4)
C(5)-C(7)	1.495(4)
C(6)-H(6)	0.9300
C(7)-O(3)	1.252(4)
C(7)-O(4)	1.268(4)
C(8)-N(2)	1.452(4)
C(8)-C(9)	1.483(5)
C(8)-H(8A)	0.9700
C(8)-H(8B)	0.9700
C(9)-C(10)	1.326(6)
C(9)-O(5)	1.344(4)
C(10)-C(11)	1.421(8)
C(10)-H(10)	0.9300
C(11)-C(12)	1.298(9)
C(11)-H(11)	0.9300
C(12)-O(5)	1.367(6)
C(12)-H(12)	0.9300
C(13)-C(18)	1.385(3)
C(13)-C(14)	1.401(4)
C(13)-S(2)	1.762(3)
C(14)-C(15)	1.368(4)
C(14)-Cl(2)	1.736(3)
C(15)-C(16)	1.411(4)
C(15)-H(15)	0.9300
C(16)-N(4)	1.356(3)
C(16)-C(17)	1.419(4)

C(17)-C(18)	1.385(4)
C(17)-C(19)	1.506(3)
C(18)-H(18)	0.9300
C(19)-O(9)	1.246(3)
C(19)-O(8)	1.261(3)
C(20)-N(4)	1.454(4)
C(20)-C(21)	1.489(5)
C(20)-H(20A)	0.9700
C(20)-H(20B)	0.9700
C(21)-C(22)	1.303(5)
C(21)-O(10)	1.336(5)
C(22)-C(23)	1.415(8)
C(22)-H(22)	0.9300
C(23)-C(24)	1.280(9)
C(23)-H(23)	0.9300
C(24)-O(10)	1.410(7)
C(24)-H(24)	0.9300
C(25)-N(5)	1.334(4)
C(25)-C(26)	1.386(5)
C(25)-C(30)	1.478(5)
C(26)-C(27)	1.367(7)
C(26)-H(26)	0.9300
C(27)-C(28)	1.354(7)
C(27)-H(27)	0.9300
C(28)-C(29)	1.374(6)
C(28)-H(28)	0.9300
C(29)-N(5)	1.339(5)
C(29)-H(29)	0.9300
C(30)-N(6)	1.350(4)
C(30)-C(31)	1.389(4)
C(31)-C(32)	1.363(6)
C(31)-H(31)	0.9300
C(32)-C(33)	1.369(6)
C(32)-H(32)	0.9300
C(33)-C(34)	1.381(4)
C(33)-H(33)	0.9300
C(34)-N(6)	1.343(4)
C(34)-H(34)	0.9300

N(1)-S(1)	1.602(3)
N(1)-H(1A N)	0.9238
N(1)-H(1BN)	0.8689
N(2)-H(2N)	0.8660
N(3)-S(2)	1.599(3)
N(3)-H(3A N)	0.9083
N(3)-H(3BN)	0.8080
N(4)-H(4N)	0.8856
N(5)-Zn(1)	2.134(3)
N(6)-Zn(1)	2.125(2)
O(1)-S(1)	1.437(2)
O(2)-S(1)	1.438(2)
O(3)-Zn(1)	2.336(2)
O(4)-Zn(1)	2.159(2)
O(6)-S(2)	1.428(2)
O(7)-S(2)	1.435(2)
O(8)-Zn(1)	1.9912(19)
O(1W)-Zn(1)	2.100(2)
O(1W)-H(1W)	0.8305
O(1W)-H(2W)	0.8461
C(1ME)-O(1ME)	1.458(7)
C(1ME)-H(1M1)	0.9600
C(1ME)-H(1M2)	0.9600
C(1ME)-H(1M3)	0.9600
O(1ME)-H(1ME)	0.8200
C(6)-C(1)-C(2)	116.9(2)
C(6)-C(1)-S(1)	121.0(2)
C(2)-C(1)-S(1)	122.2(2)
C(3)-C(2)-C(1)	122.3(3)
C(3)-C(2)-Cl(1)	117.4(2)
C(1)-C(2)-Cl(1)	120.2(2)
C(2)-C(3)-C(4)	120.8(3)
C(2)-C(3)-H(3)	119.6
C(4)-C(3)-H(3)	119.6
N(2)-C(4)-C(3)	121.1(3)
N(2)-C(4)-C(5)	121.2(3)
C(3)-C(4)-C(5)	117.7(2)

C(6)-C(5)-C(4)	119.4(2)
C(6)-C(5)-C(7)	117.6(2)
C(4)-C(5)-C(7)	123.0(2)
C(1)-C(6)-C(5)	122.8(3)
C(1)-C(6)-H(6)	118.6
C(5)-C(6)-H(6)	118.6
O(3)-C(7)-O(4)	119.9(3)
O(3)-C(7)-C(5)	120.6(3)
O(4)-C(7)-C(5)	119.5(3)
N(2)-C(8)-C(9)	113.6(3)
N(2)-C(8)-H(8A)	108.9
C(9)-C(8)-H(8A)	108.9
N(2)-C(8)-H(8B)	108.9
C(9)-C(8)-H(8B)	108.9
H(8A)-C(8)-H(8B)	107.7
C(10)-C(9)-O(5)	109.1(4)
C(10)-C(9)-C(8)	132.2(4)
O(5)-C(9)-C(8)	118.7(3)
C(9)-C(10)-C(11)	106.7(5)
C(9)-C(10)-H(10)	126.7
C(11)-C(10)-H(10)	126.7
C(12)-C(11)-C(10)	107.3(5)
C(12)-C(11)-H(11)	126.4
C(10)-C(11)-H(11)	126.4
C(11)-C(12)-O(5)	109.4(5)
C(11)-C(12)-H(12)	125.3
O(5)-C(12)-H(12)	125.3
C(18)-C(13)-C(14)	117.1(2)
C(18)-C(13)-S(2)	118.1(2)
C(14)-C(13)-S(2)	124.8(2)
C(15)-C(14)-C(13)	121.6(2)
C(15)-C(14)-Cl(2)	117.5(2)
C(13)-C(14)-Cl(2)	121.0(2)
C(14)-C(15)-C(16)	121.3(2)
C(14)-C(15)-H(15)	119.4
C(16)-C(15)-H(15)	119.4
N(4)-C(16)-C(15)	121.2(2)
N(4)-C(16)-C(17)	121.1(2)

C(15)-C(16)-C(17)	117.7(2)
C(18)-C(17)-C(16)	119.1(2)
C(18)-C(17)-C(19)	117.1(2)
C(16)-C(17)-C(19)	123.8(2)
C(13)-C(18)-C(17)	123.2(2)
C(13)-C(18)-H(18)	118.4
C(17)-C(18)-H(18)	118.4
O(9)-C(19)-O(8)	124.3(2)
O(9)-C(19)-C(17)	120.0(2)
O(8)-C(19)-C(17)	115.7(2)
N(4)-C(20)-C(21)	110.7(3)
N(4)-C(20)-H(20A)	109.5
C(21)-C(20)-H(20A)	109.5
N(4)-C(20)-H(20B)	109.5
C(21)-C(20)-H(20B)	109.5
H(20A)-C(20)-H(20B)	108.1
C(22)-C(21)-O(10)	111.9(4)
C(22)-C(21)-C(20)	125.8(4)
O(10)-C(21)-C(20)	121.7(4)
C(21)-C(22)-C(23)	106.2(5)
C(21)-C(22)-H(22)	126.9
C(23)-C(22)-H(22)	126.9
C(24)-C(23)-C(22)	107.3(5)
C(24)-C(23)-H(23)	126.3
C(22)-C(23)-H(23)	126.3
C(23)-C(24)-O(10)	110.1(5)
C(23)-C(24)-H(24)	125.0
O(10)-C(24)-H(24)	125.0
N(5)-C(25)-C(26)	120.5(3)
N(5)-C(25)-C(30)	116.0(3)
C(26)-C(25)-C(30)	123.5(3)
C(27)-C(26)-C(25)	119.8(4)
C(27)-C(26)-H(26)	120.1
C(25)-C(26)-H(26)	120.1
C(28)-C(27)-C(26)	119.5(4)
C(28)-C(27)-H(27)	120.3
C(26)-C(27)-H(27)	120.3
C(27)-C(28)-C(29)	118.6(4)

C(27)-C(28)-H(28)	120.7
C(29)-C(28)-H(28)	120.7
N(5)-C(29)-C(28)	122.6(4)
N(5)-C(29)-H(29)	118.7
C(28)-C(29)-H(29)	118.7
N(6)-C(30)-C(31)	121.0(3)
N(6)-C(30)-C(25)	116.2(3)
C(31)-C(30)-C(25)	122.8(3)
C(32)-C(31)-C(30)	119.8(3)
C(32)-C(31)-H(31)	120.1
C(30)-C(31)-H(31)	120.1
C(31)-C(32)-C(33)	119.6(3)
C(31)-C(32)-H(32)	120.2
C(33)-C(32)-H(32)	120.2
C(32)-C(33)-C(34)	118.6(4)
C(32)-C(33)-H(33)	120.7
C(34)-C(33)-H(33)	120.7
N(6)-C(34)-C(33)	122.6(3)
N(6)-C(34)-H(34)	118.7
C(33)-C(34)-H(34)	118.7
S(1)-N(1)-H(1AN)	104.8
S(1)-N(1)-H(1BN)	109.5
H(1AN)-N(1)-H(1BN)	124.9
C(4)-N(2)-C(8)	126.3(3)
C(4)-N(2)-H(2N)	113.4
C(8)-N(2)-H(2N)	120.3
S(2)-N(3)-H(3AN)	112.8
S(2)-N(3)-H(3BN)	113.5
H(3AN)-N(3)-H(3BN)	130.2
C(16)-N(4)-C(20)	124.1(3)
C(16)-N(4)-H(4N)	114.1
C(20)-N(4)-H(4N)	118.0
C(25)-N(5)-C(29)	118.9(3)
C(25)-N(5)-Zn(1)	115.3(2)
C(29)-N(5)-Zn(1)	125.8(3)
C(34)-N(6)-C(30)	118.3(3)
C(34)-N(6)-Zn(1)	126.7(2)
C(30)-N(6)-Zn(1)	115.0(2)

C(7)-O(3)-Zn(1)	87.09(18)
C(7)-O(4)-Zn(1)	94.79(19)
C(9)-O(5)-C(12)	107.5(4)
C(19)-O(8)-Zn(1)	124.52(17)
C(21)-O(10)-C(24)	103.8(4)
Zn(1)-O(1W)-H(1W)	118.6
Zn(1)-O(1W)-H(2W)	120.5
H(1W)-O(1W)-H(2W)	110.7
O(2)-S(1)-O(1)	117.39(13)
O(2)-S(1)-N(1)	107.67(14)
O(1)-S(1)-N(1)	107.14(14)
O(2)-S(1)-C(1)	108.48(13)
O(1)-S(1)-C(1)	108.12(13)
N(1)-S(1)-C(1)	107.68(13)
O(6)-S(2)-O(7)	118.70(15)
O(6)-S(2)-N(3)	106.62(15)
O(7)-S(2)-N(3)	107.40(16)
O(6)-S(2)-C(13)	110.02(14)
O(7)-S(2)-C(13)	105.85(12)
N(3)-S(2)-C(13)	107.81(14)
O(8)-Zn(1)-O(1W)	88.40(9)
O(8)-Zn(1)-N(6)	123.29(8)
O(1W)-Zn(1)-N(6)	90.55(9)
O(8)-Zn(1)-N(5)	92.88(9)
O(1W)-Zn(1)-N(5)	166.22(9)
N(6)-Zn(1)-N(5)	77.28(10)
O(8)-Zn(1)-O(4)	141.91(8)
O(1W)-Zn(1)-O(4)	93.21(9)
N(6)-Zn(1)-O(4)	94.76(9)
N(5)-Zn(1)-O(4)	94.22(10)
O(8)-Zn(1)-O(3)	84.04(8)
O(1W)-Zn(1)-O(3)	91.14(8)
N(6)-Zn(1)-O(3)	152.66(8)
N(5)-Zn(1)-O(3)	102.64(9)
O(4)-Zn(1)-O(3)	57.90(8)
O(1ME)-C(1ME)-H(1M1)	109.5
O(1ME)-C(1ME)-H(1M2)	109.5
H(1M1)-C(1ME)-H(1M2)	109.5

O(1ME)-C(1ME)-H(1M3)	109.5
H(1M1)-C(1ME)-H(1M3)	109.5
H(1M2)-C(1ME)-H(1M3)	109.5
C(1ME)-O(1ME)-H(3BN)	130.0
C(1ME)-O(1ME)-H(1ME)	109.2
H(3BN)-O(1ME)-H(1ME)	109.9

Table 3: Anisotropic displacement parameters ($\text{\AA}^2 \times 10^3$) for complex **4**. The anisotropic displacement factor exponent takes the form: $-2\pi^2 [h^2 a^2 U_{11} + \dots + 2 h k a^* b^* U_{12}]$.

	U^{11}	U^{22}	U^{33}	U^{23}	U^{13}	U^{12}
C(1)	27(1)	34(1)	41(1)	9(1)	9(1)	9(1)
C(2)	25(1)	44(2)	49(2)	12(1)	-1(1)	7(1)
C(3)	37(2)	51(2)	40(2)	18(1)	4(1)	10(1)
C(4)	32(1)	33(1)	45(2)	11(1)	11(1)	11(1)
C(5)	25(1)	29(1)	42(1)	5(1)	6(1)	9(1)
C(6)	30(1)	31(1)	36(1)	5(1)	5(1)	10(1)
C(7)	29(1)	29(1)	60(2)	8(1)	3(1)	9(1)
C(8)	55(2)	56(2)	51(2)	22(2)	24(2)	21(2)
C(9)	48(2)	58(2)	51(2)	14(2)	8(2)	21(2)
C(10)	63(3)	62(3)	152(5)	19(3)	13(3)	15(2)
C(11)	131(5)	68(3)	129(5)	-3(3)	0(4)	50(4)
C(12)	128(5)	121(5)	84(3)	35(3)	42(3)	91(4)
C(13)	32(1)	34(1)	29(1)	7(1)	12(1)	5(1)
C(14)	43(2)	41(2)	27(1)	11(1)	10(1)	12(1)
C(15)	33(1)	47(2)	31(1)	8(1)	1(1)	8(1)
C(16)	30(1)	32(1)	35(1)	7(1)	8(1)	8(1)
C(17)	29(1)	29(1)	30(1)	7(1)	8(1)	8(1)
C(18)	31(1)	33(1)	28(1)	5(1)	7(1)	6(1)
C(19)	31(1)	27(1)	31(1)	6(1)	10(1)	7(1)
C(20)	35(2)	57(2)	53(2)	13(2)	-3(1)	1(1)
C(21)	33(2)	43(2)	64(2)	-2(2)	-2(1)	0(1)
C(22)	84(3)	64(2)	106(4)	21(2)	56(3)	31(2)

C(23)	54(3)	154(6)	138(6)	61(5)	44(3)	15(3)
C(24)	120(5)	55(3)	106(4)	11(3)	12(4)	-35(3)
C(25)	44(2)	38(2)	54(2)	13(1)	8(1)	9(1)
C(26)	76(3)	37(2)	120(4)	14(2)	34(3)	12(2)
C(27)	95(4)	47(2)	147(5)	-2(3)	38(4)	26(2)
C(28)	97(4)	73(3)	114(4)	-6(3)	40(3)	44(3)
C(29)	71(3)	67(2)	82(3)	12(2)	35(2)	32(2)
C(30)	39(2)	38(2)	41(2)	12(1)	8(1)	1(1)
C(31)	56(2)	49(2)	63(2)	17(2)	22(2)	-2(2)
C(32)	56(2)	77(3)	70(2)	23(2)	35(2)	1(2)
C(33)	55(2)	73(2)	63(2)	13(2)	33(2)	15(2)
C(34)	42(2)	47(2)	46(2)	9(1)	14(1)	9(1)
Cl(1)	29(1)	94(1)	81(1)	48(1)	-8(1)	1(1)
Cl(2)	63(1)	86(1)	35(1)	29(1)	9(1)	8(1)
N(1)	45(1)	42(1)	43(1)	11(1)	16(1)	12(1)
N(2)	33(1)	62(2)	56(2)	26(1)	14(1)	14(1)
N(3)	58(2)	69(2)	45(2)	17(1)	26(1)	28(2)
N(4)	29(1)	48(1)	35(1)	6(1)	4(1)	-2(1)
N(5)	47(1)	43(1)	47(1)	12(1)	14(1)	16(1)
N(6)	32(1)	37(1)	36(1)	11(1)	8(1)	6(1)
O(1)	38(1)	39(1)	53(1)	2(1)	11(1)	2(1)
O(2)	37(1)	56(1)	59(1)	4(1)	18(1)	17(1)
O(3)	39(1)	49(1)	55(1)	14(1)	-7(1)	4(1)
O(4)	28(1)	60(1)	73(2)	20(1)	11(1)	7(1)
O(5)	74(2)	99(2)	90(2)	41(2)	37(2)	46(2)
O(6)	65(2)	43(1)	57(1)	18(1)	32(1)	7(1)
O(7)	39(1)	75(2)	36(1)	7(1)	12(1)	-7(1)
O(8)	36(1)	50(1)	27(1)	11(1)	5(1)	-1(1)
O(9)	33(1)	46(1)	38(1)	15(1)	14(1)	5(1)
O(10)	137(3)	70(2)	125(3)	12(2)	60(3)	27(2)
O(1W)	50(1)	38(1)	37(1)	10(1)	14(1)	11(1)
S(1)	29(1)	36(1)	43(1)	7(1)	12(1)	7(1)
S(2)	37(1)	43(1)	32(1)	8(1)	16(1)	2(1)
Zn(1)	27(1)	36(1)	30(1)	11(1)	7(1)	6(1)
C(1ME)	73(3)	141(5)	142(5)	65(5)	44(4)	27(3)
O(1ME)	80(2)	122(3)	161(4)	69(3)	35(3)	43(2)

Table 4: Hydrogen coordinates ($\times 10^4$) and isotropic displacement parameters ($\text{\AA}^2 \times 10^3$) for complex **4**.

	x	y	z	U(eq)
H(3)	546	894	1453	54
H(6)	1997	58	4268	40
H(8A)	1951	1513	765	61
H(8B)	3384	2238	910	61
H(10)	3911	4625	1149	117
H(11)	2573	5869	1322	137
H(12)	592	4572	1414	115
H(15)	9601	2473	9514	48
H(18)	6000	1113	7110	39
H(20A)	11589	3134	8837	66
H(20B)	11106	3951	9384	66
H(22)	12915	4160	7774	93
H(23)	14133	6302	7783	139
H(24)	13428	7473	8678	137
H(26)	8423	6350	4564	94
H(27)	7574	7174	5524	116
H(28)	6219	5964	6188	109
H(29)	5726	3954	5867	83
H(31)	9418	5499	3882	72
H(32)	10293	4481	3079	83
H(33)	9543	2436	2842	75
H(34)	7985	1464	3465	55
H(1AN)	601	-2001	4335	61(11)
H(1BN)	551	-975	5016	45(9)
H(2N)	3780	1945	2336	50(10)
H(3AN)	4965	1050	9725	56(10)
H(3BN)	4585	1637	8900	77(15)
H(4N)	10039	3390	7548	53(10)
H(1W)	6124	-118	4566	70(13)
H(2W)	6211	127	3730	80(14)
H(1M1)	4149	3535	6853	174

H(1M2)	4009	2201	6645	174
H(1M3)	5315	3141	7206	174
H(1ME)	3316	2642	7823	174

Appendix B: Mass spectra of complexes (1-8).

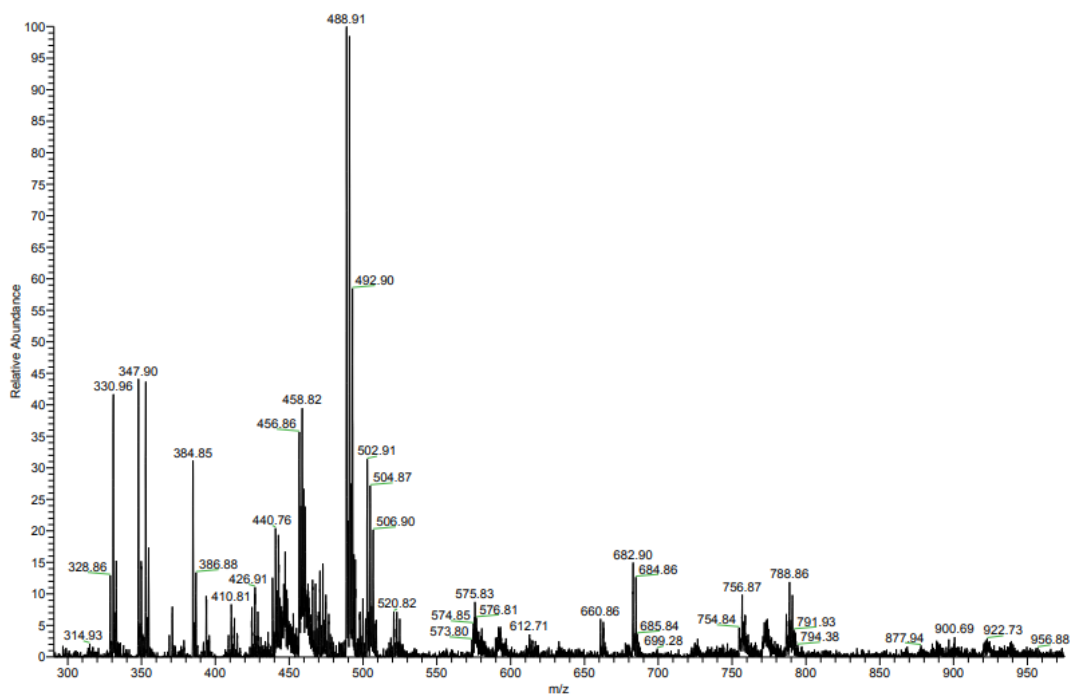


Figure 1: Mass spectra of complex 1.

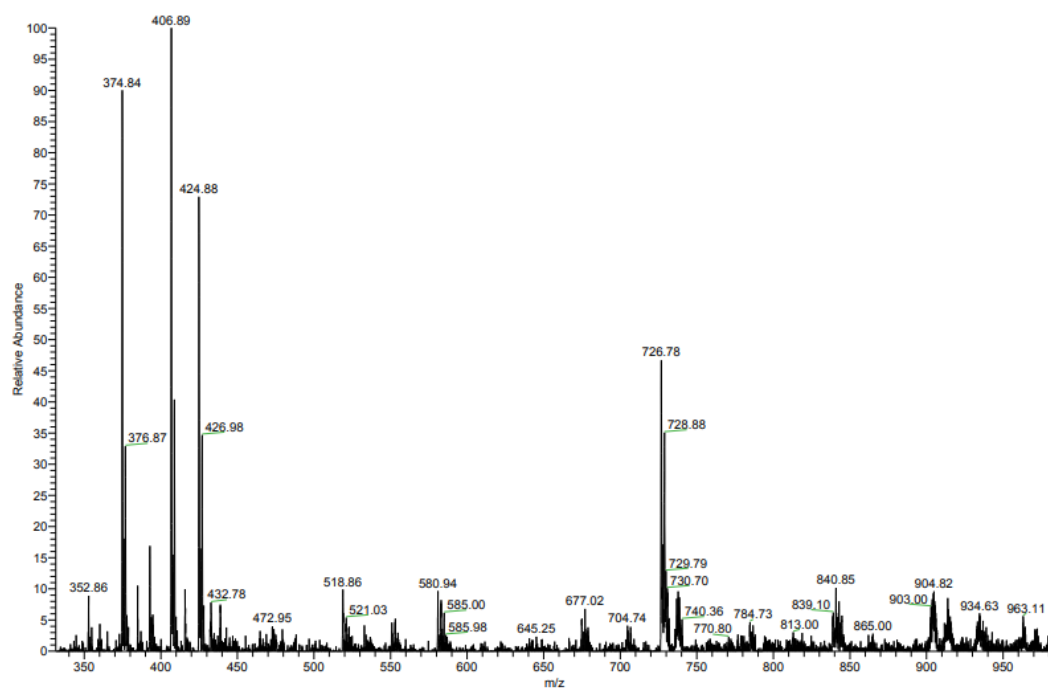


Figure 2: Mass spectra of complex 2.

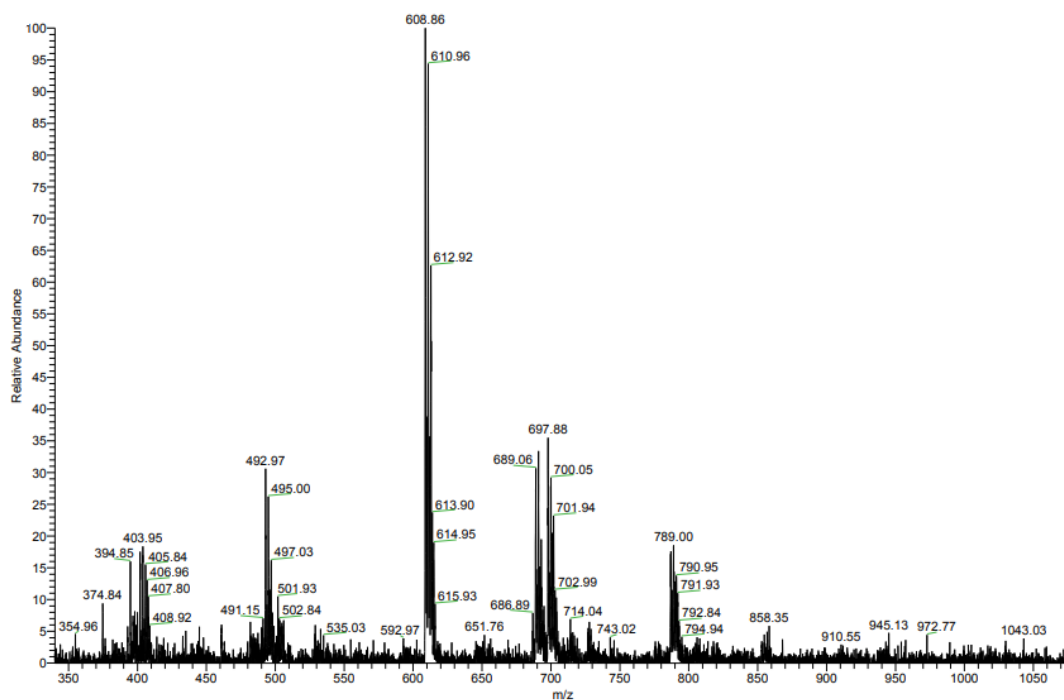


Figure 3: Mass spectra of complex 3.

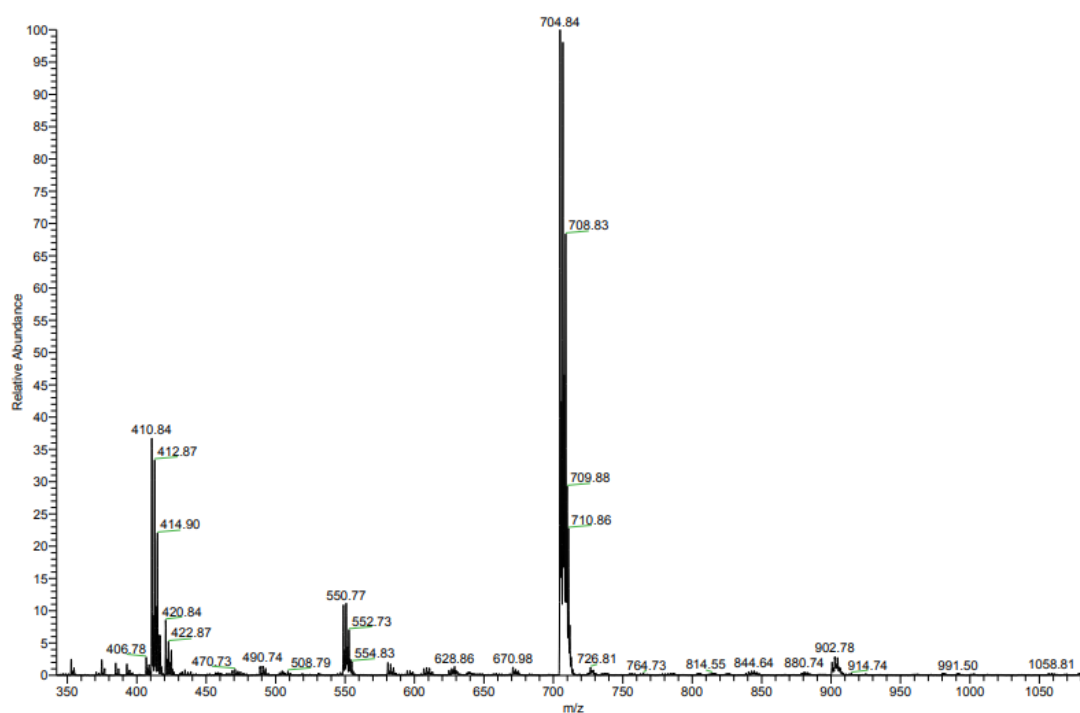


Figure 4: Mass spectra of complex 4.

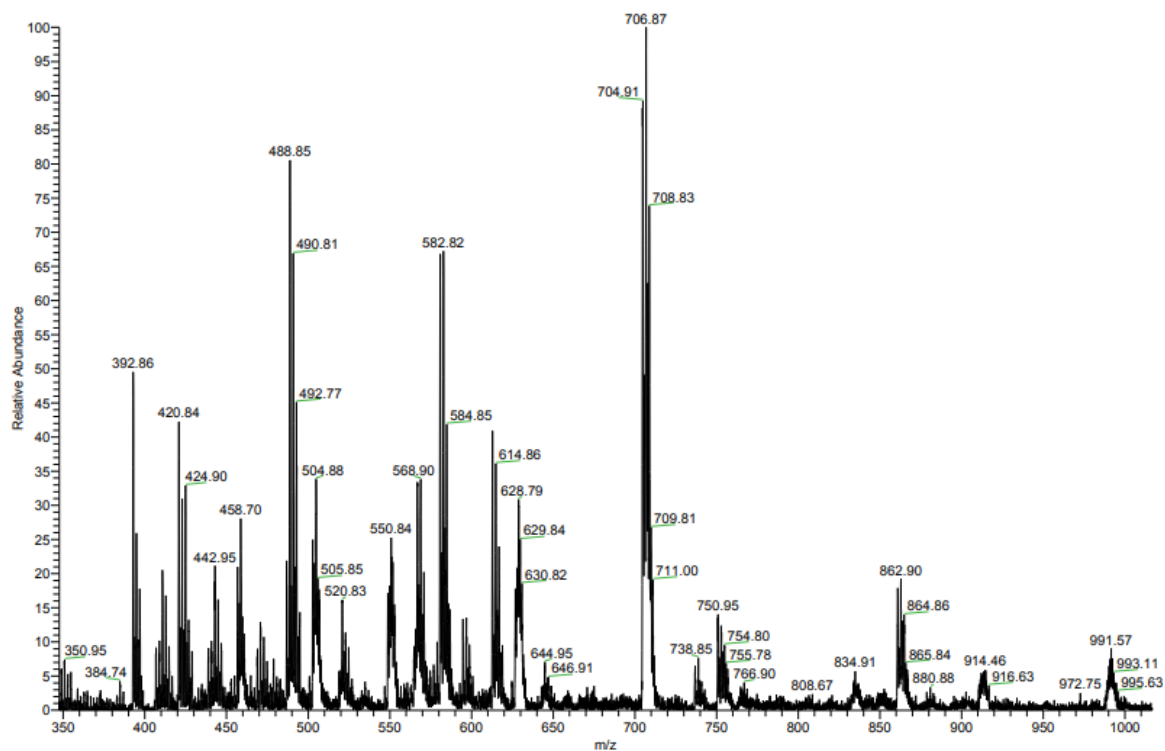


Figure 5: Mass spectra of complex 5.

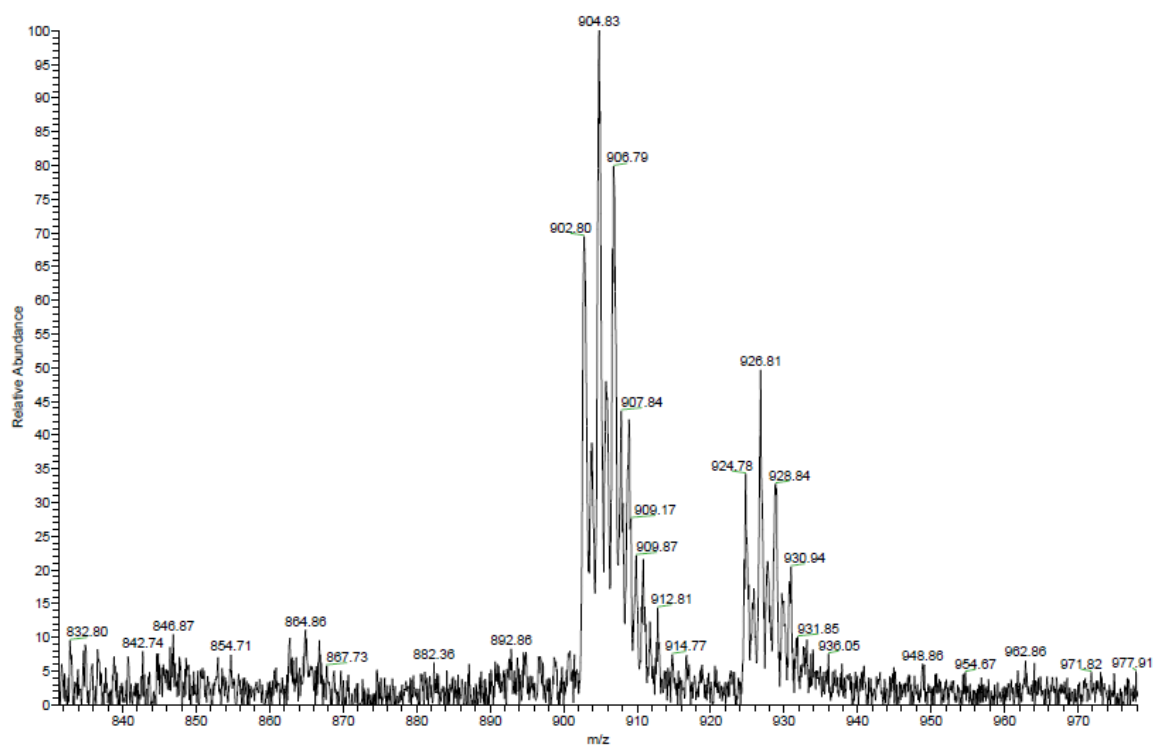


Figure 6: Mass spectra of complex 6.

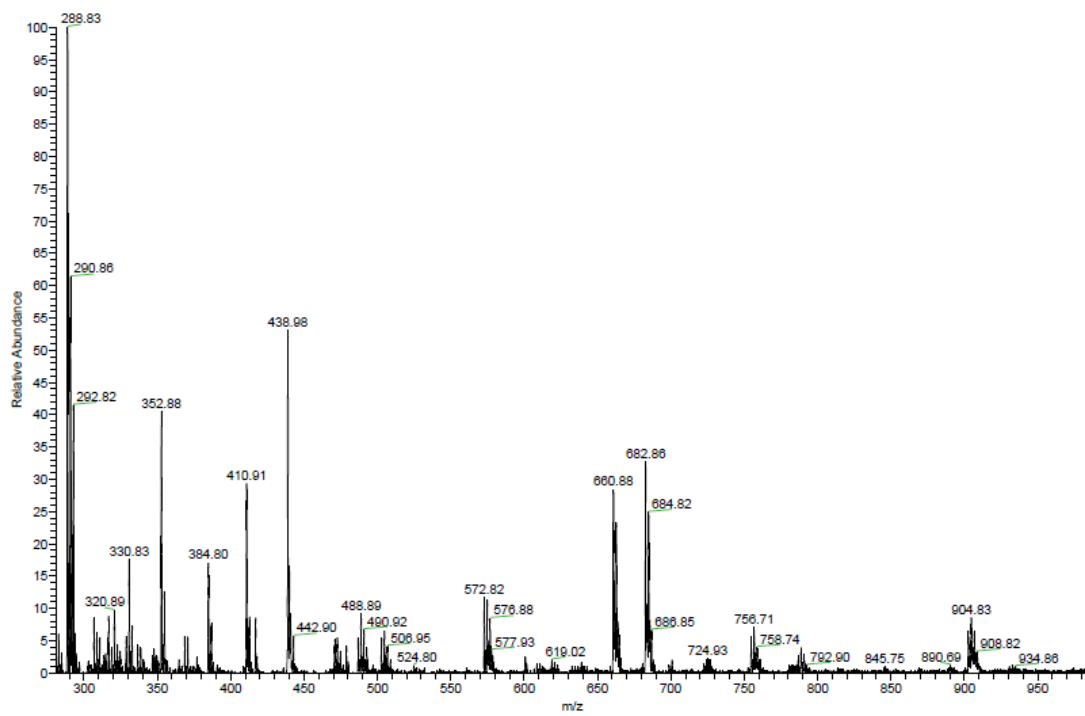


Figure 7: Mass spectra of complex 7.

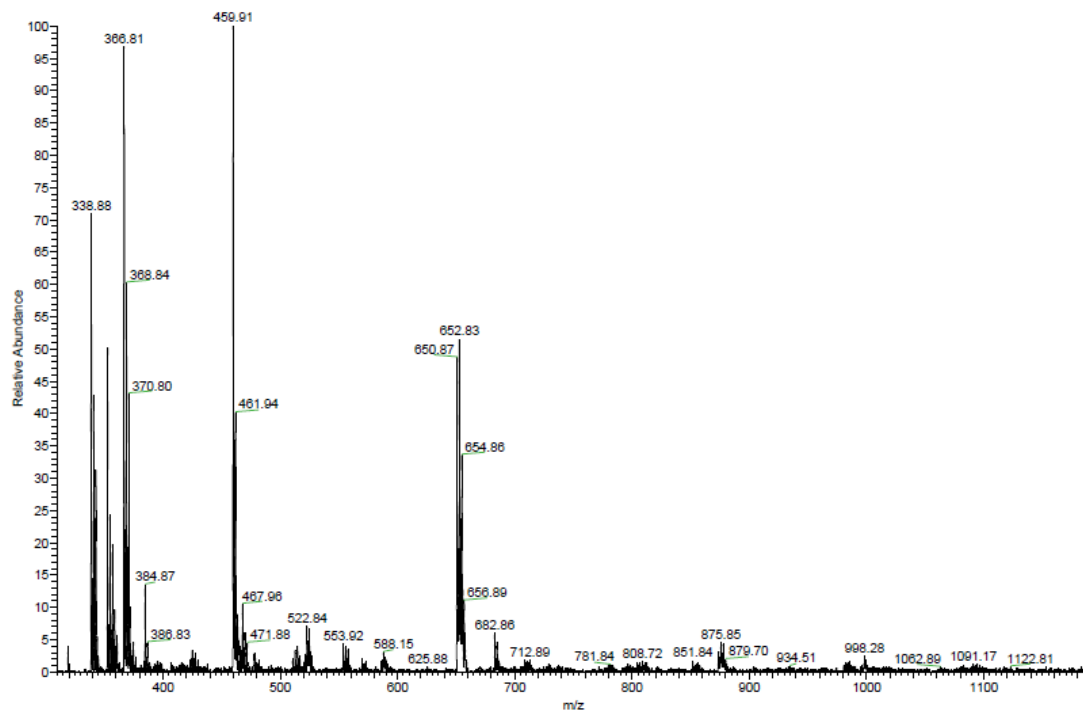


Figure 8: Mass spectra of complex 8.